UNIVERSITAT DE BARCELONA

Essential functions of *Cpeb4* in tissue homeostasis

Carlos Maíllo Carbajo

Essential functions of *Cpeb4* in tissue homeostasis

Carlos Maíllo Carbajo

Barcelona, 2016

INSTITUTE
FOR RESEARCH
IN BIOMEDICINE

UNIVERSITAT DE
BARCELONA

Universidad de Barcelona

IRB Barcelona

Doctorado en Biomedicina

Essential functions of Cpeb4 in tissue homeostasis

Memòria presentada per Carlos Maíllo Carbajo per optar al grau de doctor per la Universitat de Barcelona.

Doctorando: Carlos Maíllo Carbajo

Director de la tesis: Raúl Méndez de la Iglesia

Tutor de la tesis: Antonio Zorzano Olarte

Barcelona, 2016

A mis padres, mi hermana, y a Ágata.

Index

Abbreviations

ALT: Alanine Transaminase

CPE: Cytoplasmic Polydenylation Element

CPEB: Cytoplasmic Polyadenylation Element Binding Proteins

$CPEB4^{KO}$: CPEB4 ubiquitous knockout

$CPEB4^{LKO}$: CPEB4 liver-specific knockout

EE: Energy Expenditure

ER: Endoplasmic Reticulum

FFA: Free Fatty-Acid

GSEA: Gene Set Enrichment Analysis

GWAS: Genome Wide Association studies

HFD: High-Fat Diet

H&E: Hematoxylin and Eosin

KO: Knockout

LD: Lipid Droplet

mtDNA: Mitochondrial DNA

MEF: Mouse Embryonic Fibroblast

ORC: Oxygen Consumption Rate

RER: Respiratory Exchange Ration

RIP-seq: RNA Immunoprecipitation Sequencing

TGA: Triglyceride

TG: Thapsigargin

TM: Tunicamycin

uORF: Upstream Open Reading Frame

UPR: Unfolded Protein Response

UTR: Unstranslated Region

VLDL: Very-Low Density Lipoprotein

WT: Wild-Type

ZT: Zeitgeber Time

Abstract

The Cytoplasmic Polyadenylation Element Binding (CPEB)-family of RNA-binding proteins is composed of four paralogs in mammals, CPEB1-4. The CPEBs control the translation of the targeted mRNAs by modulating the length of their poly(A) tail. This regulatory mechanism activates maternally stored mRNAs in oocytes and drives oocyte maturation and early embryogenesis.

Genome-wide studies have revealed that the CPEBs are expressed in various adult tissues and potentially regulate up to 20% of the vertebrate transcriptome. However, the specific roles and regulation of each CPEB are poorly understood beyond the embryonic stage.

In this study, we aimed to define the functions and regulation of CPEB4 in adult tissues of mammalian organisms. For this purpose, we have generated ubiquitous and tissue-specific loss of function mouse models for CPEB4. The characterization of these genetic models has revealed that CPEB4-mediated translation is essential for mammalian organisms to cope with metabolic stress. Moreover, we have identified the molecular mechanism by which CPEB4 establishes a translational program to maintain cellular homeostasis during metabolically challenging conditions.

Altogether, our results reveal a novel function of CPEB4 in gene expression regulation during metabolic stress.

Introduction

1. Gene expression and regulation

The expression of the genomic information is arguably the most important process to life. It allows the use of the bidimensional information contained in the DNA to build and maintain exquisite molecular machines with the capacity to survive and adapt to the environmental challenges. Biochemically, the gene expression pathway comprises the group of molecular processes that uses the DNA sequence as a template for the synthesis of specific gene products, commonly proteins. This is accomplished by the transcription of a sequence of nucleotides from the DNA into an intermediary molecule called messenger RNA (mRNA), which is then translated into the sequence of amino acids that forms a protein. This sequential process of events, known as the central dogma of molecular biology, was already outlined in 1958 (Crick, 1970; Crick, 1958) and has maintained its validity after more than 50 years.

Because not all proteins are required to be produced at the same levels and at the same time, the regulation of the genetic information flow is instrumental for the control of cell structure and function, and it is the foundation of cell adaptability to environmental changes. In higher organisms, it becomes even of greater importance, since the genome contains the instructions to generate and guide the deployment of all cellular identities during embryonic and postembryonic development. Beyond that, precise control of genes allows the establishment of the multiple cell types that will conform the adult organism and will meet the environmental challenges.

Being such a central process for the maintenance and evolution of life, gene expression regulation is a complex, interconnected and multilayered process in which every step of the pathway is tightly monitored and controlled to ensure

optimal cellular adaptation to the environmental and physiological demands (Moore, 2005) (Orphanides and Reinberg, 2002). However, most of the research in the last decades has focused on the first step of the pathway: the regulation of transcription. This has led to the vast accumulation of knowledge regarding the cis-regulatory elements, trans-acting factors, chromatine structures and epigenetic modifications that govern the transcription of genes (Kornberg, 1999). The main reasons of this focus are historical: pioneer studies in the control of genes were carried out in bacteria (Jacob and Monod, 1961), in which most of the regulation is takes place at the transcriptional level. However, given that in eukaryotes transcription and translation are physically separated, evolution had the opportunity to develop a plethora of additional regulatory steps to temporally and spatially fine-tune the production of proteins. It was not until the advent of novel high-throughput techniques that we began to get a glimpse of the post-transcriptional gene regulatory networks that govern all aspects of the eukaryotic mRNA life (Lackner and Bähler, 2008) (Halbeisen et al., 2008).

2. Post-transcriptional gene regulation

In eukaryotes, post-transcriptional mRNA processing is composed of several stages that increase the genome coding capacity and provide additional regulatory opportunities. Here, we will make a brief overview of the most prominent post-translational steps.

2.1 Nuclear processing

The post-transcriptional processing and regulation of a gene starts concomitantly

to the transcriptional process (Aguilera, 2005). As soon as the first 20-30 nucleotides of the nascent pre-mRNA have been produced by the RNA polymerase II, the mRNA is capped with an m^7G structure at the 5' end (Topisirovic, 2011). The process occurs in three consecutive reactions: first the mRNA is cleaved, then a GMP is linked in a reverse orientation by a unique 5'–5' triphosphate bond to the 5' end, and finally the GMP is methylated at position N^7. The cap structure is necessary for nuclear export of the mRNA and precludes 5'–3' exonucleotide degradation (Topisirovic, 2011). In addition, it is required for proper mRNA translation (see Translational control of gene expression). These regulatory activities are mediated by cap-binding proteins: nuclear cap binding proteins complex (nCBC) in the nucleus and eukaryotic translation initiation factor 4E (eIF4E) in the cytosol.

Most eukaryotic genes contain intronic regions that must be removed to obtain a mature and functional mRNA (Papasaikas and Valcarcel, 2016). This is generally achieved by a ribonucleotide complex called the spliceosome, which excise the introns and ligates together the flanking exons of the pre-mRNA (Papasaikas and Valcarcel, 2016). This process, far from being constitutive and rigid, allows the combinatorial removal of different intronic regions expanding the coding capabilities of a single gene. In addition, it generates broad opportunities to regulate the production of different protein isoforms from a single locus depending external and internal signals. The fact that more than 90% of the human genes are alternatively spliced underscores the importance of this mechanism in the maintenance of cellular proteostasis (Papasaikas and Valcarcel, 2016).

Once the polymerase has transcribed an entire gene, the pre-mRNA must be released and its 3' end must be processed to generate a functional transcript (Di Giammartino et al., 2011). Except mRNAs encoding for replication-dependent histones, the 3' ends of all eukaryotic transcripts are generated by a two-step reaction: first, the pre-mRNA is endonucleolytically cleaved and released; second,

it is appended with a non-templated polyadenylate [poly(A)] tail. This process requires the cooperative action of specific regulatory elements in the pre-mRNA sequence and various RNA binding proteins (RBPs) that will recognize and bind those elements. The cleavage and polyadenylation specific factor (CPSF) and the cleavage stimulating factor (CstF) recognize the poly(A) signal (AAUAAA) and the U/GU-rich element, respectively, on the 3' region of the pre-mRNA. Then, the coordinate action of cleavage factors I and II (CFI, CFII), and the subsequent action of a poly(A) polymerase (PAP), lead to the cleavage and addition of a poly(A) tail some nucleotides downstream of the poly(A) signal (Di Giammartino et al., 2011). The coating of the newly synthesize poly(A) by the poly(A) binding protein nuclear I (PABNI) is essential to increase PAP processivity and to avoid transcript degradation. Interestingly, the length of the tail varies greatly among species (from 70-80 adenines in yeast up to 250-300 in humans) but it is an essential element for proper export, stability and translation of mature transcripts in all of them. Until very recently, it was thought that the 3' end processing of the transcripts was a default mechanism. However, genome-wide studies have revealed that, similarly to the regulation of splicing, more than half of mammalian transcripts can be cleaved and polyadenylated at various sites, thereby allowing the generation of transcripts with different 3' UTRs that will contain or exclude specific regulatory elements that determine their localization, stability and translation (Elkon et al., 2013). Although the molecular details of such process are still being worked out, it seems that the action of specific RBPs acting on regulatory elements of the pre-mRNA is vital for the 3' UTR determination (Bava et al., 2013).

Finally, and before reaching the cytoplasm, mature transcripts can be enzymatically modified on specific nucleotides. Examples of this are RNA pseudouridilation, cytidine deamination or adenine methylation. In particular, reversible methylation of adenosines in the position N6 (m^6A) has emerged has a widespread modification of mRNAs and controls their expression and stability (Fu et al., 2014). Considering

that there are more than 100 types of chemical modifications known to occur on the RNA and that we know very little about the biological function and distribution of most of them, our knowledge on RNA-epigenetics is expected to rise dramatically in the near future.

2.2 Cytosolic crossroad

Once the mature mRNA reaches the cytosol, its fate will be predetermine by the regulatory structures and sequences acquired in the nucleus. As we have seen, the structure of a mature transcript will be composed of an m^7G cap at the 5' end, followed by a coding sequence that is flanked by two untranslated regions, and tailored by a poly(A) tail **(Figure 1).** Every component of the mRNA exerts specific regulatory tasks that control whether it is translated into proteins, degraded by exonucleases, repressed in a latent state or localized to specific cellular compartments.

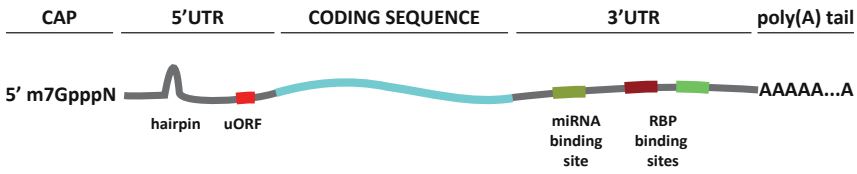

Figure 1. Eukaryotic mRNA structure and regulatory elements. The m7G cap structure at the 5' end and the poly(A) tail at the 3' end are essential components for translation initiation. Secondary structures (hairpins) and uORFs at the 5' UTR can negatively regulate mRNA translation. In the 3' UTR, the presence of miRNA/RBP binding sites can alter mRNA stability and/or translation through the recruitment of protein complexes that block the cap structure, modify the poly(A) tail length or cleave the transcript.

3. The cytosolic fate of mRNAs

Here we will analyze the common cytoplasmic fates of an mRNA (namely translation, degradation, and localization), emphasizing the regulatory function exerted by its different parts.

3.1 mRNA decay

Once in the cytoplasm, the mRNA has to subsist long enough in order to be translated. The task is not trivial due to the ubiquitous presence of endo- and exo-nucleases. The stability of a given transcript is grossly determined by its poly(A) tail length. Although every transcript is nuclearly endowed with a 250 nt poly(A) tail, when it reaches the cytoplasm the action of deadenylases can trim the tail triggering the decay of the mRNA. Transcript deadenylation is commonly followed by decapping by the decaping enzymes 1 and 2 (DCP1 and DCP2) rendering the mRNA accessible to 5'-3' exonucleases and the cytoplasmic exosome which will degrade it (Halbeisen et al., 2008).

As opposed to this general degradation pathway, the mRNA decay can also be controlled in a transcript-specific fashion by regulatory sequences located in the untranslated regions that recruit protein effectors. These effectors can actively remove the poly(A) tail or trigger the cleavage of the mRNA (see Translational control by cytoplasmic polyadenylation).

3.2 mRNA localization

RNA localization at specific cellular compartments allows a tight spatial control

of the protein production process. Active transport of mRNAs mediated by RBP-motor protein complexes is the most widely-studied mechanism of subcellular RNA localization (Halbeisen et al., 2008). Transcript-specific localization by this mechanism is achieved by regulatory elements on the mRNA sequence that recruit RBPs effectors, which repress the translation of the transcript and engage in transportation to specific cellular compartments, such as the endoplasmic reticulum, mitochondria, dendrites, etc, (Nagaoka et al., 2012) (Huang et al., 2003).

3.3 mRNA translation

The translational efficiency of an mRNA is fundamentally determined by its capacity to recruit the ribosomal machinery. Although there are alternative modes of recruitment (Weingarten-Gabbay et al., 2016), it generally occurs through the m^7G cap-structure **(Figure 2)**.

Cap-mediated translation begins with the formation of the 43S pre-initiation complex (Gray and Wickens, 1998; Jackson et al., 2010; Sonenberg and Hinnebusch, 2009). This is attained by the recruitment of the ternary complex (TC), formed by eIF2 (a heterotrymer of α, β and γ subunits), GTP and a methionyl-initiator tRNA (Met-$tRNA_i^{Met}$) to the 40S ribosomal subunit, which is aided by eIF1, eIF1A and eIF3. The recruitment of the newly formed pre-initiation complexes to the transcript is mediated by the eIF4F complex. eIF4F is formed by eIF4E, a cap-binding protein; eIF4G, a scaffolding protein; and eIF4A, an RNA helicase that assists the scanning. In addition to eIF4F, the cytosolic poly(A) binding protein (PABP) is essential to initiate translation. It binds both the poly(A) tail and eIF4G bridging together the two ends of the mRNA in a process of pseudo-circularization (Tarun and Sachs, 1995) (Sachs et al., 1997). This conformation, known as the "closed-loop model", increases ribosome recycling and has been shown to be

essential for translation initiation, at least in yeast. When the 43S pre-initiation complex reaches the start codon it forms the 48S initiation complex, which recruits the 60S subunit to form a 80S translationally competent ribosome.

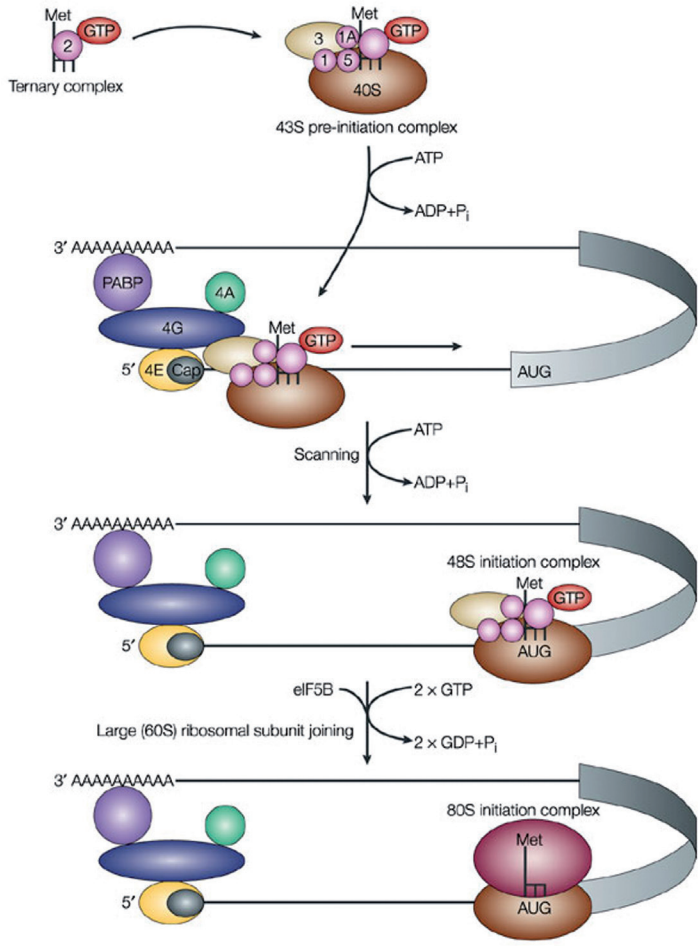

Figure 2. Cap-mediated translation initiation. Translation begins with the formation of the ternary complex (TC) by eIF2, GTP and the initiator tRNA. The TC is then recruited to the ribosomal 40S subunit to form the 43S pre-initiation complex, which is in turn recruited to the mRNA by eIF4F. The complex then can start scanning the transcript until the initiation codon is reached. At that point, the 48S initiation complex is formed and the 60S ribosomic subunit is recruited to a form a 80S full ribosome. Modified from Gebauer et al., 2004.

While translation initiation is directly regulated by more than 25 proteins, the elongation and termination processes require a minimum number of them, underscoring the preponderance of the initiation step over the other two (Lackner and Bähler, 2008). However, in recent years, condon usage and acyl-tRNA availability have emerged as important determinants of translation elongation and protein synthesis (Richter and Coller, 2015).

4. Translational control of gene expression

Global gene expression analysis in mammalian cells has revealed that translation efficiency is the single best predictor of protein expression (Schwanhausser et al., 2011) and is under strong evolutive selection (Khan et al., 2013; Wu et al., 2013), underlying the importance of this last step in the gene expression cascade.

4.1 Global translational control

The formation of the TC is the major checkpoint that the cell uses to regulate global protein production **(Figure 2)**. eIF2 is a G-protein that cycles between and active form (GTP-bound) and inactive form (GDP-bound). eIF2B is the guanine nucleotide exchange factor (GEF) that regulates the transition towards the active form by catalyzing the GTP-GDP exchange. However, when eIF2α is phosphorylated in S51 (in humans), the GEF activity of eIF2B is inhibited such that the generation of new TC is halted. Several signaling pathways converge on the phosphorylation of eIF2α by the action of different kinases, what is collectively known as the integrated stress response (IRS). These kinases are the interferon-induced double-stranded RNA (dsRNA)-dependent eIF2α kinase (PKR), activated

by viral infection (Galabru et al., 1989); the general control nonderepressible 2 (GCN2), activated by amino acid deprivation (Berlanga et al., 1999); the heme-regulated inhibitor kinase (HRI), triggered by heme deficiency (Lu et al., 2001), and the endoplasmic reticulum (ER)-resident kinase (PERK), triggered by the accumulation of misfolded proteins inside the ER (Shi et al., 1998) (see Translation at the ER: a surveillance system).

The cap-binding protein eIF4E is another node of general protein synthesis regulation and is controlled by direct phosphorylation or sequestration by eIF4E binding proteins (4EBPs) (Richter and Sonenberg, 2005).

Most of the translational activity in a cell occurs at a specialized organelle called the endoplasmic reticulum (ER), which, given its importance, has develop its own global translational control mechanism.

4.2 Translation at the ER: A surveillance system

The vast majority of proteins that are destined for cellular organelles, cell membrane or secretion are synthesized, folded, matured and transported at the ER (Cnop et al., 2012). Since they account for more than 75% of the proteins produced in a given cell, their synthesis is one of the most energy consuming cellular processes (Proud, 2002) and thus, it is tightly controlled. The ER is a specialized eukaryotic organelle formed by an intricate network of tubes and flattened sacs connected by a lumen that contains a molecular environment particularly favorable for protein maturation. In it reside numerous chaperons, protein disulfure isomerases and peptidyl-prolyl isomerases, which assist in the process of protein folding and modification. Moreover, the ER lumen chemical properties are also adapted to the folding process: it contains Ca^{2+}, which is fundamental for chaperone function, 4 orders of magnitude more concentrated than the cytoplasm (0.1mM compared to

10nM). In addition, its redox potential is highly oxidizing thereby benefiting the formation of disulfide bonds (Oakes and Papa, 2015).

In spite of all the molecular mechanisms set in place to assist it, protein folding is the most error prone phase of the gene expression cascade. It is estimated that, in highly synthetic organs like the liver, up to 50% of the proteins fail to assume their properly folded forms (Hotamisligil, 2010). Moreover, the flux of proteins into the ER can vary up to one order of magnitude in very short periods of time (Itoh and Okamoto, 1980). Therefore, cells face the fundamental task of preventing the accumulation of misfolded proteins in the ER, a condition commonly known as ER stress (Ron and Walter, 2007) (Walter and Ron, 2012). Far from being an unlikely event, accumulation of misfolded proteins by a loss of ER homeostasis can be caused by a variety of events such as increased in protein synthesis, decreased proteosomal activity, excess or deficiency of nutrients, alterations in calcium homeostasis or redox hoemostasis, etc., (Wang and Kaufman, 2016).

Considering the wide range of perturbations that can affect ER function, eukaryotic cells have evolved a surveillance and quality control system to monitor whether the folding capacity of the ER is in balance with the protein synthesis demands. This system is composed by a signal transduction pathway called the unfolded protein response (UPR) **(Figure 3)** (Ron and Walter, 2007) (Walter and Ron, 2012), which is conserved from yeast to mammals. The UPR is formed by three different branches regulated by three sensors: IRE1α, PERK and ATF6α (Bertolotti et al., 2000) (Harding, 1999). All of them are transmembrane proteins located at the ER and characterized by a luminal domain with the capacity of detecting the accumulation of misfolded proteins. In homeostatic conditions, BiP, which is an abundant ER chaperone, is bound to the intraluminal domains of these sensors and precludes their activation. However, since BiP presents higher binding affinity to misfolded proteins, when they accumulate inside the lumen of the ER, BiP is titrated away

from the UPR sensors leading to their activation (Bertolotti et al., 2000) (Shen et al., 2002) **(Figure 3)**.

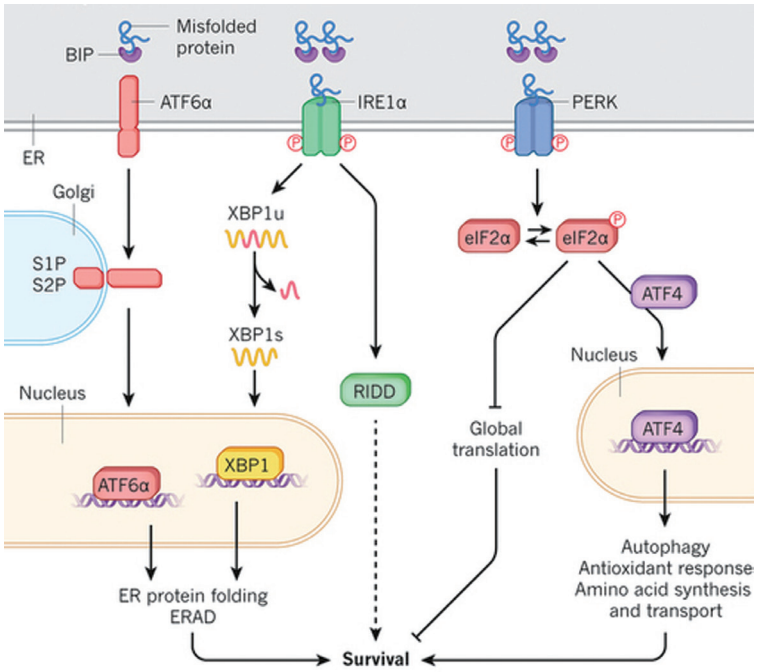

Figure 3. The UPR pathway. Three parallel branches comprise the UPR pathway. Every branch contains a different sensor: ATF6α, IRE1α and PERK. The accumulation of misfolded proteins in the ER-lumen titrates BiP away from the luminal domain of the three sensors. Once released from BiP, ATF6α travels to the Golgi were the action of the proteases S1P and S2P release a cytosolic fragment that travels to the nucleus and activates the transcription o several genes. The release of BiP from IRE1α and PERK triggers their dimerization and activation. IRE1α catalyzes the cytosolic splicing of XBP1u, generating XBP1s, which is active in transcription. In addition, IRE1α activation triggers the degradation of ER-located transcripts (RIDD). Active PERK phosphorylates eIF2α, which attenuates global protein synthesis and stimulates the translation of uORF-containing mRNAs such as Atf4. The three pathways cooperate to promote adaptation to the stress conditions and to increase cell survival. Modified from Wang et al., 2016.

When BiP is released from ATF6α, it unmasks two Golgi localization sequences

(GLS) in its luminal domain that drive its transport to the Golgi (Shen et al., 2002). Then, the ATF6α cytoplasmic N-terminus, that contains a basic leucine zipper motif that functions as a transcription factor, is proteolitically cleaved allowing its translocation to the nucleus where it binds to cAMP response elements (CRE) and ER stress response elements (ERSE) of the DNA promoting the production of proteins that mediate protein folding, ER-associated degradation (ERAD) and ER biogenesis **(Figure 3)**.

Conversely, IRE1α and PERK are activated by the dimerization-driven trans-autophosphorylation that occurs when BiP dissociates from their luminal domains. In the case of IRE1α, autophosphorylation activates the cytoplasmic endoribonuclease catalytic domain, which carries out the splicing of the Xbp1 mRNA by an unconventional spliceosomal-independent mechanism **(Figure 3)** (Yoshida et al., 2001) (Calfon et al., 2002) (Lee et al., 2003). The mature XBP1 mRNA generates a protein able to bind and stimulate the transcription of genes under the control of ERSE. On the other hand, activated PERK phosphorylates eIF2α by its cytoplasmic kinase domain thereby eliciting a global suppression of translation (Wek et al., 2006) (Harding, 1999) (see The UPR translational regulation is mediated by uORFs). Interestingly, eIF2α phosphorylation leads to the specific production of the transcription factor ATF4 and other genes. ATF4 activates the transcription of genes that allow adaptation to the ER stress conditions **(Figure 3)**.

In summary, the three pathways act together in order to achieve the same goal: increase the cell folding capacity by expanding the ER and elevating the amount of chaperons while reducing general protein synthesis to decrease the number of client proteins in the ER (Walter and Ron, 2012). However, this adaptive response cannot last forever. If the ER stress is excessive, the adaptive response switches into a cell-death response (Rutkowski et al., 2006). This is achieved by the ATF4-

mediated production of the transcription factor CHOP, which then triggers the core mitochondrial apoptotic cascade suppressing the prosurvival factor BCL2, while stimulating proapoptotic BIM, PUMA and NOXA (Tabas and Ron, 2011). Although the molecular details are still poorly understood, it seems that the duration and intensity of the insult to the ER determines the life/death switch of the UPR.

4.3 The UPR translational regulation is mediated by uORFs

While in yeast the genetic regulation triggered by the UPR is mainly transcriptional, as we have seen, in higher eukaryotes it is accompanied by a powerful translational regulation **(Figure 3)** (Pavitt and Ron, 2012). The RNAase activity of IRE1a has been shown to degrade several ER-located mRNAs in a process named regulated IRE1-depdendent decay (RIDD) **(Figure 3)** (Hollien et al., 2009). More interestingly, it has also been shown to regulate microRNA levels during ER stress to specifically modulate gene expression (Chitnis et al., 2013).

However, the UPR branch that more strongly regulates mRNA translation during the UPR is the PERK pathway (Harding et al., 2000). It simultaneously regulates bulk protein synthesis and specific protein production. As described above, PERK inhibits global protein synthesis by phosphorylating eIF2α, thereby hindering the production of new TCs. **(Figure 3)**. By doing so, it shrinks the workload placed on the ER allowing it to recover before protein synthesis ensues.

Paradoxically, there are a number of mRNAs whose translation benefit from eIF2α phosphorylation. They all contained specific regulatory sequences in their 5' UTR called upstream open reading frames (uORFs) (Harding et al., 2000) (Harding et al., 2003). These sequences repress the translation of the main ORF in homeostatic conditions while promoting its translation whenever the TC availability is reduced. This regulatory system has been thoroughly studied on Atf4 mRNA (Vattem and

Wek, 2004) **(Figure 4)**. The 5' UTR of Atf4 mRNA contains two uORFs, uORF1 is only three codons long and uORF2 overlaps with the main ORF. When the ribosome scans from the cap towards the main ORF and encounters uORF1, it gets translated. After termination, the ribosome reinitiates the scanning from that point and, given the high abundance of TCs, it is highly probable that the 40S subunit is able to form the 43S pre-initiation complex before reaching the uORF2. Thus, the translation of the uORF2 prevents the decodification of the main ORF **(Figure 4)**. On the contrary, in conditions of low TC availability caused by eIF2α phosphorylation, most of the 40S subunits exiting the uORF1 will not acquire a TC before reaching the uORF2, therefore bypassing its inhibitory function and allowing the translation of the main ORF **(Figure 4)**. This mechanism applies to all mRNAs regulated by uORF although with small variations depending on the number of uORFs, their position and whether or not they overlap with the main ORF. Accordingly, this counterintuitive but effective system has been shown to allow the production of some of the main UPR mediators such as ATF4, ATF5, CHOP and GADD34 (Pavitt and Ron, 2012).

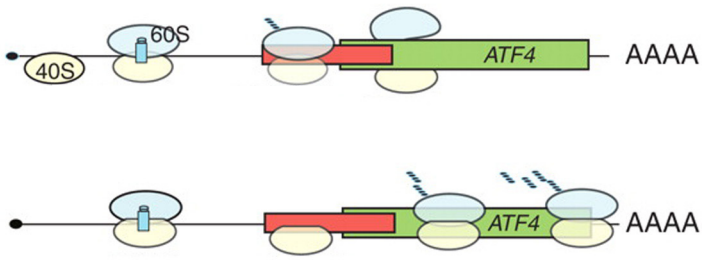

Figure 4. uORF-mediated translational regulation. During normal conditions (high TC abundance) the two uORFs of the Atf4 mRNA get translated (in blue and red) precluding the translation of the main ORF (green). However, upon eIF2α phosphorylation, the low availability of the TC hinders the formation of the 43S pre-initiation complex before reaching the uORF2. In this conditions a

higher number of scanning subunits reach de main ORF allowing it to be translated. Modified from Pavitt and Ron, 2012.

Altogether, the combination of transcriptional, translational and post-translational regulation entailed by the UPR generates exceptionally rapid and sharp changes in the cellular proteome to recover ER homeostasis.

4.4 mRNA-specific translational control: The RBPs

The translational regulatory mechanisms presented so far, based on eIF2α phosphorylation and eIF4E inhibition, targeted the recruitment of the ribosomes to the transcripts in a generalized manner. Conversely, there are a group of regulatory machineries that act in a transcript-specific manner. They rely on the presence of cis-acting sequences in the mRNAs that recruit specific trans-acting factors: the RNA-binding proteins (RBPs).

RBPs are central components in RNA metabolism. They regulate all aspects in the life cycle of the mRNA: RNA synthesis, processing, maturation, export, stability, transport and translation (Gerstberger et al., 2014) (Singh et al., 2015) (Glisovic et al., 2008). Indeed, as soon as the pre-mRNA is produced it is rapidly packed into ribonucleoprotein (RNP) complexes through the binding of a myriad of RBP to its different elements. The identity and dynamics of single RBPs on mRNP complex varies through the life cyle of the mRNA through processes of remodelling (Singh et al., 2015). Intriguingly, RBPs not only regulate every step of RNA metabolism but also connect them together generating regulatory networks with the capacity to counteract perturbations in one step of the pathway by modulating others (Orphanides and Reinberg, 2002). Moreover, it has been propose that RBPs form RNA-regulons, in which every RBP controls several mRNAs encoding proteins

that function in the same biological process (Keene, 2007). For instance, the neuro oncologic ventral antigen (Nova) RBP coordinates the translation of a subset of mRNAs involved in the inhibitory activity of synapses in neurons (Keene, 2007).

Recent advances in high-throughput sequencing and mass spectrometry have revealed that in eukaryotes up to 20% of total expressed protein-coding transcripts encoded RBPs (Gerstberger et al., 2014), underscoring that RNA metabolism is not only and essential cellular process but also one that demands the highest protein copy number. Furthermore, RBPs are commonly subjected to post-translational modifications allowing them to integrate signals and to couple the expression of genes to the cellular demands. Interestingly, RBPs are highly enriched in intrinsically disorder domains or low-complexity sequences that enables them to constitute dynamic aggregates like P-bodies, stress-granules or transport granules (Gerstberger et al., 2014).

While some RBPs bind structural elements of the mRNA such as the m^7G cap (cap-binding proteins, CBPs) or the poly(A) tail (poly(A)-binding proteins, PABPs) and some are left behind by the splicing machinery (exon-junction complex, EJC), there are some others that bind with high specificity to regulatory sequences commonly located in the UTRs. The latter category constitutes a highly interesting subgroup of RBPs that endow eukaryotic cells with the potential to deploy particular regulatory features to every single mRNA.

5. Translational control by cytoplasmic polyadenylation

As we have seen above, the poly(A) tail of the mRNA is a dynamic structure that controls many aspects of mRNA metabolism like transcript stability, translation and transport. Thus, modulating the poly(A) tail length of mature mRNAs constitutes a fast and reversible regulatory mechanisms than enables the cell to quickly respond to environmental stimuli by simultaneously degrading, inhibiting or activating the translation of different subsets of transcripts in a temporal and spatial regulated manner (Weill et al., 2012).

This regulation is accomplished by the coordinate action of cytosolic deadenylases, microRNA-RBPs (miRNPs) and cytoplasmic polyadenylation complexes. All these RNP-complexes recognize cis-regulatory elements either by direct protein interaction or through small RNA molecules (Weill et al., 2012). Most commonly, the target sequences are located in the 3' UTR of the mRNAs, the only region of the transcript that is not cleared by the progression of the ribosome. Given the pseudo-circularized conformation that mRNAs acquire, the RBPs bound to the 3' UTR are in close proximity to both the poly(A) tail and the cap-structure, the two main determinants of mRNA stability and translation.

5.1 The CPEB-family of proteins

One interesting family of RBPs is the Cytoplasmic Polyadenylation Element Binding Protein (CPEB)-family, which regulate mRNA translation and stability through the modulation of the poly(A) tail length of target mRNAs (Ivshina et al., 2014) (Fernandez-Miranda and Mendez, 2012).

In mammals, the CPEB-family is comprised of four paralogs: CPEB1-4. Because CPEB2-4 contain higher sequence identity compared to CPEB1, they are usually clustered into a separated subfamily (Fernandez-Miranda and Mendez, 2012) (Ivshina et al., 2014) **(Figure 5)**. Comparison between species reveals that the CPEBs are better conserved across species than across paralogs (Wang and Cooper, 2010) suggesting strong evolutionary selective pressure to maintain their different identities. However, some species contain different number of CPEBs, for instance, in the arthropod *Drosophila melanogaster* there are two CPEBs called Orb1 and Orb2, whereas in the mollusc *Aplysia californica* there is just one, aCPEB (Fernandez-Miranda and Mendez, 2012) **(Figure 5)**.

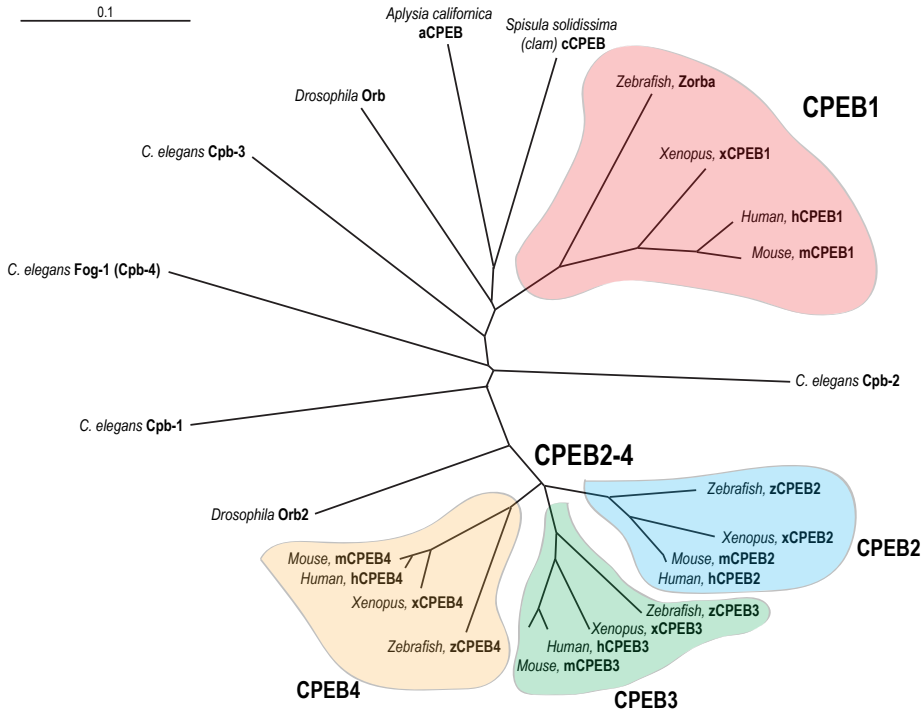

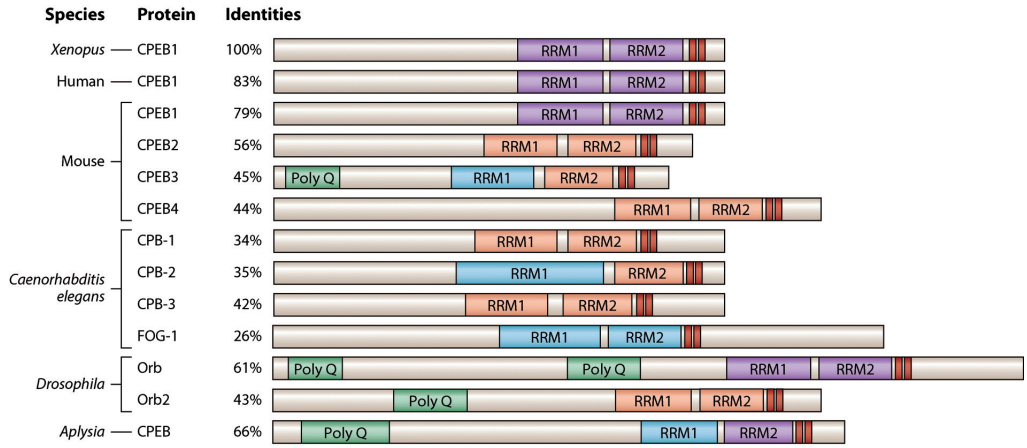

Figure 5. Phylogenetic analysis of the CPEBs. (Upper panel) Unrooted phylogenetic tree of the main orthologs and paralogs in the CPEB-family. In red, CPEB1 orthologs; more distant, and in blue, green and yellow, the orthologs of CPEB2, CPEB3 and CPEB4, respectively. (Lower pannel) Structural comparison of the CPEBs from various species. The colour of the RRMs (RNA recognition motives) reflects their differential similarities. Poly Q refers to polyglutamine stretches and the double vertical red bars depict the ZZ domains. Modified from Fernández-Miranda and Méndez, 2012; and from Ivshina et al., 2014.

It is now well established that, although with different affinities, all the CPEBs are able to bind a specific type of AU-rich sequence, called cytoplasmic polyadenylation element (CPE) that resides in the 3' UTR of some mRNAs, indicating that their target population of mRNAs may overlap (Igea and Mendez, 2010) (Novoa et al., 2010; Ortiz-Zapater et al., 2012). The first CPE motives identified consisted on UUUUAAU or UUUUAU sequences, although several non-consensus variants have been subsequently discovered. Alternatively, and based on *in vitro* selex experiments, it was proposed that CPEB3-4 may recognize a U-rich loop motif (Huang et al., 2006); however, it remains to be tested whether this interaction occurs in any biological context. Genome-wide studies have suggested that up to 20% of the genome is under the control of the CPEBs (Belloc and Mendez,

2008; Novoa et al., 2010; Pavlopoulos et al., 2011) indicating that CPEB-mediated translational control might be a widespread mechanism to fin-tune cellular protein production in metazoans.

Structurally, the CPEBs share common features. They all contain an unstructured N-terminal regulatory domain (NTD) and a RNA-binding C-terminal domain (CTD) **(Figure 5 lower panel)**. While the former is highly variable and is subject to various post-transcriptional modifications depending on the CPEB (Mendez et al., 2000a; Mendez et al., 2000b; Drisaldi et al., 2015; Theis et al., 2003), the latter is very much conserved, suggesting that while all the CPEBs can bind the same targets, they may integrate different signals and affect the mRNA targets in various ways, generating a complex regulatory network that couples the expression of the CPE-containing mRNAs to several signalling pathways.

The RNA-binding properties of the CTD are conferred by the presence of two RNA-recognition motives (RRMs) and a ZZ-domain, in which the latter adopts a cross-braced zinc coordination topology (Merkel et al., 2013). The crystal structure of the domain was recently solved and revealed that target specificity is mostly given by the first RRM. Initially, it was thought that the ZZ domain mediated the recruitment of sumoylated proteins (Merkel et al., 2013), however, and unexpectedly, the structure of the whole CTD revealed that the ZZ domain is involved in the RNA binding activity, although it does not confer specificity (Huang et al., 2006) (Hake et al., 1998).

The sequence similarity degree of the NTD between the different CPEBs is quite low, ranging from 40% among the CPEB2-4 subfamily to 10% when compared to CPEB1. Hence, every CPEB-NTD is modified by different enzymes. CPEB1 is known to be phosphorylated by Aurora A, CDK1 and PLK1, and it undergoes rapid degradation mediated by a PEST-box domain (Mendez et al., 2000a) (Mendez et al., 2000b). Phosphorylation, although by different kinases, also seems to regulate

CPEB4 function: the hyperphosphorylation of its NTD regulates its activity by modulating its aggregation status (data not published). Alternatively, SUMOylation, monoubiquitination and polyQ-sequence-dependent-aggregation seem to be the regulatory modifications that control CPEB3 activity, at least in neurons (Drisaldi et al., 2015) (Theis et al., 2003); on the other hand, the posttranslational modifications that regulate the activity of CPEB2 remain to be elucidated.

Several mechanisms have been shown to control the expression levels of the CPEBs. In the case of CPEB1 and CPEB4, they have been described to autoregulate their own expression through binding to the CPE-elements harboured in their own 3' UTRs (Igea and Mendez, 2010) (Hu et al., 2014). In the case of CPEB4, this has been shown to generate both positive and negative regulatory feedback loops that confer ultra-sensitivity properties to CPEB4 expression. Cpeb1 gene undergoes epigenetic silencing during gastric cancer progression by heavy methylation of its promoter. A recent report on circadian transcriptomics in mouse liver revealed the rhythmic expression of Cpeb2 and Cpeb4 mRNAs during the day (Kojima et al., 2012). This study showed that the circadian expression of the CPEBs in liver correlates with the differential polyadenylation of various transcripts at different times of the day, suggesting a strong temporal regulation of the CPEBs' function by the molecular clock (Kojima et al., 2012).

Regarding the regulatory activities exerted by the CPEBs on their target mRNAs, they have been mainly studied during *Xenopus laevis* oocyte maturation. However, in recent years, data unveiling their functions and mechanisms of action in different biological contexts has started to emerge.

5.2 The activatory and repressory functions of the CPEBs

CPEB1 has been shown to exert both activatory and repressory activities on the translation of target mRNAs depending on its phosphorylation status (Fernandez-Miranda and Mendez, 2012). When unphosphorylated, CPEB1 represses the translation of the mRNAs by a mechanism that is still controversial. There are three alternative and mutually exclusive models proposed for CPEB1-repressing function **(Figure 6, left)**: (1) CPEB1 inhibits translation by recruiting the deadenylase PARN to the mRNA, which outcompetes the cytosolic poly(A)-polymerase (Gld2) and therefore shortens the poly(A) tail and precludes the circularization of the transcript (Barnard et al., 2004); (2) CPEB1 inhibits ribosomal recruitment to the transcript by recruiting Masking, an eIF4E binding protein that hinders the formation of the eIF4F complex (Stebbins-Boaz et al., 1999); (3) CPEB1 recruits another eIF4E binding protein, eIF4E-T, with the same outcome as in model (2) (Minshall et al., 2007).

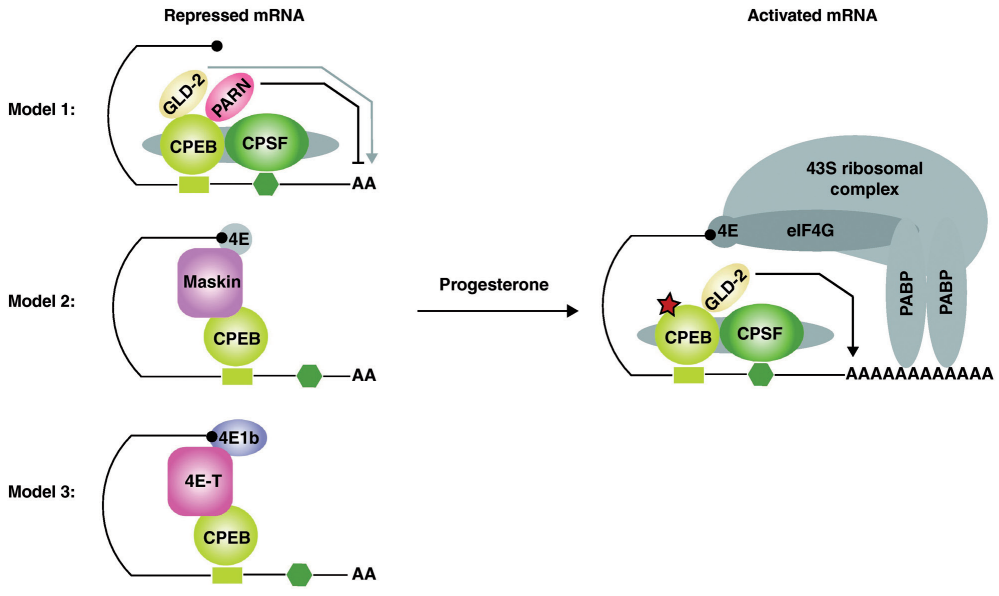

Figure 6. Regulatory functions of CPEB1. The CPE-element and the hexanucleotide are

represented as a rectangle and an hexagon in the 3' UTR on the mRNAs, respectively. Three models have been proposed for CPEB1-mediated mRNA repression (left). Progesterone treatment leads to the phosphorylation of CPEB1 (depicted as a red star), which triggers the recruitment of the polyadenylation complex (right). The increase in length of the poly(A) tail allows the binding of the PABP and the formation of the "close loop".

On the other hand, the CPEB1 activatory mechanism seems to be better established: when CPEB1 gets phosphorylated by Aurora A, the repression complex gets remodeled by an change in the affinity of CPEB1 towards CPSF (Mendez et al., 2000b), which ejects PARN from the complex and allows Gld2 to extend the length of the poly(A) tail (Kim and Richter, 2006) **(Figure 6, right)**.

An important element that determines the activity of CPEB1 is the arrangement of the CPE-elements within the 3' UTR (Pique et al., 2008). Two CPEs separated by an optimal distance of 12 nucleotides seem to be necessary for CPEB1-mediated repression, most probably because they favor the formation of a dimer (Pique et al., 2008). On the contrary, translational activation only requires the presence of a single CPE, within a range of 100 nucleotides from the poly(A) signal, being 25 nucleotides the optimal distance predicted. Quite recently it has been proposed that transient dimerization of CPEB1 might also regulate its function (Lin et al., 2012).

Beyond meiosis, the mechanism of action of CPEB1 is quite conserved, at least in neurons (Udagawa et al., 2012), although with important variations. CPEB1 represses translation by recruiting another eIF4 binding-protein called Masking, and, when phosphorylated by Aurora A or CamKII kinases, it stimulates translation through the recruitment of the cytoplasmic poly(A) polymerases Gld2 or Gld4 (Atkins et al., 2004).

CPEB2 has been proposed to repress transcript translation by inhibiting the

elongation phase through the interaction with eEF2 (Chen and Huang, 2012). Although the molecular details are not clear, CPEB2 has also been described to activate the translation of some target mRNAs (Hagele et al., 2009).

Most of the translational activity of CPEB3 has been studied in the context of synapse activity. There, it has been found that CPEB3 can either drive mRNA degradation through actively promoting deadenylation or activate translation when is subjected to monoubiquitination by Neurilized1 (Pavlopoulos et al., 2011), cleaved by Calpain2 or when it forms aggregates with prion-like properties (Drisaldi et al., 2015) (Fioriti et al., 2015; Stephan et al., 2015). More recently, it has been proposed that CPEB3 might be regulated by PKA- and CamKII-mediated phosphorylation in the NTD (Kaczmarczyk et al., 2016).

Finally, CPEB4 has been proposed to act as a repressor of translation during terminal erythroid differentiation through its interaction with eIF3 (Hu et al., 2014). However, the rest of studies that analyzed CPEB4 mechanism of action revealed and activatory role during oocyte maturation, somatic cell cycle and tumor progression (Igea and Mendez, 2010) (Novoa et al., 2010) (Ortiz-Zapater et al., 2012), mediated by the recruitment of the canonical cytoplasmic polyadenylation machinery.

5.3 The CPEBs in somatic tissues – CPEB4

Given that CPEB-mediated regulation is instrumental for meiotic progression and that CPE-regulated mRNAs are highly abundant in all biological processes, the study of the CPEBs in non-germinal tissues has dramatically increased in recent years revealing important function for each CPEB beyond meiosis.

Several reports have unveiled that CPEB1-mediated translation regulates mitotic

cell cycle (Novoa et al., 2010), cellular senescence (Burns and Richter, 2008), tumour development (Nagaoka et al., 2015) (Burns and Richter, 2008), inflammation (Ivshina et al., 2015) and synaptic plasticity (Udagawa et al., 2012). Moreover, CPEB1 seems to regulate mammalian organism homeostasis by repressing the translation of PTEN and STAT3 mRNAs in liver, thereby modulating the hepatic insulin-signalling pathway (Alexandrov et al., 2012). Therefore, CPEB1 seems to be important for both pathogenic and non-pathogenic genetic regulation.

Although the somatic functions of CPEB2 remain to be discovered, CPEB3 plays an essential role in the regulation of hippocampal memory formation (Fioriti et al., 2015), synaptic plasticity (Drisaldi et al., 2015) and thermosensation (Fong et al., 2016).

CPEB4-mediated regulation is important for the mitotic progression of tumoral cells (Novoa et al., 2010), embryonic erithroid differentiation (Hu et al., 2014), cell survival (Chang and Huang, 2014) (Kan et al., 2010), tumour malignancy (Ortiz-Zapater et al., 2012) and pathological angiogenesis (Calderone et al., 2016) (Garcia-Pras et al., 2016). In fact, CPEB4 KO mice partially suffer from neonatal lethality (Hu et al., 2014), although a similiar model does not (Tsai et al., 2013), underscoring the importance of CPEB4-mediated regulation. Interestingly, CPEB4 protein localizes at the endoplasmic reticulum of neurons, yet the significance of this localization remains unknown (Kan et al., 2010). CPEB4 seems to play a protumoral role in cancer progression (Ortiz-Zapater et al., 2012) (Boustani et al., 2016) (Sun et al., 2015) (Chen et al., 2015) (Zhong et al., 2015) (Hu et al., 2015) although some reports point in the opposite direction (Peng et al., 2014).

In spite of the growing literature regarding the roles of CPEB4, it remains to be shown whether CPEB4-mediated regulation plays any role in adult tissue homeostasis.

6. Cellular metabolism and translation

6.1 Bidirectional link between the UPR and cellular metabolism

Given that the ER is the major anabolic organelle in a cell, it plays a central role in cellular metabolism. It regulates protein synthesis, the most energetically expensive cellular process (Proud, 2002). It also constitutes a metabolic hub where many of the enzymes involved in glucose and lipid metabolism are located (Fu et al., 2012). Consequently, it is not surprising that the ER-surveillance system and the cellular metabolism are closely interconnected to couple the cellular metabolic needs to the ER folding capacity, and vice versa. Accordingly, researchers have found strong functional connections between the ER the cellular bioenergetic powerhouse, the mitochondria (Malhotra and Kaufman, 2011).

The ER and the mitochondria are functionally and physically interconnected, with 20% of the mitochondria surface in close contact with the ER membrane through specialize contact sites called mitochondrial associated membranes (MAMs). These interactions have been shown to be fundamental for Ca^{2+} signaling, lipid transport, energy metabolism and cell death (Malhotra and Kaufman, 2011). Importantly, upon ER stress the UPR increases the production of ROS and the liberation of Ca^{2+} from the ER reservoir into de cytoplasm. This Ca^{2+} is uptaken by the MAMs and modulates the activity of mitochondrial dehydrogenases and nitric oxide synthases (Malhotra and Kaufman, 2011). Through these mechanisms, the UPR pathway couples the ER folding status with the mitochondrial energy production activity. Thus, prolonged UPR activity hinders mitochondrial function. Further evidences support that in conditions of irreversible ER stress the UPR triggers mitochondrial-dependent apoptosis through the action of CHOP and the release of Ca^{2+} (Wang and Kaufman, 2016). Conversely, and although the molecular details

are not clear, there are evidences that mitochondrial dysfunction can lead to ER stress. Therefore these two organelles seem to control and regulate one another in order to maintain protein folding, energy homeostasis and Ca^{2+} equilibrium inside the cell.

6.2 The UPR and the etiology of metabolic disease

Taking in consideration the strong conection between the ER and cellular metabolism, it is no surprise that the UPR is involved in the pathogeneses of several metabolic diseases such as diabetes type 2 and non-alcoholic fatty liver disease (NAFLD) (Fu et al., 2012) (Malhi and Kaufman, 2011) (Gentile et al., 2011) (Rutkowski et al., 2008) (Oakes and Papa, 2015). NAFLD is a condition in which the hepatic-accumulated fat accounts for more than 5% of the total liver weight, in the absence of chronic alcohol consumption or any other liver disease (R. and AJ., 2013). NAFLD has become the most common cause of liver disease worldwide with a prevalence of around 30% in the western world, and up to 75% in obese populations (R. and AJ., 2013) (Feldstein, 2010).

In mammals, the liver acts as a metabolic hub that process and distributes all nutrients to the different organs. Under homeostatic conditions, the main sources of fat that arrive at the liver are plasma non-sterified fatty acids (FFA) released from the white adipose tissue or absorbed by the intestine from dietary sources **(Figure 7)**. Moreover, the liver actively synthesizes lipids by a process known as *de novo* lipogenesis. Once inside the liver, FFAs can enter the mitochondrial β-oxidation pathway for energy production or can be esterified into triacylglicerides (TGA). TGA are then stored inside the hepatocytes as lipid droplets or secreted into the bloodstream as very low density lipoproteins (VLDL). Therefore, excessive fat accumulation inside the liver can occur as result of increased FFA uptake, increased

lipogenesis, decreased β-oxidation or decreased lipoprotein secretion **(Figure 7)** (Postic and Girard, 2008) (Browning and Horton, 2004) (Anderson and Borlak, 2008).

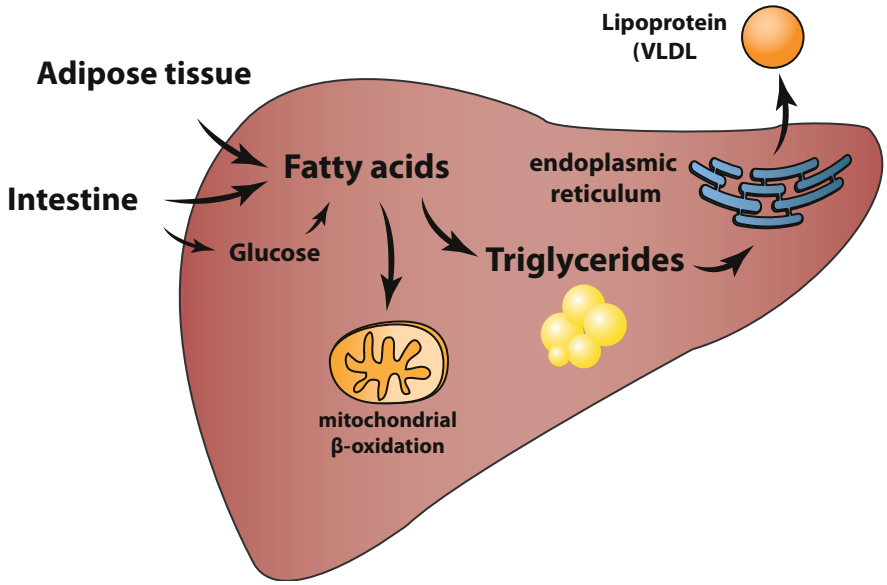

Figure 7. Hepatic lipid metabolism. Hepatic free fatty-acids (FFA) come from dietary sources, adipose tissue release or de novo lipogenesis. FFA can be then used as a source of energy through mitochondrial β-oxidation. Alternatively, they can be esterified into TGA molecules that are stored in the form of cytosolic lipid droplets or secreted as very low-density lipoproteins (VLDLs). Hepatic steatosis occurs when the influx of FFA increases (uptake or synthesis) or when the output pathways capacity decreases (β-oxidation or lipoprotein secretion).

In some individuals, hepatosteatosis progresses to steatohepatitis, in which the accumulation of fat is accompanied by liver fibrosis and inflammation (Angulo, 2002). NAFLD constitutes a major risk factor for the development of cirrhosis, liver failure, cardiovascular disease and hepatocellular carcinoma (Angulo, 2002).

However, the molecular mechanisms underlying the disease are poorly understood (Feldstein, 2010). For instance, there is no current explanation for the variable susceptibility to the disease among different human populations, the increasing prevalence in individuals with low BMI or why the disease progresses at different speeds depending on the individual.

In recent decades the UPR has been proposed to play a central role in the progression of NAFLD (Ozcan et al., 2004). On the one hand, hyperlipidemia causes hepatic ER stress through a variety of mechanism: an imbalance in the cellular lipid pool that leads to alterations of membrane fluidity, increased in protein palmitoylation and generation of ROS, all of which are triggers of the UPR (Wang and Kaufman, 2014) (Volmer and Ron, 2015). Conversely, several genetic mouse models have demonstrated that the UPR pathway is key to limit hepatic lipid accumulation. Genetic ablation of any of the UPR branches leads to the development of hepatosteatosis in mice by decreasing the secretion of liver lipoproteins (by inducing the degradation of ApoB100), decreasing mitochondrial β-oxidation of fatty acids and/or increasing hepatic lipogenesis (Lee et al., 2008) (Wang, 2012) (So, 2012).

Indeed, chemical chaperons are being tested for the treatment of NAFLD (Maerkeen, 2010) (Ozcan et al., 2006). These compounds prevent ER stress by stabilizing protein-folding intermediates. In a seminal work, researches proved that treating obese mice with 4-phenyl butyric acid (PBA) or taurine-conjugated ursodeoxycholic acid (TUDCA) alleviated ER stress and prevented the development of hepatosteatosis and insulin resistance (Ozcan et al., 2006). Indeed, TUDCA treatment has been shown to ameliorate hepatic and muscular ER stress and to increase insulin sensitivity in obese men and women (Maerkeen, 2010). This and other studies position the UPR/ER stress pathway as an attractive therapeutic target for drugs against metabolic diseases.

7. The circadian clock

Over the past few years a growing body of evidence has unveiled that almost every molecular process that occurs in living organisms is under the control of an endogenous time-keeping mechanism known as the circadian clock (Wijnen and Young, 2006) (Asher and Schibler, 2011). Molecularly, this system consists on a network of transcription factors interconnected by positive and negative feedback loops that generate waves of gene expression with a periodicity of approximately 24 hours **(Figure 8)**. This system can run autonomously, in the absence of external stimuli, but can also be entrained by environmental cues. In mammals, the circadian clock is organized in a central pacemaker formed by the neurons of the suprachiasmatic nucleus (SCN) that maintain proper phase alignment of peripheral tissue clocks present in all cells (Bass and Takahashi, 2010).

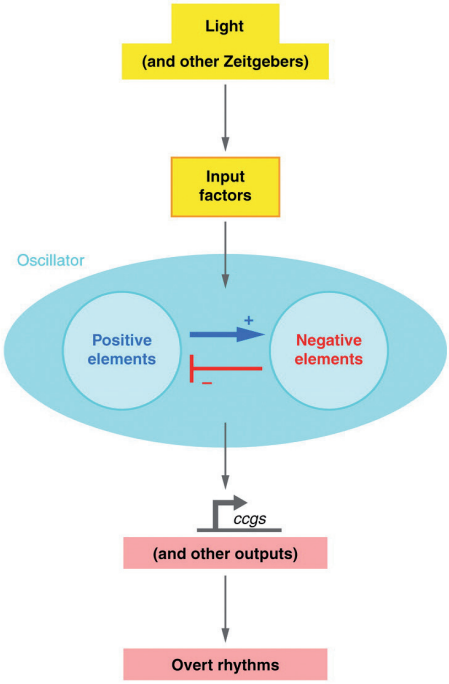

Figure 8. The mammalian circadian clock architecture. The core of the molecular clock , which is located in almost every cell, comprises positive and negative feedback circuits that generate autonomous oscillations in gene expression with a 24 h periodicity. Clock rhythmicity can be entrained by environmental and organic cues (input factors) to maintain cellular synchronicity. Circadian regulation of the clock-controlled genes (ccgs) allows the temporal modulation of the physiology, behaviour and metabolism of mammalian organisms. Modified from Wijnen and Young, 2006.

7.1 Post-transcriptional gene regulation by the clock

Importantly, the molecular clock modulates organism physiology and behavior by controlling the expression of hundreds of genes (Eckel-Mahan et al., 2012) **(Figure 8)**. It is not surprising that most of the studies on the genetic regulation exerted by the molecular clock focused at the transcriptional level; however, recent findings have broadened this view by revealing extensive clock-mediated post-transcriptional circadian gene regulation. Therefore it is now well established that the processes of splicing, alternative polyadenylation, translation and cytoplasmic polyadenylation are regulated by the circdaian clock (Gachon and Bonnefont, 2010) (Douris et al., 2011) (Janich et al., 2015) (Kojima et al., 2015) (Garbarino-Pico and Green, 2007) Accordingly, in mouse liver 50% of the rhythmic proteins are translated from non-rhythmic mRNAs (Atger et al., 2015) and circadian rhythms exist in anucleated cells (JS. and Reddy, 2011) underscoring the importance of post-transcriptional mechanism in the cell rhythmic physiology.

7.2 Circadian regulation of mammalian metabolism

As expected, cellular metabolism seems to be under the strict control of the circadian clock (Bass and Takahashi, 2010) (Asher and Schibler, 2011) (Eckel-Mahan et al., 2012). In the metabolic organs of mammals, the timing-system plays a central role in the adaptation and anticipation of the feeding-fasting cycles that constitute the daily behavior. In accordance, genetic disruption of the clock in mice leads to a plethora of metabolic alterations such as obesity, diabetes and NAFLD (Birky and Bray, 2014) (Bray and Young, 2011) (Wijnen and Young, 2006) (Reinke and Asher, 2016). Interestingly, clock disruption in mice leads to a hepatic steatosis that can be reverted by the treatment with the chaperone TUDCA, indicating a strong connection between the circadian clock, ER stress and metabolic disease (Cretenet

et al., 2010). In accordance, intervention strategies targeted at circadian oscillator components are being tested to prevent or treat NAFLD (Cho et al., 2012) (Reinke and Asher, 2016) (Solt et al, 2012; Reinke et al, 2016).

At a subcellular level, it is well established that the function of the major metabolic organelles are under circadian control. The circadian peacemaker generates daily oscillations of mitochondrial oxidative activity through rhythmic regulation of NAD+ levels (Peek et al., 2013). Similarly, the UPR signaling pathway shows daily oscillations in activity (Cretenet et al., 2010).

Although our understanding of this temporal aspect of gene regulation has tremendously expanded, much remains to be explored about the post-transcriptional regulatory circuits that coordinate the circadian clock with the cellular metabolism.

Objectives

The goal of this study is to gain a deeper understanding of the post-translational regulatory mechanism mediated by CPEB4 and their contribution to mammalian physiology, with special emphasis in cellular metabolism and its circadian control.

The specific goals that we have pursued are:

1. Generation and phenotypic characterization of genetically engineered loss of function mouse models for CPEB4.

2. Study of the pathophysiological conditions caused by the genetic ablation of CPEB4 and the underlying etiology.

3. Analysis of the molecular mechanisms that drive the biological alterations caused by CPEB4 depletion.

4. Identification of CPEB4 mRNA targets and in depth study of the regulatory mechanism exerted by CPEB4.

5. Analysis of the subcellular localization of CPEB4 in mammalian cells.

6. Characterization of the regulatory mechanisms that control CPEB4 expression.

7. Exploration of the regulation exerted by the circadian clock on the biological functions of CPEB4.

8. Investigation of the potential impact of these findings in the understanding and treatment of human disease.

Methods

Generation of constitutive and liver-specific Cpeb4 knockout mice

To generate a CPEB4 conditional knockout mouse ($CPEB4^{lox/lox}$), mouse ES cells carrying a βgeo-cassette [β-galactosidase gene fused to neomycin resistance gene] in *Cpeb4* intron 1 and loxP sites flanking the exon 2 (clone EPD0060_4_E10; Sanger Institute) were microinjected into developing blastocysts. The resulting positive chimeric mice ($CPEB4^{+/loxfrt}$) were crossed with C57BL6/J mice. Subsequently, the βgeo-cassette was removed by mating with mice expressing the FlpO recombinase (Tg.pCAG-Flp), thereby generating conditional knockout animals ($CPEB4^{lox/lox}$). To obtain an ubiquitous and constitutive depletion of CPEB4, $CPEB4^{lox/lox}$ mice were crossed with animals expressing the DNA recombinase Cre under the control of a human cytomegalovirus minimal promoter (B6.C-Tg(CMV-cre)1Cgn/J). The excision of exon 2 of the *Cpeb4* gene leads to a frame shift in the mRNA generating several new premature stop codons, resulting in mice that are deficient in CPEB4 protein ($CPEB4^{KO}$). The offspring was maintained in a C57BL/6J-129S mixed background. Liver-specific CPEB4 knockout mice ($CPEB4^{LKO}$) were obtained by crossing $CPEB4^{lox/lox}$ mice with albumin-Cre transgenic animals. The offspring was backcrossed for five generations onto the C57BL/6J background. Routine genotyping was performed by PCR.

Animal studies

Animals were maintained under a standard 12-h light-dark cycle, at 21°C, with free access to food and water. At 6 weeks of age, male mice were randomly assigned to either an HFD (60% fat, 20% protein, and 20% carbohydrates; D12492, Research Diets) or a control regular chow diet (7.42% fat, 17.49% protein, and 75.09% carbohydrate; RM1, SDS). Only male mice between 2 and 5 months of age were used, unless otherwise stated. For circadian experiments, mice were caged in a

reverse light-cycle room. All experimental protocols were approved by the Animal Ethics Committee at the University of Barcelona.

Intraperitoneal glucose tolerance test and pyruvate tolerance test

The glucose tolerance test (GTT) was performed on mice after an overnight fast. Blood glucose was measured a time 0 with a Bayer glucometer, followed by i.p. injection of glucose (2 g/kg body weight). Blood glucose was measured at 15, 30, 60 and 120 min after injection. Plasma insulin levels were measured with an Ultrasensitive Mouse Insulin Elisa Kit (Cristalchem) at 0, 30, and 60 min after injection. For the pyruvate tolerance test (PTT), overnight-fasted mice were injected with pyruvate (2 g/kg body weight) and glucose levels were measured at 30, 60 and 90 min after injection. For the glucagon tolerance test (GTT), overnight-fasted mice were injected with glucagon (15 μg/kg body weight) and glucose levels were measured at 15, 30, 60 and 90 min after injection.

Hepatic VLDL production assay

Mice were fasted for 5 h and then intravenously injected with tyloxapol (500 mg/kg body weight; Sigma). Aliquots of tail vein blood were taken at 60 and 120 min after injection for plasma triglyceride (TGA) determination using the Serum Triglyceride Determination Kit (Sigma).

Indirect respirometry analysis

The Oxymax-CLAMs indirect calorimetry system was used to determine metabolic phenotypes. Mice were left to acclimate in individual metabolic cages

for 2 consecutive days prior to data collection. Metabolic parameters (oxygen consumption, carbon dioxide production and locomotor activity) were then measured every 20 min for 3 consecutive days.

Primary hepatocyte isolation

Collagenase perfusion (0.5 U/mL) via the inferior cava vein was used to isolate hepatocytes from fed 12-week-old male mice. Cells were suspended in Dulbecco's Modified Eagle's Medium (DMEM) supplemented with 10 mM glucose, 10% fetal bovine serum (FBS), 100 nM insulin, and 100 nM dexamethasone and then seeded onto plates treated with 0.01% (w/v) collagen solution (Sigma). After 3 h, cells were washed with PBS, and the media were replaced with fresh serum-free DMEM without glucose for 16 h.

Mouse embryonic fibroblast (MEF) isolation

MEFs were extracted from 14.5-day-old embryos, following standard procedures (Hogan et *al.* 1994). Briefly, pregnant female mice were euthanized at day 14.5 of gestation, and embryos were extracted. After removal of heads and livers, embryos were minced, incubated in trypsin for 5 min, disaggregated, and resuspended in culture medium. MEFs were cultured in high glucose-DMEM supplemented with 10% FBS, 2 mM L-glutamine and 1% penicillin/streptomycin at 37°C in a 5% CO_2 incubator. Only primary MEFs up to passage 5 were used in all the experiments except for the circadian synchronization analysis in which 3T3-immortalized MEFs were used.

Mouse embryonic fibroblast clock synchronization

WT and CPEB4^{KO} immortalized MEFs were starved in 0.5% FBS-containing DMEM for 2 consecutive days. Next, their clocks were synchronized with a 100 nM dexamethasone shock and protein and RNA samples were collected every 6 h for 2 days.

Fatty acid oxidation, uptake and incorporation

Palmitate oxidation to CO_2 was measured in primary hepatocytes grown in 6-well plates. On the day of the assay, cells were washed in Krebs-Ringer bicarbonate HEPES buffer (KRBH buffer: 135 mM NaCl, 3.6 mM KCl, 0.5 mM NaH_2PO_4, 0.5 mM $MgSO_4$, 1.5 mM $CaCl_2$, 2 mM $NaHCO_3$, and 10 mM HEPES pH 7.4) that contained 0.1% BSA. Cells were preincubated at 37ºC for 30 min in KRBH 1% BSA and then washed again in KRBH 0.1% BSA. Then, they were incubated for 3 h at 37ºC with fresh KRBH containing 2.5 mM glucose and 0.8 mM carnitine plus 0.25 mM palmitate and 1 _Ci/ml [1-^{14}C]palmitate bound to 1% BSA. Oxidation measurements were performed by trapping the radioactive CO_2 in a parafilm-sealed system. The reaction was stopped by the addition of 40% perchloric acid through a syringe that pierced the parafilm.

For palmitate incorporation, cells were incubated for 16 h at 37ºC in serum-free medium containing 0.25 mM palmitate and 1 _Ci/ml [1-^{14}C]palmitate bound to 1% BSA. On the day of the assay, cells were washed in PBS, and lipids were extracted by chloroform-methanol extraction. Total lipids were dissolved in 30 µl of chloroform and separated by thin-layer chromatography to measure the incorporation of labeled fatty acid into phospholipids (PL), diacylglycerol (DAG), triglycerides (TGA) and non-esterified labelled palmitate (NEPalm).

Glucose production assay

Primary hepatocytes were plated at 1.740.000 cells/60-mm dish, and after 3 h the medium was replaced by DMEM supplemented with 2 mM glutamine without glucose, FBS or sodium pyruvate. The day after, cells were treated for 4 h with the indicated compounds and cell medium was collected for glucose quantification.

Cellular oxygen consumption

Cellular oxygen consumption rate (OCR) was measured using the Seahorse XF24 analyzer and following the manufacturer's instructions (Seahorse Biosciences). MEFs were plated at a concentration of 50.000 cells/well, and OCR measurements were made after the sequential addition of 1 μg/ml oligomycin, 1 μM carbonyl cyanide p-trifluoromethoxyphenylhydrazone (FCCP), and 1 μM rotenone plus 1 μM antimycin A (Rot+AA). Oligomycin treatment inhibits complex V, thus distinguishing the oxygen consumption devoted to ATP synthesis from the oxygen consumption required to overcome the natural proton leak across the inner mitochondrial membrane. Applying FCCP uncouples the electron chain, unveiling the maximal respiratory capacity. Final treatment with rotenone (complex I inhibitor) plus antimycin A (complex III inhibitor) reveals the non-mitochondrial respiration. The OCRs measured were normalized to total protein content, and routine and maximal respiration was calculated by subtracting the non-mitochondrial respiration to the basal or FCCP-mediated respiration, respectively.

Respiratory chain function analysis from isolated mitochondria

The respiration of isolated liver mitochondria was measured at 37ºC by high-resolution respirometry with an Oxygraph-2k (Oroboros Instruments, Innsbruck,

Austria). Mitochondria were obtained from mouse liver by differential centrifugation and then resuspended in buffer II (0.5 M sucrose, 50 mM KCl, 5 mM EDTA, 1 mM sodium pyrophosphate, 5 mM $MgCl_2$ pH7.4, and protease inhibitors). 500 µl of mitochondria suspension was brought to a final volume of 2.1 ml with respiration medium (0.5 mM EGTA, 3 mM $MgCl_2.6H_2O$, 20 mM taurine, 10 mM KH_2P0_4, 20 mM HEPES,1 g/l BSA, 60 mM K-lactobionate, 110 mM sucrose, pH 7.1) and added to the oxygraph chamber. All respiration measurements were done in triplicate. Resting respiration (state 2, absence of adenylates) was assessed by the addition of 10 mM glutamate and 2 mM malate as the complex I substrate supply, and then state 3 respiration by the addition of 2.5 mM ADP. The integrity of the outer mitochondrial membrane was established by the addition of 10 µM cytochrome c. No stimulation of respiration was observed. The addition of 10 mM succinate provided state 3 respiration with parallel electron input to complexes I and II. We examined ADP control of coupled respiration and uncoupling control through the addition of the protonophore carbonylcyanide-4-(trifluoromethoxy)-phenylhydrazone (FCCP). The addition of 0.5 µM rotenone resulted in inhibition of complex I, thereby allowing examination of O_2 flux with complex II substrate alone, while 2.5 µM antimycin A was added to inhibit complex III in order to observe non-mitochondrial respiration. The concentrations of substrates and inhibitors used were based on prior experiments conducted to optimize the titration protocols.

Cell culture and analysis

HepG2 and HEK-293 cells were cultured in high glucose DMEM, supplemented with 10% FBS, 2 mM L-glutamine and 1% penicillin/streptomycin at 37°C and 5% CO_2.

Treatment of mouse embryonic fibroblasts (MEFs) with tunicamycin (T7765, Sigma) and thapsigargin (T9033, Sigma) was done as described in (Rutkowski et *al.*, 2006). Cells were plated at a concentration of 360,000 cells/60-mm dish and allowed to rest overnight before the application of the stress. Apoptosis was measured with FITC Annexin V Apoptosis Detection Kit I (BD Pharmigen), following the manufacturer's instructions.

Tunicamycin injection and tissue analysis

Mice were injected intraperitoneally with TM at 1 mg/kg body weight. At the indicated times, mice were killed and livers were extracted. Various lobules were separated and snap-frozen in liquid nitrogen, formalin-fixed, or frozen in OCT. Frozen livers were pulverized in liquid nitrogen and stored at -80ºC. Protein extracts were obtained by resuspending frozen liver powder in RIPA buffer (50 mM Tris, 150 mM NaCl, 0.1% SDS, 0.5% deoxycholate, 1% NP-40, 1 mM EDTA, 1 mM DTT, 1 mM PMSF) containing protease inhibitors cocktail (11873580001, Roche) and phosphatase inhibitors cocktail 2 and 3 (P5726, Sigma). Samples were thoroughly vortexed and sonicated for 10 min at maximal intensity, then centrifuged at 16000 rpm for 10 min at 4ºC. The supernatant was then stored at -80ºC. RNA was extracted as described below, and lipids were obtained by chloroform-methanol extraction.

TUDCA treatment

Mice on a high-fat diet (HFD) for 12 weeks received intraperitoneal injections of 250 mg/kg TUDCA (Merck) twice a day during the last two weeks of HFD administration. Then, mice were killed and livers were collected as indicated above.

Histological analysis

Livers were fixed in 10% neutral buffered formalin and stained with H&E or Sirius Red. For Oil-red O staining, liver tissue was frozen in OCT, sectioned, and stained.

Immunoblotting

Protein extracts were quantified by DC Protein assay (Bio-Rad), and equal amounts of proteins were separated by SDS-polyacrylamide gel electrophoresis. After transfer of the proteins onto a nitrocellulose membrane (GE10600001, Sigma) for 1 h at 400 mA, membranes were blocked for 1 h in 5% milk, and specific proteins were labeled with the following antibodies: anti-CPEB4 (Abcam, Ab83009); anti-ATF4 (Santa Cruz, sc-200); anti-CHOP (Santa Cruz, sc-575); anti-phosphorylated eIF2α (Cell Signaling, 9721); anti-VDUP1 (anti-TXNIP) (Santa Cruz, sc-166234); anti-vimentin (Abcam, ab8978); anti-tubulin (Sigma, T9026); anti-BIP (BD Bioscience, 610978); anti-TIMM44 (BD Biosciences, 612582); anti-Calnexin (Santa Cruz, 11397); anti-GAPDH (Life Technologies, AM4300); and anti-Vinculin (Abcam, ab18058).

Immunofluorescence

Cells were fixed with 4% PFA for 10 min followed by permeabilization with 0.1% Triton X-100 for 5 min. Then, cells were blocked with 10% FBS in 0.03% Triton X-100 for 1 h. Primary antibodies were incubated overnight at 4ºC followed by 1 h incubation with the corresponding secondary antibody. Images were obtained on an inverted Leica TCS SP5 confocal microscopy.

RNA analysis

Total RNA was either extracted by TRIzol reagent (Invitrogen) or RNAspin Mini Kit (GE Healthcare), followed by Turbo DNA-free Kit (Ambion) treatment. One microgram of RNA was reverse-transcribed with oligodT and random primers using SuperScript III (ThermoFisher), following the manufacturer's recommendations. Quantitative real-time PCR was performed in a LightCycler 480 (Roche) using SYBRGreen I Master (Roche). The primer sequences are listed in Supplementary Table. All quantifications were normalized to endogenous control [TATA-binding protein (TBP) or 18s].

Lipid extraction

Lipids were extracted following the method of Salmon and Flatt. Liver powder was digested in potassium ethanol overnight, then centrifuged, and diluted in 50% ethanol. Samples were mixed with 1M magnesium, incubated on ice for 10 min, and centrifuged. Supernatant was used for TGA quantification.

DNA extraction and mtDNA quantification

Liver powder was digested with Proteinase K at 50ºC for 16 h. DNA was isolated by standard phenol-chloroform extraction and ethanol precipitation. mtDNA was quantified by qPCR using primers designed against mitochondrial DNA and a nuclear encoded mitochondrial gene (SHD).

RNA-immunoprecipitation-sequencing analysis

CPEB4^{KO} and wild-type primary hepatocytes were cultured in DMEM supplemented with 10% FBS, rinsed twice with 10 ml PBS, and incubated with FBS-free DMEM and 0.5 % formaldehyde for 5 min at room temperature under constant soft agitation to crosslink RNA-binding proteins to target RNAs. The crosslinking reaction was quenched by addition of glycine to a final concentration of 0.25 M for 5 min. Cells were washed twice with 10 ml PBS, lysated with scraper and RIPA buffer [25 mM Tris-Cl pH7.6, 1% Nonidet P-40, 1% sodium deoxycholate, 0.1% SDS, 100 mM EDTA, 150 mM NaCl, protease inhibitor cocktail, RNase inhibitors], and sonicated for 10 min at low intensity with Standard Bioruptor Diagenode. After centrifugation (10 min, max speed, 4ºC) supernatants were collected, precleared, and immunoprecipitated (4 h, 4ºC, on rotation) with 10 μg of anti-CPEB4 antibody (Abcam), or rabbit IgG (Sigma) bound to 50 _l of Dynabeads Protein A (Invitrogen). Beads were washed 4 times with cold RIPA buffer supplemented with Protease inhibitors, resuspended in 100 _l Proteinase-K buffer with 70 _g of Proteinase-K (Roche), and incubated 60 min at 65ºC. RNA was extracted by standard phenol-chloroform. Samples were processed at the IRB Functional Genomics Facility following standard procedures.

Subcellular fractionation

The endoplasmic reticulum was purified from whole livers of overnight-fasted mice using the Endoplasmic Reticulum Isolation Kit (ER0100-1KT, Sigma) and following the manufacturer's protocol. Then, proteins and RNA were extracted following the protocols described above.

Microscopy analysis

Stained sections were visualized with a Nicon Eclipse Ci-E microscope. Images from several regions of the tissue sections were then acquired by a Nikon DS-Fi2 camera. Digitalized images were analyzed by computerized imaging software Image J.

Plasmid constructions, cell transfections, and luciferase assays

The cDNA fragment encoding the 5' UTR of CPEB4 mRNA was inserted between HindIII and NcoI restriction sites in a pGL3-Promoter vector. The resulting PSV40-CPEB4-Luc plasmid contains the 5' UTR of CPEB4 fused to a luciferase reporter downstream of a constitutive SV40 promoter. 0.5 μg of pSV40-CPEB4-Luc construct were transiently contransfected with 0.5 μg of a Renilla reporter plasmid pRL-SV40 in HepG2 cells for 24 h using Lipofectamine 3000 (Thermo Fisher Scientific) following the manufacturer's instructions. Transfected cells were then incubated with 0.1 μM TG for 6 h. Luciferase activity was determined with the Dual-GLO Luciferase Assay System (Promega). RNA was extracted and quantified by RT-qPCR to normalize for transfection variability.

Statistics

Data are expressed as means±SEM. Dataset statistics were analyzed using the GraphPad Prism software. Comparisons between groups were carried out with the Student's t test and two-way ANOVA followed by the Bonferroni post-hoc test, and differences under $p<0.05$ were considered statistically significant (*$P<0.05$, **$P<0.01$, ***$P<0.001$).

Results

1. Generation of Cpeb4 ubiquitous knockout mice

To examine the somatic functions of CPEB4, we generated a global loss-of-function genetic mouse model (CPEB4^{KO}) by targeted deletion of exon 2 of the *Cpeb4* gene, as described in Methods. Since the excision of exon 2 of the *Cpeb4* gene leads to a frame shift that generates several new premature stop codons, these animals were depleted of CPEB4 protein in all the tissues tested, as demonstrated by immunobloting **(Figure 9a)**, and immunohistochemistry **(Firgure 9b)** and had reduced levels of *Cpeb4* (truncated) mRNA **(Figure 9c)**.

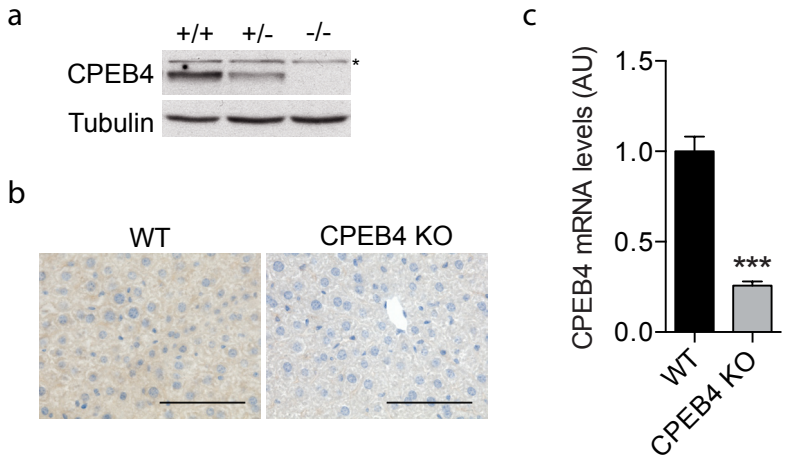

Figure 9. CPEB4 depletion by gene-targeting. **a**, Immunoblot displaying CPEB4 and α-tubulin protein levels in CPEB4$^{+/+}$, CPEB4$^{+/-}$ and CPEB4$^{-/-}$ liver extracts. **b**, Immunohistochemistry against CPEB4 in WT and CPEB4^{KO} liver sections. Scale bar, 100 μm. **c**, *Cpeb4* mRNA expression in WT and CPEB4^{KO} livers, normalized to TBP transcript levels.

CPEB4^{KO} mice were born in the expected Mendelian and male/female ratios, thereby ruling out an essential role of this protein during embryonic development. However, we observed that not all knockout mice reached the age of weaning because of a certain degree of neonatal lethality that varied depending on the

genetic background (30% in C57BL6/J, 129/sv mixed background and 94% in C57BL6/J pure background). A recent report has identified defective embryonic erytroid differentiation in CPEB4^{KO} livers as the probable cause of this early neonatal lethality (Hu et al., 2014).

2. CPEB4 prevents the development of fatty liver disease

Comprehensive histological analysis of animals deficient in CPEB4 revealed no overt phenotype at young ages and under unchallenged conditions. Furthermore, CPEB4^{KO} mice were viable, fertile and grossly normal compared with wild-type (WT) mice. Accordingly, CPEB4-deficient mice showed a body weight increase comparable to that observed in WT animals **(Figure 10a)**. However, when let to age for 80 weeks, CPEB4^{KO} old mice developed a hepatic steatotic phenotype with significantly increased liver weight **(Figure 10b)** and excessive accumulation of cytosolic lipid droplets (LD) as detected by H&E and Oil Red staining of livers **(Figure 10c)**, compared with WT aged mice.

To address whether this aging-induced steatotic phenotype can be recapitulated in young CPEB4^{KO} animals under feeding conditions that favor obesity, we fed 20 weeks-old CPEB4^{KO} mice with high-fat diet (60% HFD) for 12 weeks. Indeed, we found that WT mice were able to adapt to a HFD and to remain nonsteatotic, whereas mice lacking CPEB4 failed to adapt and developed hepatic steatosis **(Figure 11a-c)**. Thus, HFD-fed CPEB44^{KO} mice also had exacerbated liver steatosis, characterized by enhanced liver weight **(Figure 11a)**, excessive intrahepatic triglyceride content **(Figure 11b)**, and substantially increased fat deposits and accumulation of triglycerides in the cytoplasm of hepatocytes, as illustrated by H&E and Oil Red histological stainings **(Figure 11c)**. Moreover, and in agreement with the known inhibitory effect of lipid accumulation in hepatic insulin signalling (Postic and Girard, 2008), steatotic HFD-fed CPEB4^{KO} mice

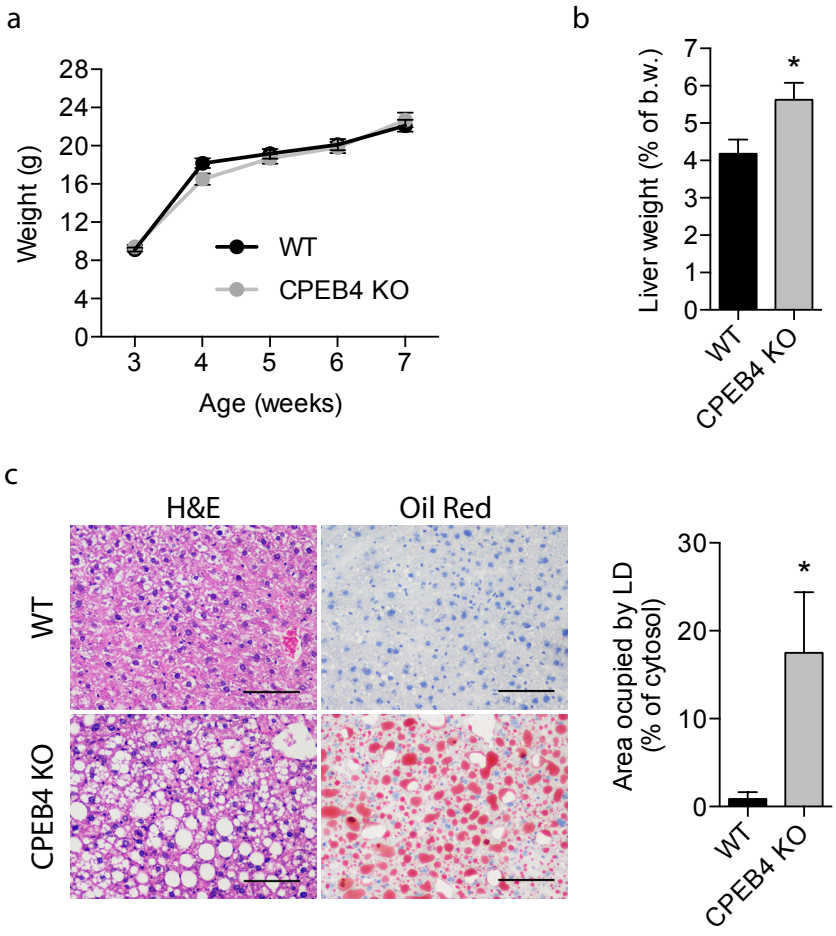

Figure 10. CPEB4 depleted mice develop liver steatosis. **a**, Changes in body weight of WT and CPEB4^{KO} mice fed with normal diet, n=16-24. **b**, Liver weight of 80-week-old WT and Cpeb4^{KO} mice on normal diet normalized to body weight, n=6-7. Scale bar, 100 μm. **c**, Left: H&E staining and Oil Red O staining of liver sections from the same mice. Right: Quantification of area occupied by lipid droplets (LD), showing accumulation of hepatic lipids in Cpeb4^{KO} aged mice.

suffered from fed and fasted hyperglycemia **(Figure 11d).** In some CPEB4^{KO} mice, hepatic steatosis was also accompanied by fibrosis, as assessed by Sirius Red staining **(Figure 11e)** The intolerance to metabolism imbalance present in CPEB4-

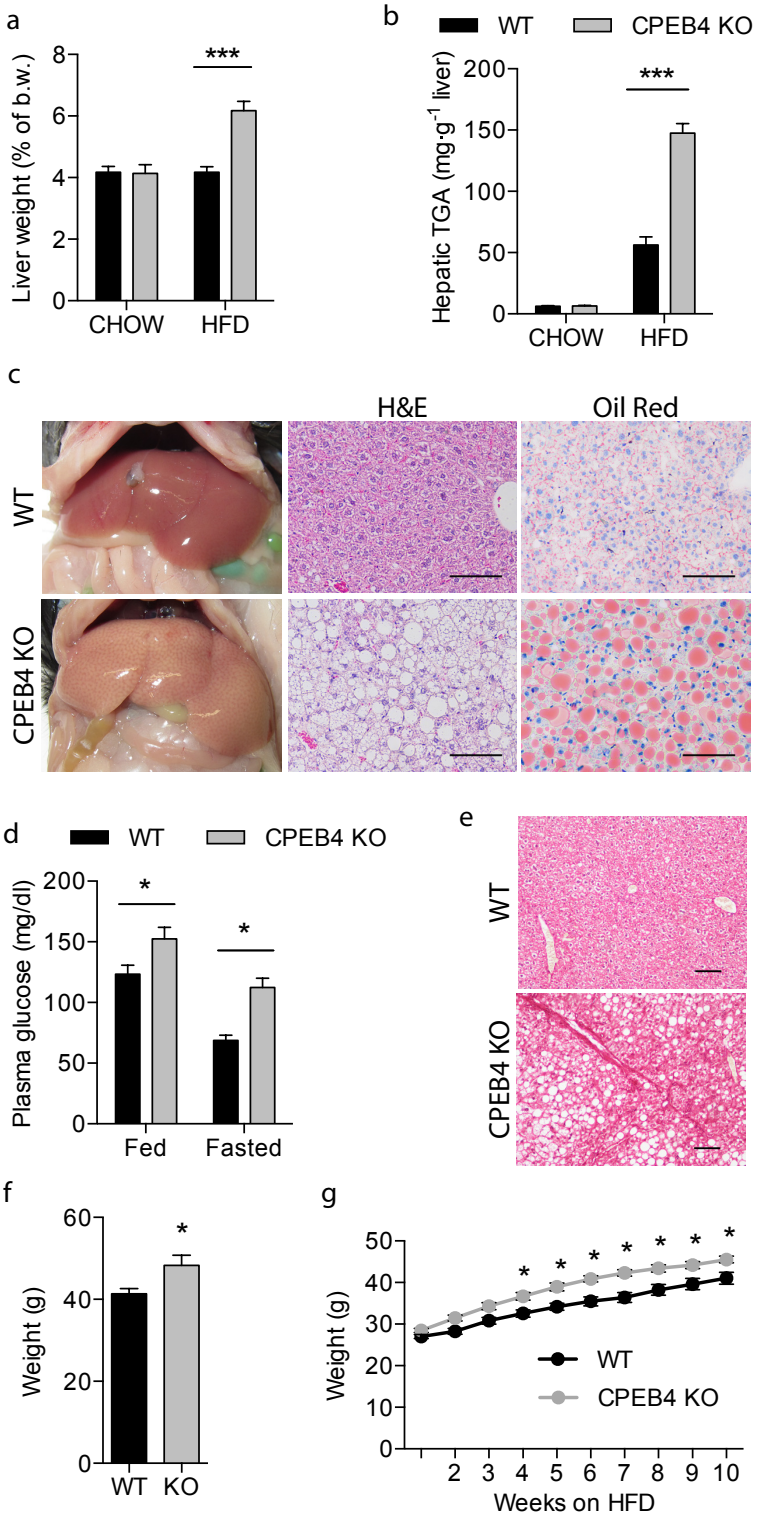

Figure 11. HFD accelerates steatosis in CPEB4^{KO} mice. **a,** Liver weight normalized to body weight

of 20-week-old WT and CPEB4^{KO} mice fed with a regular diet (CHOW) or with a HFD, n=8-15. **b**, Triglyceride content of livers from the same animals. **c**, Representative photograph of the liver (left), H&E staining (middle) and Oil Red O staining (right) of liver sections from 20-week-old WT and CPEB4^{KO} mice on HFD. Scale bar, 100 μm. **d**, Plasma glucose levels of WT and CPEB4^{KO} mice on HFD in fasted and fed conditions, n>4. **e**, Sirius Red staining of liver sections from 20-week-old WT and Cpeb4^{KO} mice on HFD. Scale bar, 100 μm. **f**, Body weight of 80-week-old WT and KO mice on normal diet, n=5-8. **g**, Changes in body weight of WT and CPEB4^{KO} mice fed with a HFD, n=14-20. *P<0.05; ***P<0.001.

depleted animals was further supported by the increased body weight of aged and HFD-fed CPEB4^{KO} animals compared to WT counterparts **(Figure 11f,g).**

Behavioural alterations seemed not to be the cause of the phenotype because we did not detect any difference in food or water intake **(Figure 12a,b)** or locomotor activity **(Figure 12c)** in the absence of CPEB4. Neither could we find differences in respiratory exchange ratio (RER) **(Figure 12d)** or energy expenditure (EE) **(Figure 12e)** in CPEB4^{KO} young animals. Taken together, these results indicate that deficiency of CPEB4 predisposes to liver steatosis in two different settings of metabolic homeostasis imbalance (i.e., aging and fat-rich diet feeding).

As CPEB1 knockout mice develop hepatic insulin resistance as a result of altered translation of mediators in the insulin-signalling pathway (Alexandrov et al., 2012), which is strongly associated with hepatic triglyceride accumulation (Browning and Horton, 2004), we next analysed whether glucose metabolism defects could be the cause of the hepatosteatosis in the CPEB4^{KO} mice. CPEB4 deficiency did not promote by itself any obvious glucose metabolicabnormality, either *in vivo* in mice fed a standard diet or *in vitro* in primary hepatocytes. In this regard, we did not find any alteration in plasma glucose **(Figure 13a)**, insulin **(Figure 13b)**, or free-fatty acid levels **(Figure 13c)**, in fed or fasted conditions. Neither were detectable differences in the plasma glucose or insulin profile during a glucose tolerance test,

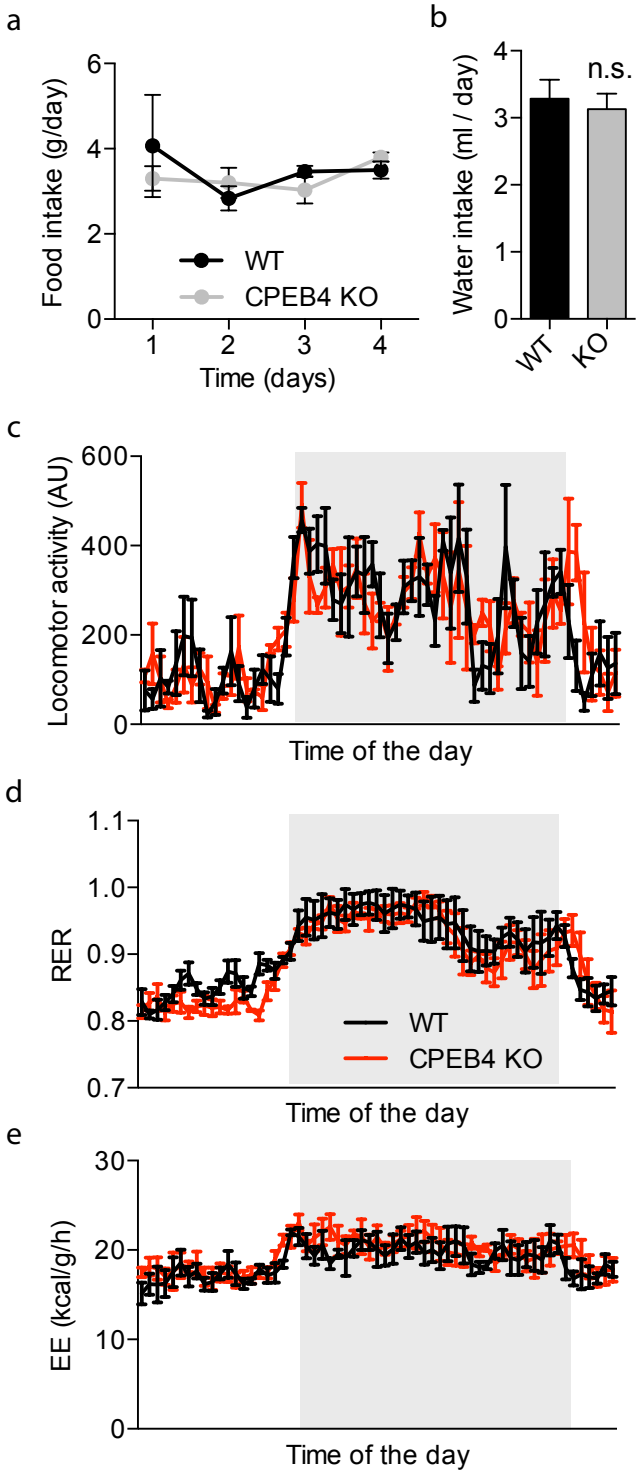

Figure 12. Depletion of CPEB4 does not elicit alterations in behaviour. **a**, Food intake (g/day) during 4 consecutive days of animals on HFD, n=4. **b**, Water intake in a 24h period, n=6. **c-d**, 24-hours time course of locomotor activity (**c**), RER (**d**) and EE (**e**) of mice fed a normal diet, n=3.

thereby ruling out the direct involvement of CPEB4 in insulin signalling and contrasting with the role of CPEB1 **(Figure 13d,e)** Liver gluconeogenesis was also unaffected in the CPEB4^{KO} animals, as shown *in vivo* by a glucagon tolerance test **(Figure 13f)** or *in vitro* by a glucose production assay on primary hepatocytes **(Figure 13g)**. However, *in vivo* glucose production from pyruvate substrate measured by a pyruvate tolerance test was enhanced in CPEB4^{KO} mice **(Figure 13h)** probably indicating the existence of a subjacent alteration of the glucose metabolism that however did not have a clear repercussion in the ability of the liver to respond to insulin or to maintain plasma glycemia **(Figure 13a,d)**. Together, these results suggest that CPEB4 depletion-induced liver steatosis is not due to a general dysfunction in glucose metabolism.

3. CPEB4 prevents hepatic steatosis autonomously

Given that CPEB4-depleted mice are heavier upon HFD-feeding or aging, a possible mechanism to account for abnormal hepatic lipid could be increased lipolysis in visceral and peripheral adipose tissue and subsequent transport of free fatty acids to the liver (Fabbrini et al., 2010) (Deng et al., 2012). However, our findings demonstrating absence of behavioral differences **(Figure 12a,b,c),** normal levels of circulating free fatty acids in CPEB4^{KO} mice **(Figure 13c)** and high CPEB4 protein expression in hepatocytes **(Figure 9b)**, argue against this possibility. Therefore, we next sought to determine whether hepatic steatosis arose as a cell-autonomous defect in the knockout hepatocytes. For this purpose, we mated animals with a floxed *Cpeb4* allele with transgenic mice expressing Cre recombinase under the control of the albumin gene promoter, thus generating a hepatocyte-specific depletion of CPEB4 in the postnatal state (Postic et al., 1999). This model is advantageous in two ways: first, the expression of the Cre is hepatocyte-specific, thereby rules out the contribution of any other hepatic cell

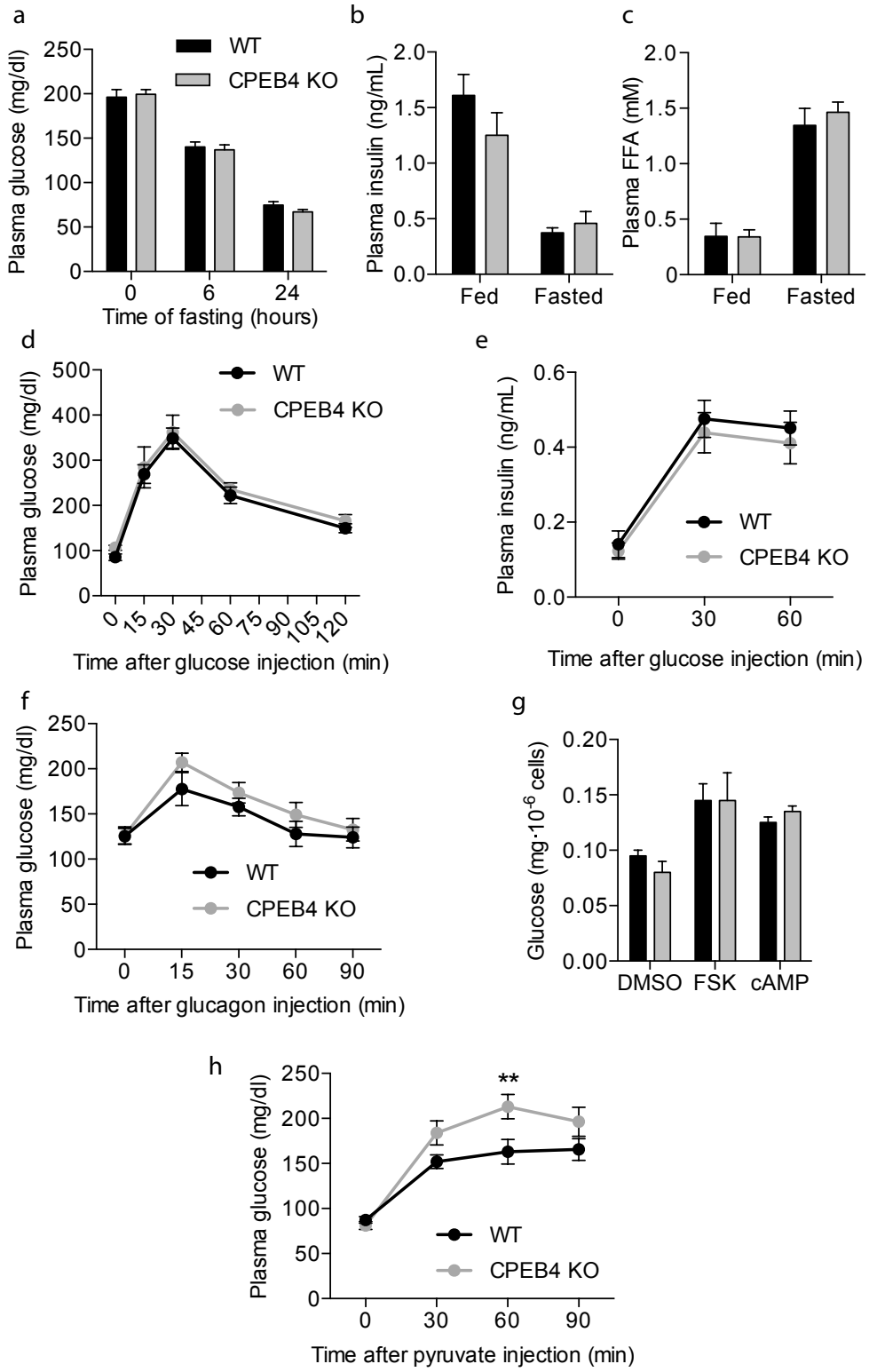

Figure 13. Absence of major alterations in glucose metabolism in CPEB4^{KO} mice. **a,** Plasma glucose

levels of fed, 6h- and 24h-fasted mice, n=6-11. **b-c**, Fed and overnight fasted plasma insulin levels (**b**) and free fatty acid (FFA) plasma levels (**c**), n=8-9. **d-e**, Glucose levels (**d**) and insulin levels (**e**) during a glucose tolerance test, n=6. **f**, Glucagon tolerance test after 6h fasting, n=6. **g**, Glucose produced by primary hepatocytes in culture after treatment for 4h with vehicle (DMSO), with the combination of 10 μM forskolin, 20 mM lactate and 2 mM pyruvate (FSK) or with the combination of 300 μM dibutyryl-cAMP and 100 nM dexamethasone (cAMP), n=3. **h**, Pyruvate tolerance test after overnight fasting, n=13. **i**, Fed and overnight fasted plasma glucose levels of mice fed a HFD, n>4. *P<0.01; ***P<0.001.

type; second, it is expressed postnataly, so it allows to discard that any alteration present in the adult animal is originated during the embryonic development. The resulting CPEB4^{LKO} mice were born at the expected Mendelian ratio and expressed normal levels of CPEB4 in all organs tested except in the liver, in which it was completely absent at 8 weeks of age **(Figure 14a,b)**.

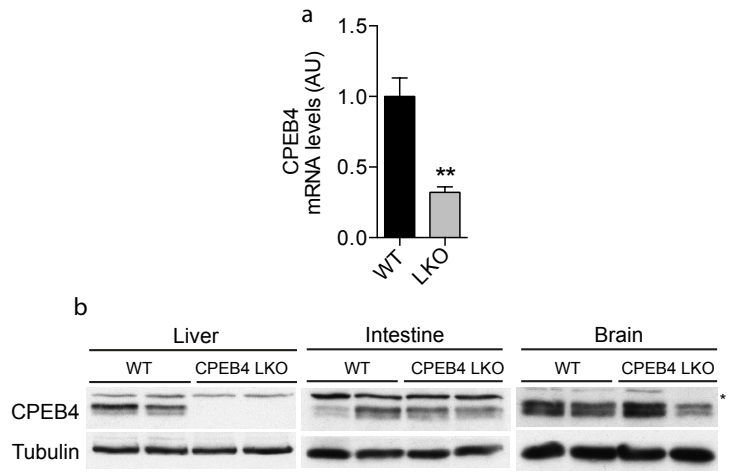

Figure 14. Hepatic CPEB4 depletion in liver-specific CPEB4^{KO}. **a**, *Cpeb4* mRNA expression in WT and liver-specific Cpeb4^{KO} (Cpeb4^{LKO}) livers, n=4. **b**, Immunoblot displaying CPEB4 and α-TUBULIN protein levels in different tissues of WT and CPEB4^{LKO} mice.

As in global CPEB4^{KO} mice, liver-specific CPEB4 deletion was not deleterious per se, having little effect on body weight **(Figure 15a)** and glucose metabolism **(Figure 15b)**, compared with WT mice. Neither did it increase plasma alanine transaminase (ALT) levels **(Figure 15c)**, excluding gross hepatic injury. However, when animals were challenged with a HFD for 12 weeks, CPEB4^{LKO} mice developed a lipid deposition phenotype, in a manner very similar to global CPEB4^{KO} animals fed a HFD. Thus, CPEB4^{LKO} exhibited increased liver weight **(Figure 15c)** and enhanced intrahepatic triglyceride content **(Figure 15d)**, along with histologically visible accumulation of triglyceride within hepatocytes **(Figure 15e)**, compared to WT counterparts. However, CPEB4^{LKO} did not exhibit increased body weight gain upon HFD administration **(Figure 15g)**, thereby further discarding that the hepatic steatosis of the ubiquitous KO mice was secondary to the increase in obesity. These results indicate that the development of fatty liver observed in CPEB4-deficient mice in response to HFD-feeding relies on a cell-autonomous defect in hepatocytes, rather than a metabolic alteration in adipose tissue.

4. CPEB4 deletion causes mitochondrial dysfunction and defective lipid metabolism in hepatocytes

To identify the cell-autonomous anomalies that make CPEB4-depleted hepatocytes prone to abnormal retention of lipids, we next turned our attention to other lipid metabolism processes of the liver. We found no differences in the expression of hepatic fatty-acid synthase and stearoyl-CoA desaturase between CPEB4^{LKO} and WT mice under a control diet **(Figure 16a)**, indicating that the capacity of the liver to synthesize fatty acids de novo (ie, lipogenesis) was not altered by CPEB4 deficiency and consequently did not contribute to hepatic fat deposition in CPEB4^{LKO} mice. Neither were there changes in the fatty acid uptake capacity of primary hepatocytes isolated from CPEB4^{KO} mice, compared with WT hepatocytes

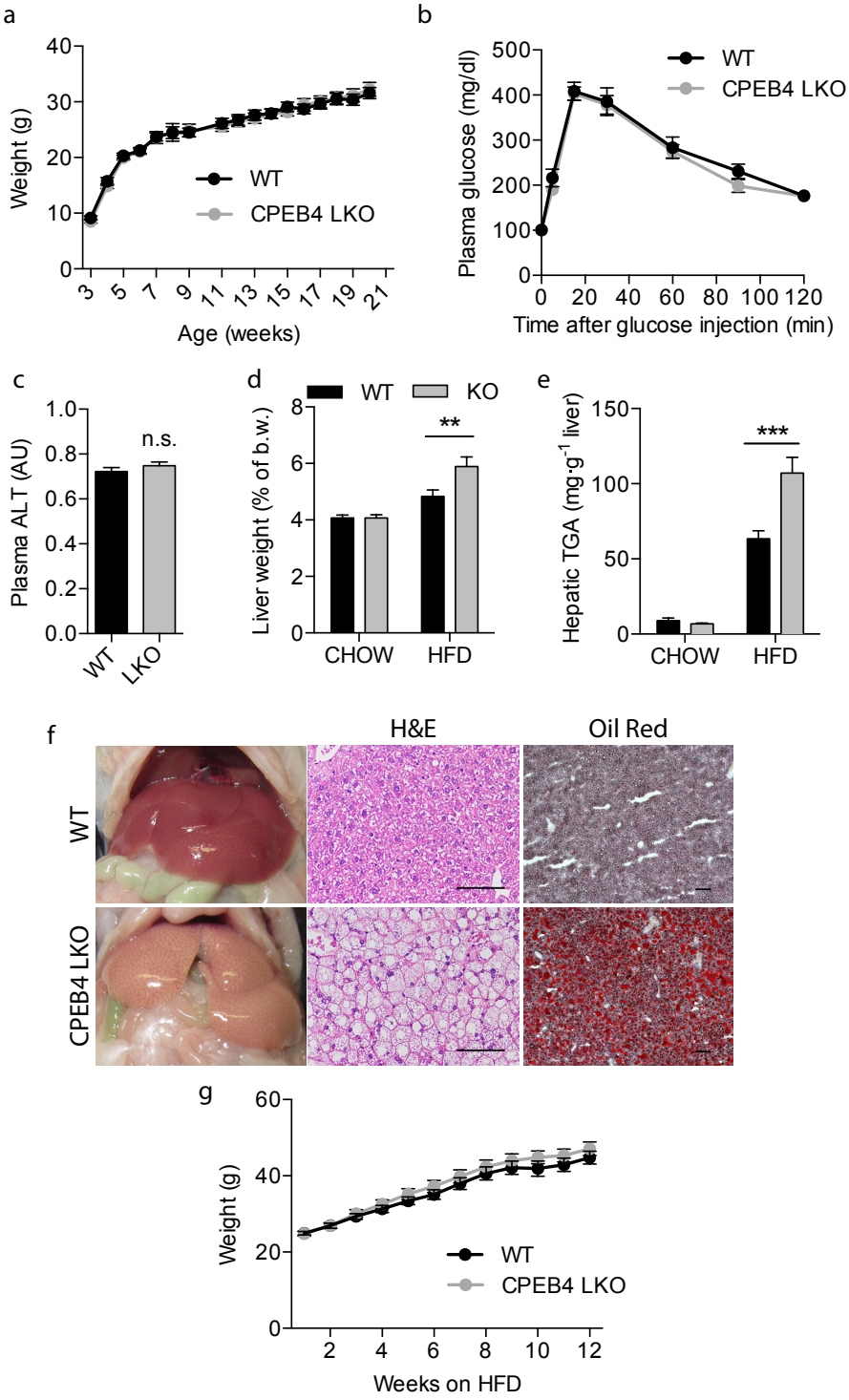

Figure 15. CPEB4 prevents hepatic steatosis autonomously. **a**, Weight evolution of WT and

CPEB4^{LKO} mice fed a regular diet, n=13-15. **b**, Glucose tolerance test after overnight fasting, n=8. **c**, Plasma alanine aminotransferase levels of mice fed a regular diet, n=7-8. **d-e**, Liver weight (**d**) and hepatic trygliceride content (**e**) of 20-week-old wild type and CPEB4^{LKO} mice fed a HFD, n=9. **f**, Representative photograph, H&E staining and Oil Red O staining of liver sections from the same animals. Scale bar, 100 μm. **g**, Growth curve of WT and CPEB4^{LKO} mice on HFD, n=11-12.

(Figure 16b). However, we found diminished mitochondrial fatty acid β-oxidation in CPEB4^{KO} hepatocytes, even after glucagon stimulation **(Figure 16c)**. This effect was concomitant with augmented incorporation of fatty acids into triglycerides in CPEB4^{KO} hepatocytes compared to control **(Figure 16d)**.

Accordingly, maximal mitochondrial activity, which is an effective indicator of the capacity of cells to manage metabolic stress was reduced both in cultured cells **(Figure 16e)** and purified mitochondria from knockout livers **(Figure 16f)** deficient for CPEB4. This reduction was more evident for complex II activity than for complex I **(Figure 16f)**, in agreement with the inability of knockout cells to utilize fatty acids as a source of energy **(Figure 16c)**. Moreover, we did not find differences in mitochondrial mass, as measured by mitochondrial proteins and DNA levels **(Figure 16g,h)**. Further evidence of mitochondrial dysfunction was provided by the observation of reduced plasma levels of ketone bodies **(Figure 16i),** which are byproducts of fatty acid metabolism in the mitochondria of liver cells.

We also assessed whether the lack of CPEB4 impaired triglyceride secretion from the liver via very low-density lipoproteins (VLDL), which could also contribute to increase hepatic lipid accumulation. CPEB4^{LKO} and WT littermates were injected with tyloxapol to block plasma lipoprotein hydrolysis and clearance, followed by the determination of plasma triglyceride (TGA) levels as an index of hepatic VLDL-TGA secretion. We found that CPEB4^{LKO} mice accumulated TGA in the plasma at a lower rate than WT mice **(Figure 16j)**, pointing to suboptimal lipoprotein export

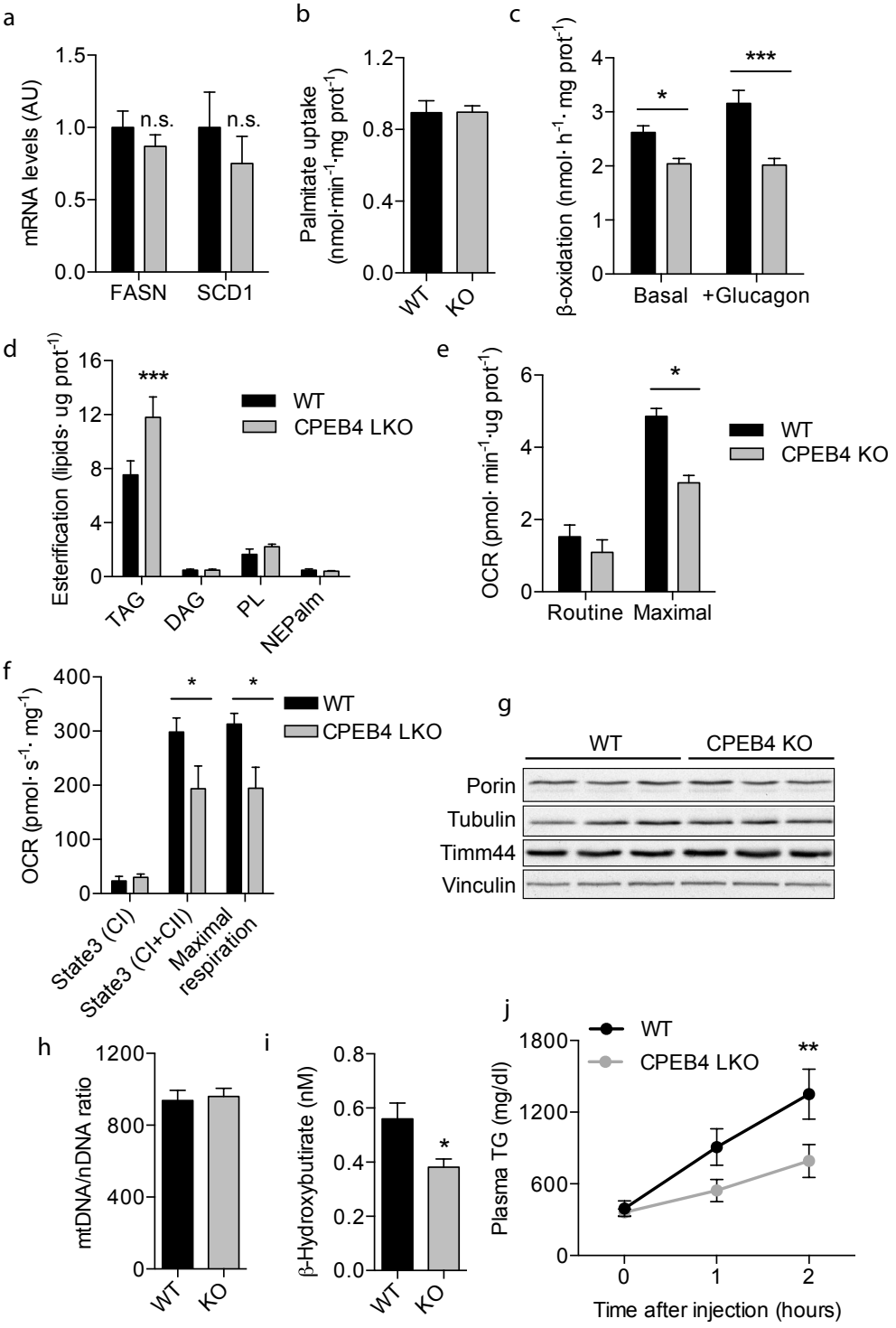
a
mRNA levels (AU)
1.5
1.0
0.5
0.0
n.s.
n.s.
FASN
SCD1
b
Palmitate uptake (nmol·min-1·mg prot-1)
1.2
0.8
0.4
0.0
WT
KO
c
β-oxidation (nmol· h-1· mg prot-1)
4
3
2
1
0
*
***
Basal
+Glucagon
d
Esterification (lipids· ug prot-1)
16
12
8
4
0
***
WT
CPEB4 LKO
TAG
DAG
PL
NEPalm
e
OCR (pmol· min-1·ug prot-1)
6
4
2
0
*
WT
CPEB4 KO
Routine
Maximal
f
OCR (pmol· s-1· mg-1)
400
300
200
100
0
*
*
WT
CPEB4 LKO
State3 (CI)
State3 (CI+CII)
Maximal respiration
g
WT
CPEB4 KO
Porin
Tubulin
Timm44
Vinculin
h
mtDNA/nDNA ratio
1200
800
400
0
WT
KO
i
β-Hydroxybutirate (nM)
0.8
0.6
0.4
0.2
0.0
*
WT
KO
j
Plasma TG (mg/dl)
1800
1200
600
0
WT
CPEB4 LKO
**
0
1
2
Time after injection (hours)

Figure 16. CPEB4 deletion causes mitochondrial dysfunction and defective lipid metabolism in hepatocytes. **a**, FASN and SCD1 gene expression analysis by qRT-PCR of livers from WT or CPEB4^{LKO} mice, n=8. **b**, Analysis of palmitate uptake in primary hepatocytes, n=2. **c**, Analysis of palmitate β-oxidation in primary hepatocytes from CPEB4^{KO} or WT mice, untreated or stimulated with 20 nM glucagon, n=2. **d**, Analysis of palmitate incorporation into triacylglycerol (TAG), diacylglycerol (DAG), phospholipids (PL) or non-esterified palmitate (NEPalm) in primary hepatocytes from CPEB4^{KO} or WT mice, n=2. **e**, Oxygen consumption rate normalized with total protein content of MEFs using an extracellular flux analyzer in basal (routine) or FCCP-induced (maximal) respiration, n=2. **f**, Oxygen consumption rate of isolated mitochondria from mouse liver analyzed by Oxygraph-2k at State3 (CI), State3 (CI+CII) and State3u (CI+II), n=3. **g**, Immunoblot for the indicated mitochondrial markers and loading controls in WT and CPEB4KO liver extracts. **h**, mtDNA quantification by qRT-PCR from WT and CPEB4^{KO} mice livers normalized to nuclear DNA content, n=8. **i**, Plasma β-hydroxybutirate levels in overnight fasted WT and CPEB4^{KO} mice fed a HFD, n=7. **j**, Hepatic VLDL secretion assay in CPEB4^{LKO} and WT animals. Plasma triglycerides were measured at 1 h and 2 h after tyloxapol intravenous injection; n=12-13. *P<0.05; **P<0.01; ***P<0.001.

in livers of CPEB4-deficient animals. No differences in body weight were detected **(Figure 15a)**, thereby precluding the possibility that the observed reduction in VLDL production was secondary to body weight changes in CPEB4^{LKO} mice.

Taken together, these data suggest that lipid accumulates in the livers of CPEB4-deficient animals because of a defect in mitochondrial fatty acid oxidation and respiration, possibly augmented by impaired lipoprotein secretion.

5. CPEB4 regulates the expression of ER-related proteins

Given that CPEB4 is a RNA-binding protein, we reasoned that the connection between CPEB4 deletion and increased susceptibility to develop fatty livers might be most readily determined by identifying which mRNAs are bound to, and therefore are translationally regulated by, CPEB4 in hepatocytes. For this purpose, we applied RNA-immunoprecipitation-sequencing (RIP-seq) with specific antibodies against endogenous CPEB4 protein using CPEB4^{KO} hepatocytes and mock IgG

immunoprecipitation as controls **(Figure 17a)**. Illumina sequencing showed that 444 mRNAs were specifically associated with CPEB4 in hepatocytes (logFC>2) and that their 3' UTRs were enriched in CPE motifs compared with the whole transcriptome **(Figure 17b)**. Intriguingly, a significant number of these CPEB4 targets encoded for endoplasmic reticulum-related proteins, such as TXNIP, HYOU1, DPM3, TAP1, HMOX1, CRELD2 and TOR3a, as revealed by Gene Set Enrichment Analysis (GSEA) **(Figure 17c)**. Many of these proteins, including DNAJC2, DNAJC8, ERP44, HYOU1, NPM3, DNAJA1, SACS, PPIL3, PPIB, PPIF, DNAJA1, SLMAP and TOR3A, are ER-resident molecular chaperones that participate in protein homeostasis, specifically helping proteins to fold and preventing their aggregation. Therefore, these data suggest that CPEB4 regulates the translation of specific mRNAs encoding ER-related proteins.

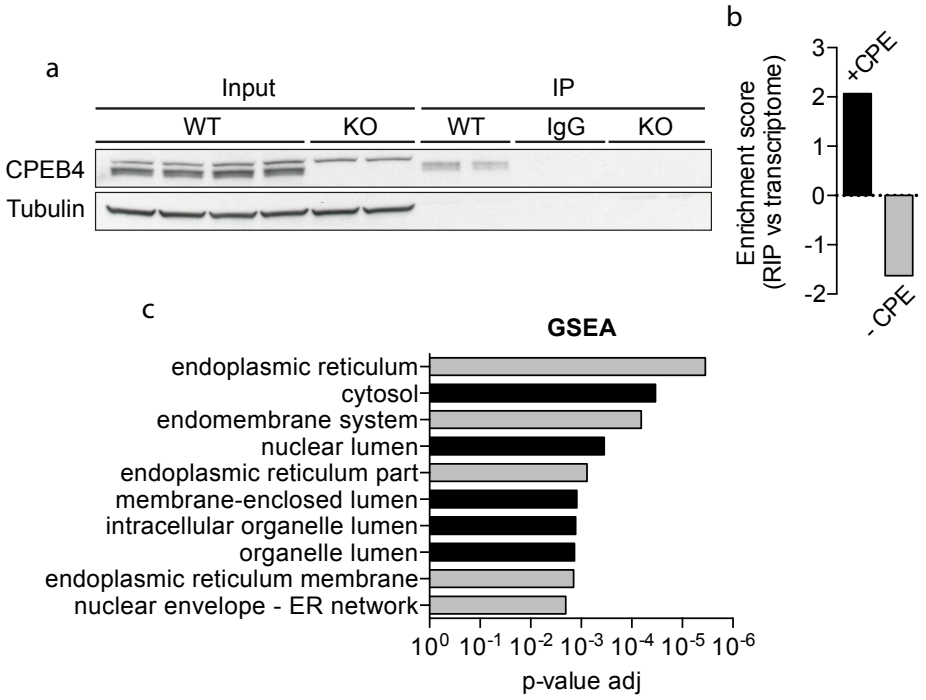

Figure 17. CPEB4 regulates the expression of ER-related proteins. **a**, Immunoblot for CPEB4 and α-TUBULIN from inputs and immunoprecipitated fractions with α-CPEB4 antibody or IgGs in

WT and CPEB4^{KO} primary hepatocytes. **b**, Enrichment score of CPE-regulated and -unregulated transcripts of RIP-targets versus the mouse transcriptome. **c**, Top enriched cell compartment categories based on RIP-seq data analyzed by DAVID bioinformatics resources.

6. CPEB4 is located at the ER, but does not localize mRNAs

The specific binding of CPEB4 to ER-related transcripts made it plausible that, in order to perform its function, CPEB4 would be located at the vicinity of the ER. Indeed, previous studies in neuronal cultures showed an ER-specific localization of CPEB4 (Kan et al., 2010). To test whether this localization was also conserved in hepatocytes, we subjected mouse livers to a subcellular fractionation, which revealed that CPEB4 was heavily skewed to the ER in livers of WT mice, being absent in mitochondrial fractions **(Figure 18a).** Immunostaining of CPEB4 in primary mouse embryonic fibroblasts (MEFs) also revealed a perinuclear staining pattern, congruent with the subcellular localization of the ER **(Figure 18b)**.

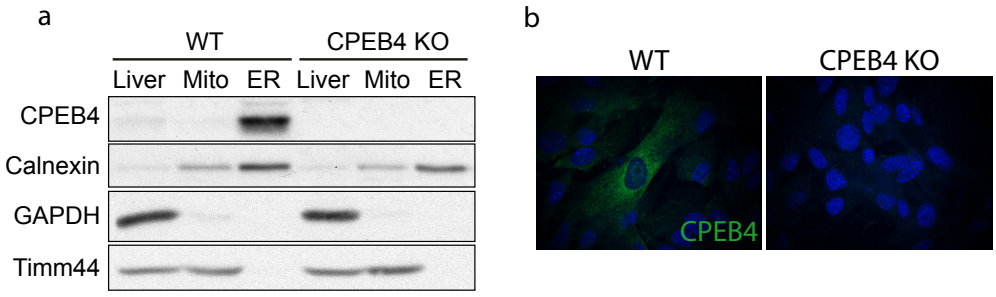

Figure 18. ER-localization of CPEB4. **a**, Immunoblot of liver-fractionated extracts for the indicated proteins. The fractions from total liver (Liver), mitochondria (Mito) and endoplasmic reticulum (ER) are shown. **b**, Immunofluorescence of CPEB4 in WT and CPEB4^{KO} MEFs. Nuclei are stained with DAPI.

Because CPEB1 has been shown to localize mRNAs to specific subcellular compartments (Weill et al., 2012), we wondered whether an analogous process could be taking place with CPEB4 at the ER. To specifically examine whether CPEB4 was necessary to localize specific mRNAs at the ER, we extracted and sequenced ER-located mRNAs from WT and CPEB4^{KO} livers. Compared with controls, only 8 mRNAs showed reduced localization to the ER in knockout livers **(Table 2)**. These mRNAs were probably mislocalized by indirect causes because none of them was a direct target of CPEB4 according to the RIP-seq data **(Table 1)**. Thus, we concluded that CPEB4 most likely regulates the translation activity, but not the localization, of specific mRNAs at the ER.

7. CPEB4 deletion sensitizes livers to dietary fat-induced ER stress

Three lines of evidence lead us to hypothesize that CPEB4 might directly participate in the response to ER-stress: (1) CPEB4 targets are enriched in proteins involved in ER homeostasis; (2) HFD feeding and aging are known to generate hepatic ER stress. (3) Hepatic ER stress impairs mitochondrial FFA oxidation and respiration, together with lipoprotein secretion (Ota et al., 2008; Raabe et al., 1999; Rao and Reddy, 2001), which are all affected in CPEB4-depleted cells.

To this end, we first determined the intrahepatic expression of a panel of ER stress markers by real-time qPCR. Following HFD feeding for 12 weeks, the ER stress markers and downstream inflammatory cytokines upregulation was significantly exacerbated in livers from CPEB4^{KO} mice **(Figure 19)**, indicating that animals with CPEB4 deficiency fail to adaptively attenuate ER stress in response to HFD feeding.

These results suggest that CPEB4 prevents the development of hepatic steatosis by promoting adaptation to ER stress

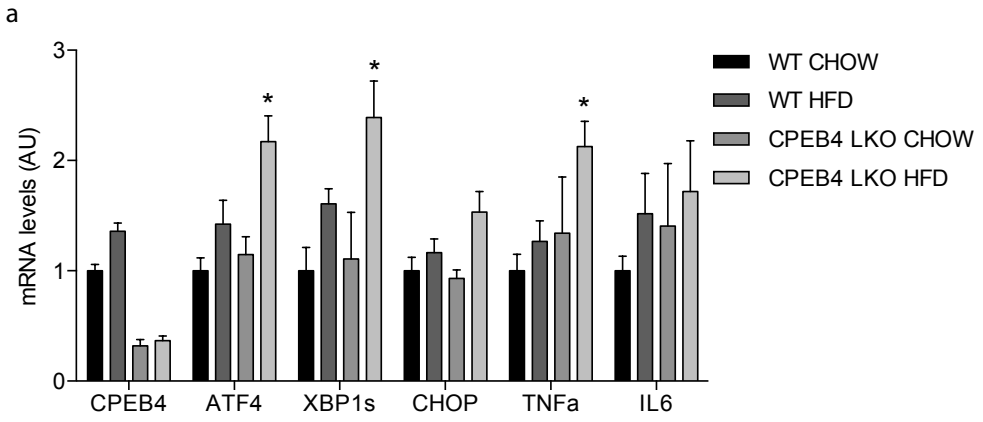

Figure 19. HFD-induced ER stress is exacerbated in CPEB4^{KO} mice. **a**, Gene expression analysis by qRT-PCR of livers from CPEB4^{LKO} and WT mice fed a normal diet (CHOW) or a high-fat diet (HFD), n=8.

8. CPEB4 depletion leads to defective adaptation to chronic ER stress

To confirm that the exacerbated liver fat accumulation in the absence of CPEB4 was a general consequence of activated and unresolved ER stress and UPR signaling, we next tested the effect of ER stress chemical-inducers in both CPEB4-deficient animals and cultured cells. Liver-specific CPEB4^{KO} animals were subjected to a single intraperitoneal injection of tunicamycin (TM), which inhibits N-linked glycosylation of newly synthesized proteins and subsequently causes accumulation of unfolded or misfolded proteins in the ER lumen and ER stress. Forty-eight hours after challenge, CPEB4^{LKO} mice developed profound hepatic steatosis as evidenced by the presence of livers much lighter in color than WT counterparts **(Figure 20a, left)**, accumulation of lipid droplets visualized by H&E staining **(Figure 20a, right)** and significantly increased liver weight **(Figure 20b)** and triglyceride content **(Figure 20c)**, as compared with WT mice treated with

TM or mice not subjected to stress. These results are consistent with our findings in HFD-induced ER stress models and suggest that CPEB4 deletion enhances the susceptibility to both chronic (dietary fat) and acute (TM) ER stress.

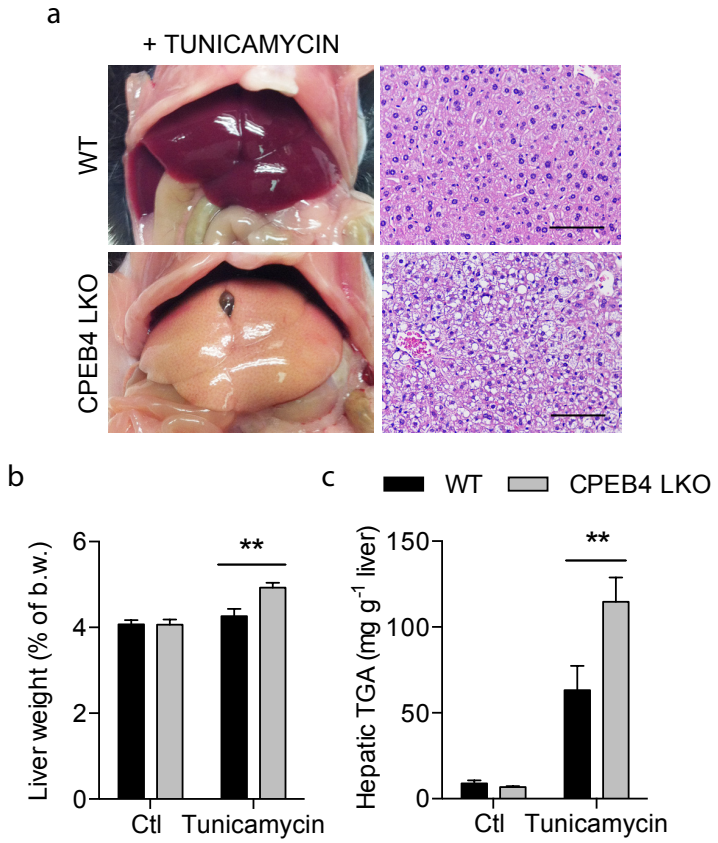

Figure 20. CPEB4 depletion leads to defective adaptation to chronic ER stress. **a**, Representative photograph and H&E staining of liver sections from WT and CPEB4^{LKO} mice injected with 1 mg TM/kg body weight and killed after 48 h. Scale bar, 100 μm. **b-c**, Liver weight (**b**) and hepatic triglyceride content (**c**) of the same animals, n=7-8.

Moreover, the transcript encoding the proapoptotic transcription factor CHOP was dramatically increased in CPEB4^{LKO} mice, compared with WT animals, after TM-induced ER stress **(Figure 21a)** and, accordingly, the percentage of apoptotic cell death was markedly increased in CPEB4^{KO} cells treated with TM for 24h

(Figure 21b). These results suggest that CPEB4 may be essential to orchestrate the adaptation to ER stress and, in its absence, the apoptotic branch of UPR is favoured. Indeed, upon mild ER stress, ATF4 and CHOP upregulation took place at lower TM doses in CPEB4^{KO} cells than in WT cells **(Figure 21c)**.

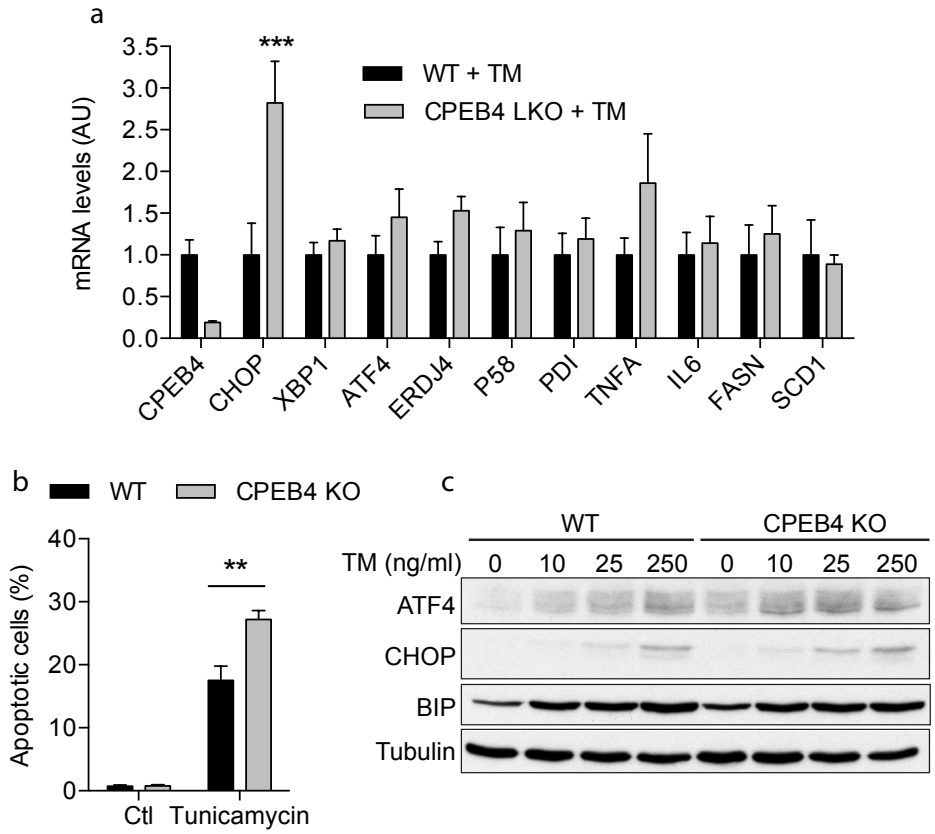

Figure 21. Depletion of CPEB4 favours the apoptotic UPR. **a**, Gene expression analysis by qRT-PCR of the indicated genes, n=6. **b**, Apoptotic analysis of WT and CPEB4^{KO} MEFs measured by flow cytometry as the percentage of annexin V-positive cells after addition of 5 μg/ml TM for 24 h. **c**, Immunoblot of ATF4, CHOP, BIP and α-tubulin of MEF extracts 24 h after the addition of the indicated doses of TM.

To buttress the conclusion that the hepatosteatotic phenotype of CPEB4^{KO} mice was at least in part caused by a failure to cope with ER stress and to attenuate

the UPR, we treated HFD-fed animals with tauroursodeoxycholic acid (TUDCA), a chemical chaperon described to protect from the ER stress-effects induced by HFD (Ozcan et al., 2006). Strikingly, TUDCA treatment restored both liver weight **(Figure 22a)** and intrahepatic triglyceride content **(Figure 22b)** of CPEB4^{KO} mice to WT levels, completely reverting the effects caused by CPEB4 absence in the context of HFD-feeding. These results confirm that the hypersensitivity to ER stress induced by CPEB4 suppression causes the development of liver steatosis in mice.

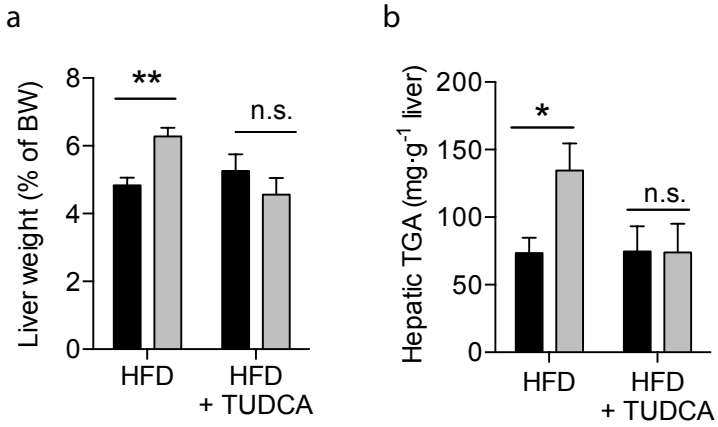

Figure 22. TUDCA rescues the CPEB4^{LKO} steatosis. **a**, Liver weight of WT and CPEB4^{LKO} mice on HFD for 12 weeks and treated with TUDCA (500 mg/day/mice) for the last 2 weeks, n=6. **b**, Triglyceride content of livers from the same animals. *P<0.05; **P<0.01.

9. CPEB4 protein levels are upregulated by the unfolded protein response

To further define the specific UPR step in which CPEB4 may participate, wild-type and CPEB4^{KO} MEFs were incubated with thapsigargin (TG), which causes ER stress by inhibiting the sarco/ER Ca^{2+} pump (Sagara and Inesi, 1991), and the expression of the UPR markers and CPEB4 were measured at short times (1, 2, 4 and 6 h) after the induction.

We found that CPEB4 protein levels were low under non-stressed conditions in WT cells, but were potently and rapidly upregulated, in a time-dependent fashion, by exposure to TG **(Figure 23a),** with a kinetic similar to that of ATF4, following eIF2α phosphorylation and preceding CHOP accumulation **(Figure 23a)**. *Cpeb4* mRNA levels, as does *Atf4* mRNA, moderately increased at early time-points **(Figure 23b)** Similar results were obtained by treating the cells with TM (data not shown).

Interestingly, the absence of CPEB4 in MEFs did not affect the activation of any of the UPR branches in response to short-term ER stress. Thus, the time courses of eIF2α phosphorylation, ATF4 and CHOP expression in CPEB4^{KO} cells after challenge with TG were very similar to those of their WT counterparts **(Figure 23a)**. These observations suggest that CPEB4 synthesis is either downstream of, or in a parallel pathway to, eIF2α phosphorylation and ATF4 translational activation, but not upstream.

Because CPEB4 follows the same expression pattern as ATF4, which mRNA is translationally activated through an uORF-dependent mechanism, we analyzed *Cpeb4* mRNA for the presence of possible uORFs. Indeed, close inspection of the 5' UTR of *Cpeb4* mRNA revealed multiple (8 in rodent and 9 in human) putative uORFs that were conserved among various mammalian species **(Figure 23c)**. Ribosome profiling analysis from published data sets (Gao et al., 2015) (GWIPS-visualization tool) indicated that these regulatory sequences are in fact translated in non-stressed conditions **(Figure 23d)** thereby precluding the translation of the coding sequence. To test whether these *Cpeb4* 5' UTR-uORFs could promote, or capacitate, translation upon the UPR induction by TG, we expressed chimeric mRNAs with either *Cpeb4* 5' UTR or a control 5' UTR followed by a reporter ORF. Indeed, *Cpeb4* 5' UTR promoted translation of a reporter ORF, when compared with a control 5' UTR after TG treatment **(Figure 23e)** without affecting the

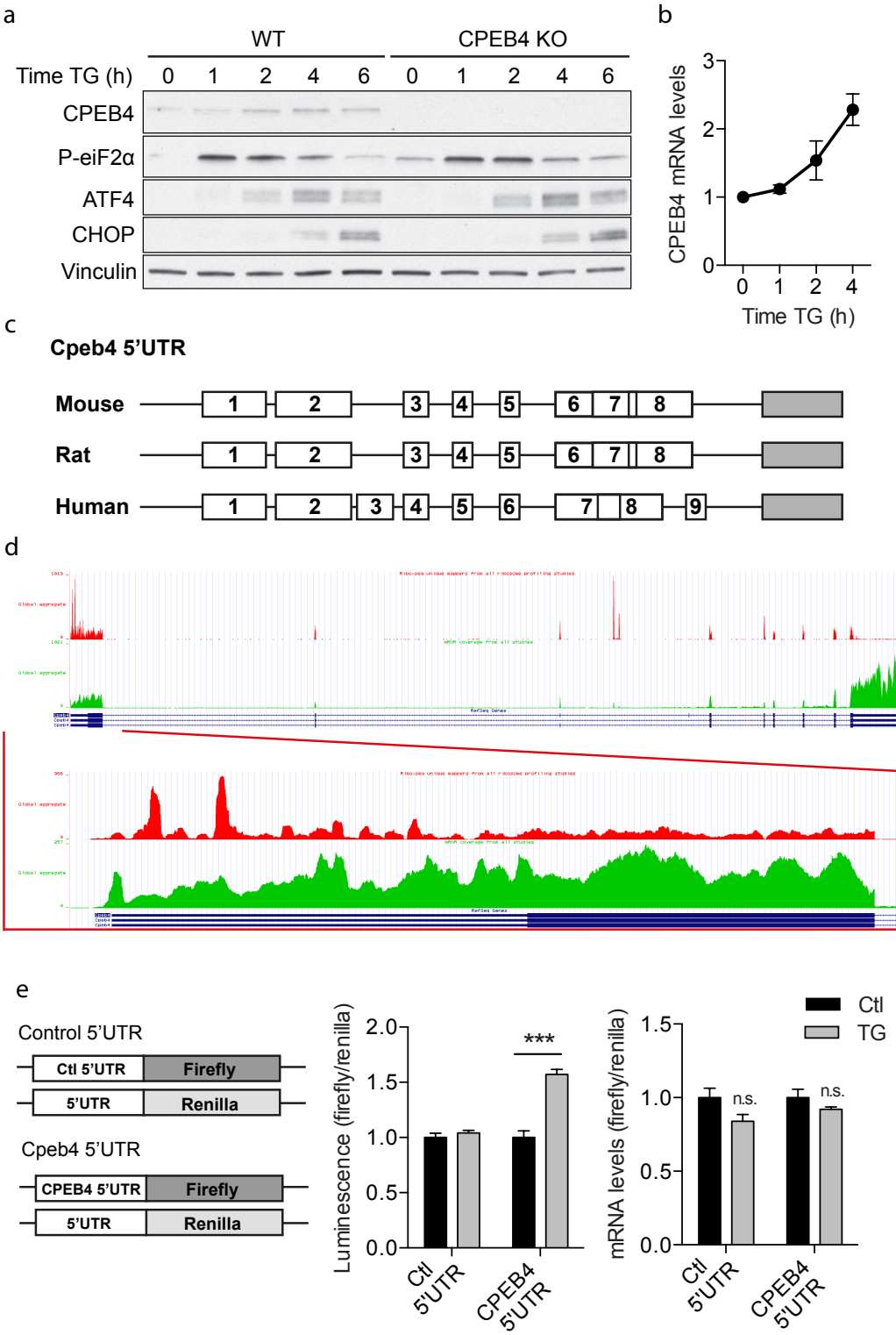
a
WT
CPEB4 KO
Time TG (h)
0 1 2 4 6 0 1 2 4 6
CPEB4
P-eiF2α
ATF4
CHOP
Vinculin
b
CPEB4 mRNA levels
Time TG (h)
c
Cpeb4 5'UTR
Mouse
Rat
Human
d
e
Control 5'UTR
Ctl 5'UTR
Firefly
5'UTR
Renilla
Cpeb4 5'UTR
CPEB4 5'UTR
Firefly
5'UTR
Renilla
Luminescence (firefly/renilla)
***
Ctl 5'UTR
CPEB4 5'UTR
mRNA levels (firefly/renilla)
Ctl
TG
n.s.
n.s.
Ctl 5'UTR
CPEB4 5'UTR

Figure 23. CPEB4 levels are regulated by the UPR. **a**, Immunoblot analysis of WT and CPEB4^{KO} MEFs treated with 1 μM TG for the indicated proteins. **b**, *Cpeb4* mRNA levels of the same cells, n=3. **c**, Schematic of the phylogenetic conservation of *Cpeb4* mRNA uORFs among different mammalian species. **d**, Visualization of ribosome footprints within *Cpeb4* mRNA (in red) and total RNA-seq reads (in green) by GWIPS-viz tool. The fragment corresponding to the 5' UTR of the mRNA is highlighted. **e**, Left: Scheme of the dual luciferase reporter assay. A Firefly luciferase reporter under the control of *Cpeb4* 5' UTR and a Renilla luciferase reporter control in HepG2 cells treated with 0.1μM TG for 6h. Middle: Luminescence values before and after the addition of TG. Right: qRT-PCR expression analysis of the constructs.

stability of the mRNA.

Therefore, these data demonstrate that CPEB4 protein levels are translationally regulated by the UPR through the uORFs located in its 5' UTR, and that this process is probably conserved throughout tissues and mammalian species.

10. CPEB4 is the only CPEB family member induced by the UPR

Because the CPEB family of proteins is composed of 4 members with overlapping target mRNA populations, we wondered whether the rest of the CPEBs were under the same UPR-translational regulation or if otherwise this was a specific mechanism of CPEB4. Bioinformatic comparison of the 5' UTRs of all 4 Cpebs showed that *Cpeb4* had a disproportionally large 5'UTR sequence compared to that of the rest of the members **(Figure 24a)**. Furthermore, neither uORFs nor ribosomal footprints were identified within the 5' UTRs of *Cpeb1-3*. Accordingly, genome-wide ribosome profiling data showed that CPEB4 was the only CPEB whose translation was stimulated by TG-induced ER stress in MEFs (Reid et al., 2014) **(Figure 24b)**, in agreement with our results **(Figure 23a,b)**. All these experiments support the notion that CPEB4 is the only member of the CPEB

family regulated during the UPR, which positions it as a unique regulator of mRNA translation during ER stress.

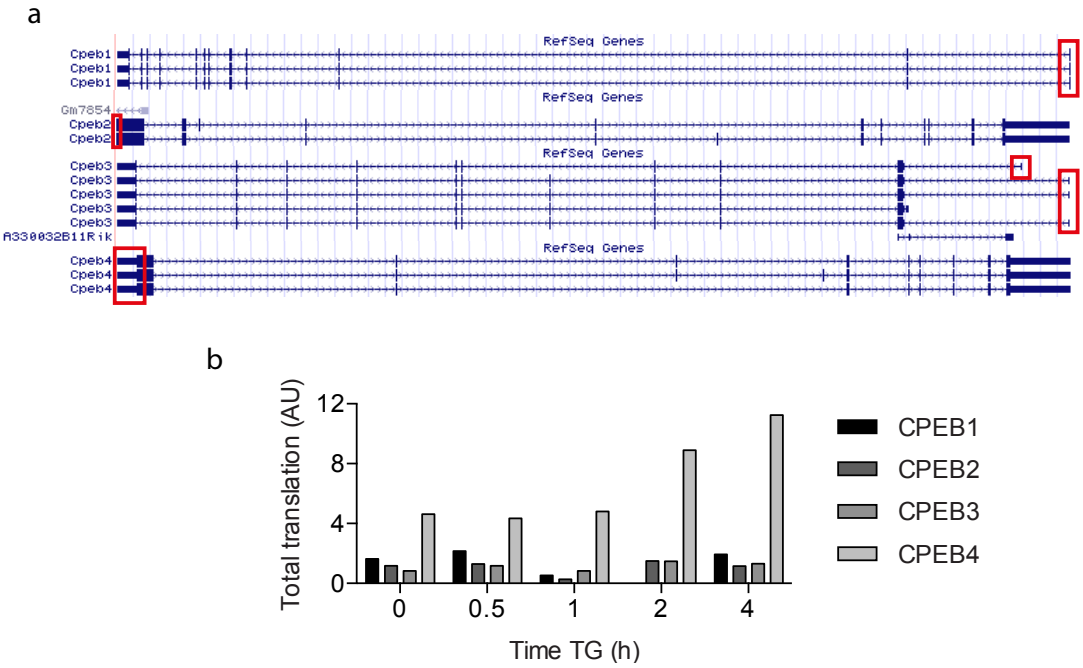

Figure 24. CPEB4 is the only CPEB regulated by the UPR. **a**, Illustration of the mRNA isoforms from all CPEB-family members in mouse. Arrows indicate the direction of the transcripts and 5' UTRs are highlighted. **b**, Total translation of the CPEB-family members assessed by ribosome profiling in MEFs treated with 1μM TG for the indicated times (analyzed from Reid D.W. et al., 2014).

11. CPE-regulated mRNAs are activated during the UPR

Mechanistic studies on the CPEB-family of proteins show that they can both activate or repress the translation of their target mRNAs. As for CPEB4, while most of the studies show that it acts as a translational activator (Igea and Mendez, 2010; Novoa et al., 2010), others point to a role in repression (Hu et al., 2014). Therefore, we next sought to determine whether the UPR-dependent increase in CPEB4 levels results in translational regulation of CPE-containing mRNAs and, if

that is the case, which is the translational activity of CPEB4 in that context. For this purpose, we used cells expressing a GFP reporter under the regulation of a 3' UTR that contains CPE regulatory elements, either functional (CPE) or inactivated by point mutations (mCPE), and a RFP reporter as normalization control (Giangarra et al., 2015). None of the reporters contained uORFs in their 5' UTRs. These cells were treated with TG and the fluorescence intensity of both proteins was followed over time. The UPR activation led to a two-fold increase in the production of GFP over RFP 8 h after the addition of TG **(Figure 25a)**. This activation was both dependent on the CPE-elements and CPEB4 levels, as it did not take places in the mCPE reporter or when CPEB4 was depleted (CPEB4 KD) **(Figure 25a)**.

Strikingly, these results indicate that CPEs and CPEB4 promote translation of specific mRNAs during the UPR, when eIF2α is phosphorylated and general protein synthesis inhibited, in a similar but independent manner than the uORFs. Therefore, a CPEB4-driven mechanism may constitute a new branch of UPR-mediated translation.

To interrogate whether this translational regulation was also occurring in endogenous CPEB mRNA targets, we analyzed the UPR-induced activation of TXNIP, an ER-resident protein in charge of maintaining redox homeostasis. TXNIP is induced in response to ER stress according to ribosome profiling data **(Figure 25b)** and is one of the most enriched targets of CPEB4 according to the RIP-seq results **(Table 1)**. *Txnip* 3'UTR contains several conserved CPEs **(Figure 25c)**. TG treatment of MEFs led to a marked increased in both TXNIP protein and mRNA peaking at 2 h after the induction **(Figure 25d,e)** as previously described **(Figure 25b)**. However, the absence of CPEB4 completely abolished TXNIP protein induction **(Figure 25d)**, while the mRNA upregulation was maintained **(Figure 25e)**, indicating that TXNIP is translationally activated by CPEB4 during the UPR.

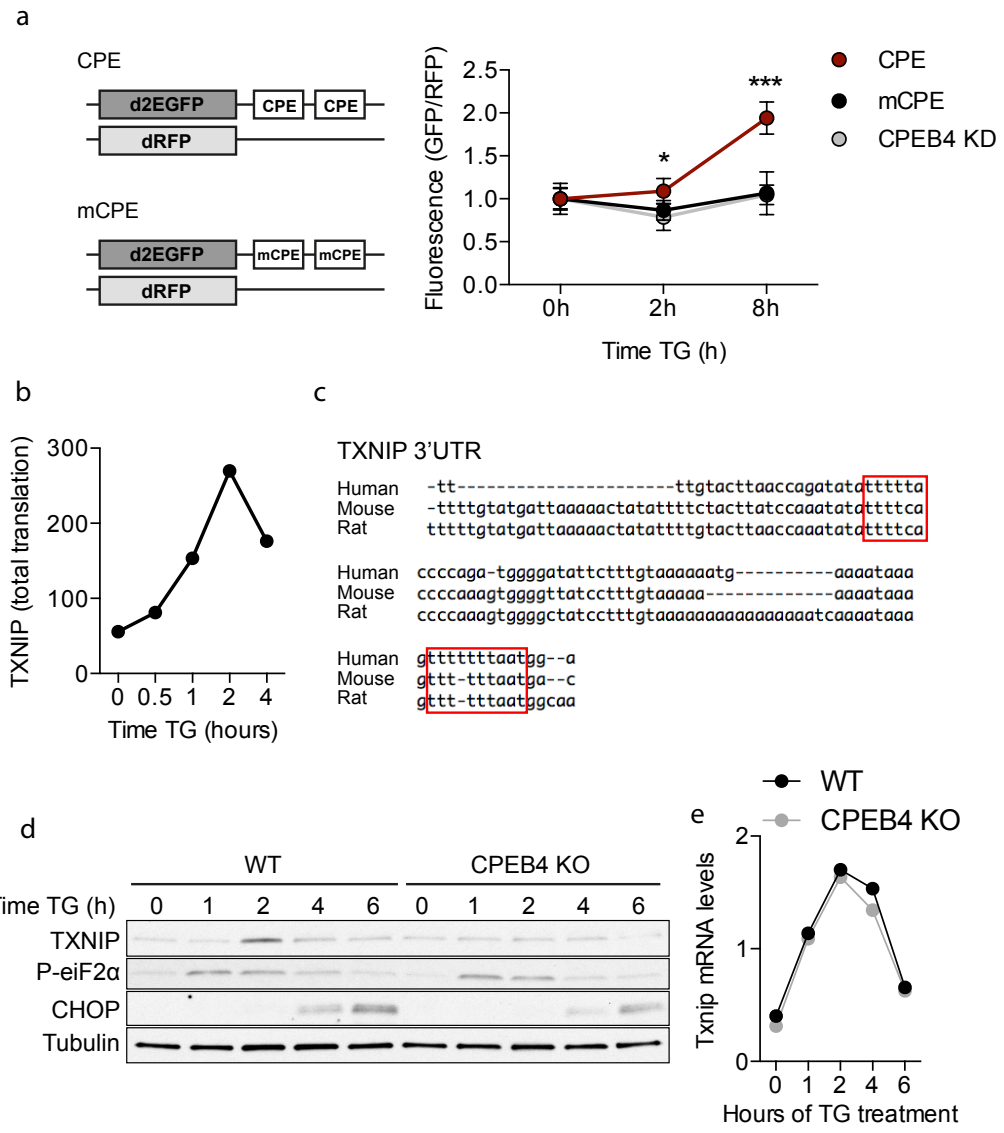

Figure 25. The UPR activates CPEB4-mediated translation. **a**, Left: Scheme of the dual fluorescence reporter assay: a destabilized GPF reporter under the control of a CPE-containing 3' UTR and a destabilized RFP reporter control in HEK-293 cells treated with 1μM TG for the indicated times. Right: fluorescence values for the indicated times. **b**, Total translation of Txnip assed by ribosome profiling in MEFs treated with 1μM TG for the indicated times (analyzed from Reid D.W. et al., 2014). **c**, Txnip 3' UTR sequence in different mammalian species. The conserved CPE-elements are highlighted. **d**, Immunoblot for the indicated proteins in WT and CPEB4^{KO} MEFs treated with TG. **e**, mRNA levels of Txnip quantified by qRT-PCR from the same samples.

Collectively, these data demonstrate that UPR-induced eIF2α phosphorylation, while inhibiting global protein synthesis, promotes the translation of uORF-containing transcripts including *Cpeb4* mRNA. In turn, CPEB4 activates the translation of CPE-regulated mRNAs in a uORF-independent manner.

12. CPEB4 mRNA levels are regulated by the molecular circadian clock

Recent studies revealed that the UPR signalling is a rhythmic process in mouse liver and it is regulated by the peripheral cell-autonomous hepatic circadian clock (Cretenet et al., 2010). Given that *Cpeb4* is known to be rhythmically transcribed in this organ (Kojima et al., 2012), we decided to investigate the potential impact of the circadian clock on the hepatic CPEB4-branch of the UPR.

Close inspection of the promoter sequence of the *Cpeb4* gene revealed several E-boxes and CT-rich regions **(Figure 26a)**, which are known binding sites of the CLOCK-BMAL1 complex, the core component of the molecular clock. Although these data suggest that CPEB4 gene might be directly regulated by the hepatic clock, we set out to gain a deeper understanding on the dynamics of *Cpeb4* mRNA throughout the circadian cycle, and based on published liver circadian transcriptomic data sets (Vollmers et al., 2009), we plotted the hepatic *Cpeb4* mRNA levels throughout the circadian cycle over a 24h period in a 12-h ligh-dark cycle. We found that hepatic *Cpeb4* mRNA levels oscillate in a circadian fashion in mouse liver peaking in the morning **(Figure 26b)**. Interestingly, at this time of the day is when the hepatic protein secretion rhythms reach their maximum (Mauvoisin et al., 2014). Both fed or fasted mice maintained *Cpeb4* oscillations, indicating that *Cpeb4* rhythmicity does not respond to the feeding status of the animal. However, the rhythms of *Cpeb4* mRNA did not persist in CRY1/CRY2 KO mice, which do not have functional circadian clocks **(Figure 26b)**. Thus, liver *Cpeb4* mRNA levels

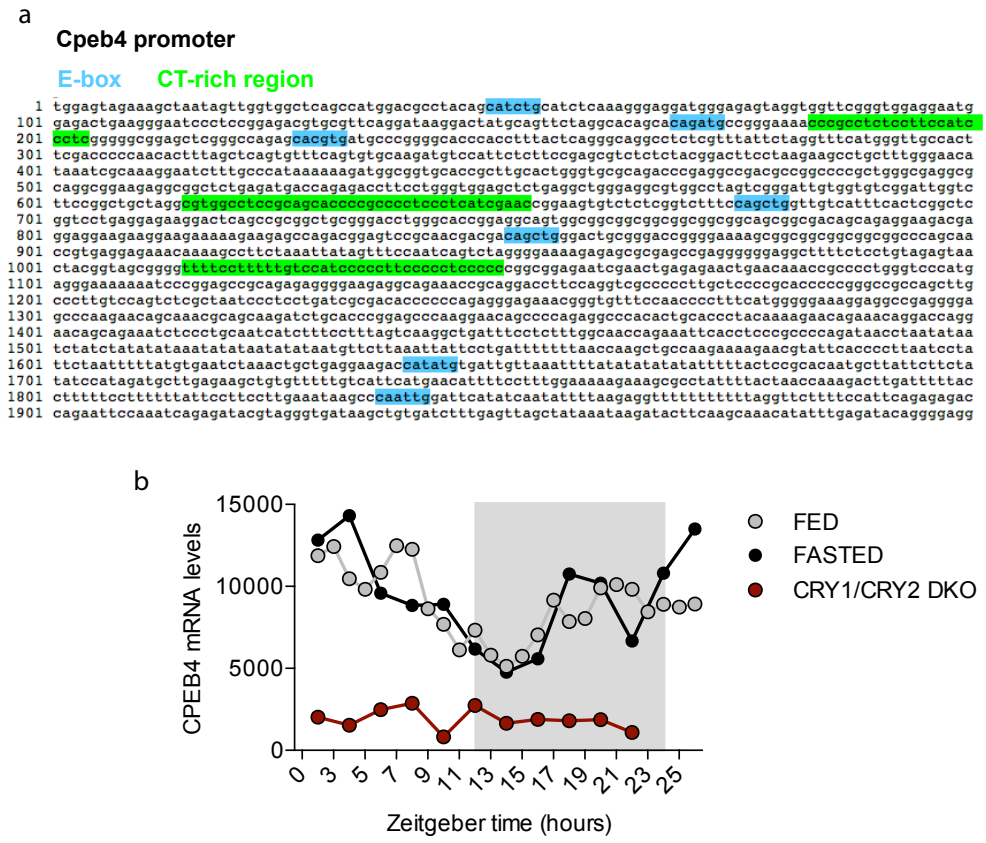

Figure 26. *Cpeb4* mRNA is regulated by the molecular clock. **a**, *Cpeb4* promoter sequence. E-boxes and CT-rich regions are highlighted in blue and in green, respectively. **b**, *Cpeb4* mRNA levels from livers of WT fed or fasted mice, and CRY1/CRY2 double knockout mice at the indicated ZT.

appear to be controlled directly by the liver circadian clock independently of feeding-related signals.

As one of the target mRNAs identified by RIP-seq was *Cry1*, a core component of the molecular clock, we hypothesiezed that CPEB4, apart from regulating ER function, could be controlling the clock rhythmicity. For this purpose, we analysed the circadian rhythmicity of livers and MEFs depleted of CPEB4. Gene expression analysis of the circadian clock genes Per2 and Bmal1 at various times of the day did not reveal any significant difference in the period or amplitude of the clock

oscillations in CPEB4 mutant livers or cells **(Figure 27a,b)**. Therefore, although *Cpeb4* levels are regulated in a circadian manner, *Cpeb4* does not appear to be an intrinsic component of the clock.

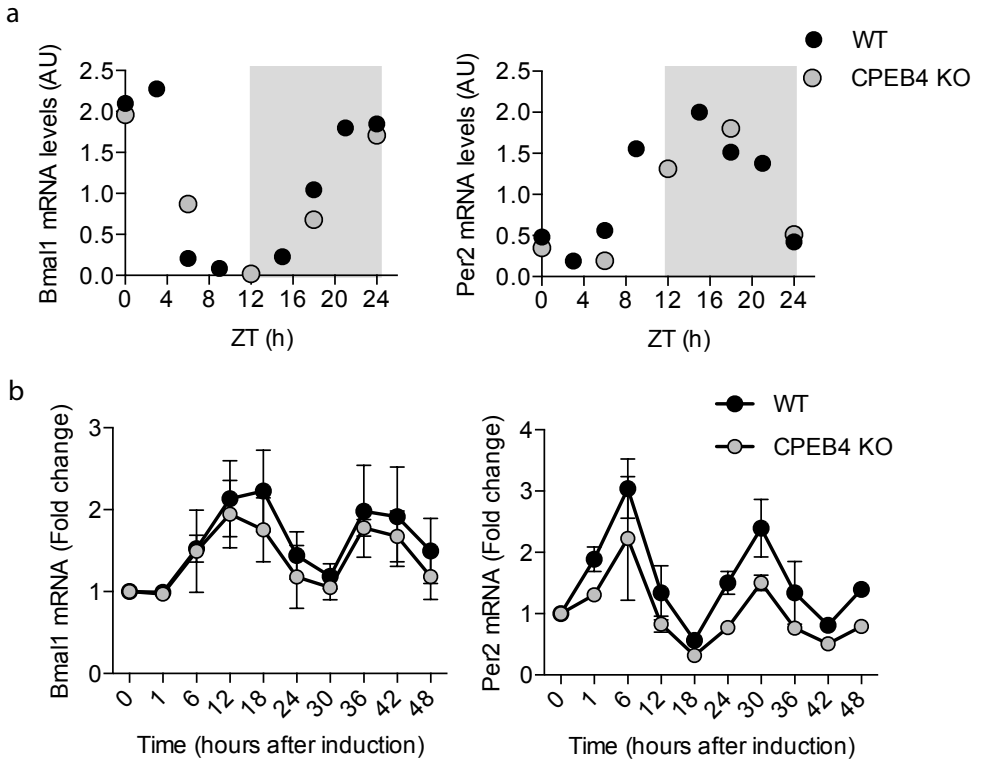

Figure 27. CPEB4 depletion does not affect the rhythmicity of the molecular clock. **a**, Gene expression analysis by qRT-PCR of Bmal1 and Per2 in WT and CPEB4^{KO} mouse livers at the indicated ZT. **b**, Gene expression analysis of the same genes in WT and CPEB4^{KO} MEFs after clock synchronization by a dexamethasone shock, n=3.

Given that *Cpeb4* mRNA is translationally repressed by the uORFs in homeostatic conditions, we reasoned that the fluctuations originated by the clock in *Cpeb4* mRNA could be dampened by the uORF translational repression and that, only upon ER stress, CPEB4 protein levels could gain circadian rhythmicity. Indeed, we

found that the circadian *Cpeb4* mRNA oscillations in the livers of our mice **(Figure 28a)** were not reflected at the protein level **(Figure 28b)**. However, upon TM-induced ER-stress CPEB4 protein levels increased in a circadian fashion **(Figure 28c).** Thus, we detected greater CPEB4 protein induction by TM at the time of the day when *Cpeb4* mRNA levels peaked (ZT2), compared to when it reached its trough (ZT14). These oscillations were not the consequence of a differential UPR induction as phospho-eIF2α and ATF4 levels were comparable.

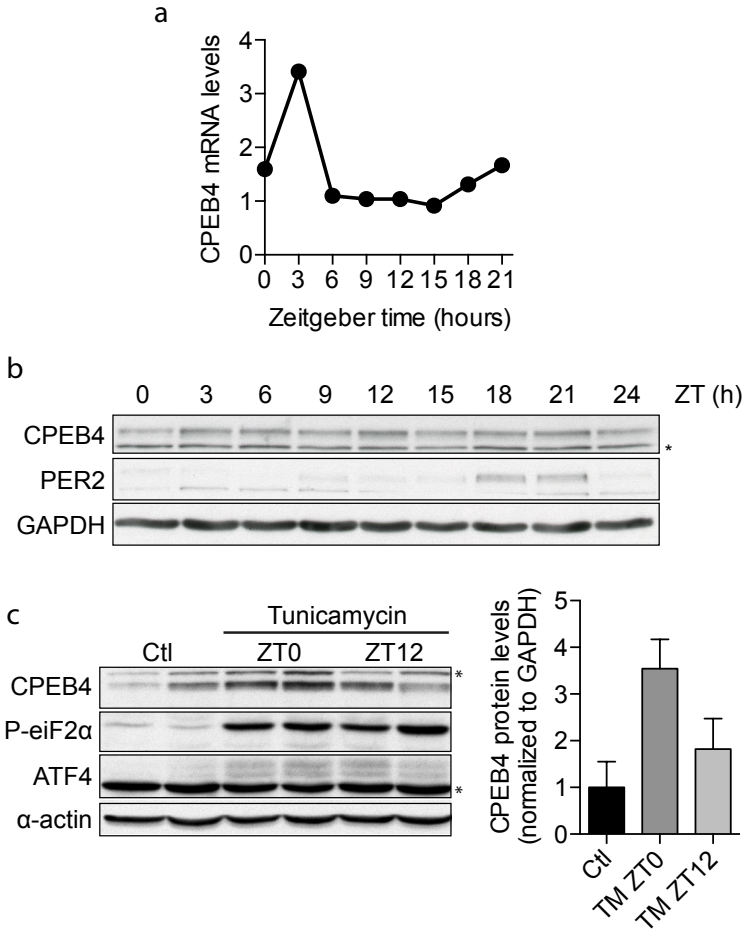

Figure 28. The circadian clock regulates the UPR-mediated CPEB4 activation. **a**, *Cpeb4* mRNA

levels in fed WT mice liver extracts at the indicated ZTs. **b**, Immunoblot for the indicated proteins from the same livers. **c**, Left: Immunoblot for the indicated proteins in liver extracts from mice treated with 1μg TM/g of animal and killed 4 hours after. The ZT of the injections are indicated. Right: quantification of normalized band intensities.

These data suggest that *Cpeb4* mRNA oscillation confers circadian sensitivity to the CPEB4-branch of the UPR response. Therefore, the circadian clock increases the "CPEB4-potential" activity during the morning, the time of the day when hepatocytes are under maximal secretory demand. This mechanism presumably allows hepatic cells to anticipate the ER stress caused by periods of great synthetic demand.

13. CPEB1/CPEB4 double knockout mice develop hepatosteatosis

According to these and previously published data, CPEB1 and CPEB4 regulate different aspects of the hepatic metabolism in such way that depletion of CPEB1 leads to hepatic insulin resistance (Alexandrov et al., 2012) while CPEB4 absence results in hepatic steatosis upon metabolic stress. Because insulin resistance can indirectly promote hepatic steatosis through increased lipogenesis and fatty acid availability, a similar condition that the one generated by HFD feeding, we next sought to investigate the phenotypic consequences of losing both regulatory activities at the same time. Thus, we mated CPEB4$^{+/-}$ with CPEB1$^{+/-}$ mice in order to obtain CPEB1/CPEB4 double knockout mice (CPEB1/4^{DKO}). Crosses between double heterozygous mice (CPEB1$^{+/-}$ CPEB5$^{+/-}$) gave rise to all six different genotypes expected. However, only 30% of the expected double-knockout mice survived the two firs weeks of age. Strikingly, all the surviving double-knockout mice presented sings of aberrant lipid accumulation in their livers as early as two months of age as observed by H&E staining of livers **(Figure 31a)** even when fed

a normal diet.

These data suggest that in a context of CPEB4 absence, the insulin resistance condition generated by the depletion of CPEB1 accelerates and worsens the

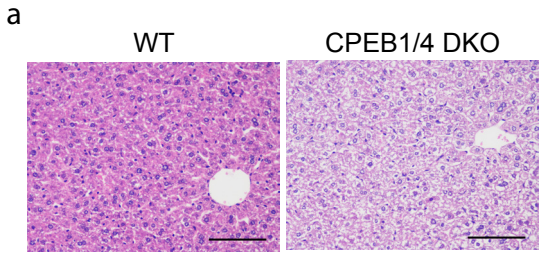

development of hepatic steatosis.

Figure 29. CPEB1/4 DKO mice develop hepatic steatosis. **a**, Representative H&E staining of liver sections from WT and CPEB1/4DKO mice 8 weeks old fed a normal diet.

Discussion

1. A novel regulatory branch of the UPR is orchestrated by CPEB4

During aging or metabolic stress, such as HFD, liver cells undergo ER stress giving rise to UPR signalling in order to maintain tissue homeostasis (Hummasti and Hotamisligil, 2010) (Brown and Naidoo, 2012). The UPR activation leads to phosphorylation of eIF2α, thereby attenuating general protein synthesis, limiting the protein load and helping cells to adapt to ER stress (Wang and Kaufman, 2016). Paradoxically, phosphorylated eIF2α selectively increases translation of mRNAs that harbour uORFs in their 5' UTR, such as *Atf4*, *Atf5* and *Chop* mRNAs. This translational mechanism allows the deployment of a gene expression program aimed to resolve the accumulation of unfolded proteins by decreasing the number of client proteins at the ER while simultaneously increasing the amount of a group of proteins involved in the folding, maturation and removal of misfolded proteins (Kaufman, 2002). In this study, we unveiled a novel adaptive translational response to ER stress mediated by the RNA-binding protein CPEB4. This new arm of the UPR is distinct and complementary to previously described branches, and it is essential to maintain cellular homeostasis and survival in conditions of ER stress **(Figures 20 and 21).** Thus, upon ER stress, CPEB4 mediates the translational activation of mRNAs that encode a group of proteins enriched in chaperones and other proteins implicated in ER homeostasis **(Figure 17) (Table 1)**.

Thus, we found that, upon UPR activation and eIF2α phosphorylation not only uORF-containing mRNAs are transnationally stimulated, but also CPE-regulated transcripts are activated **(Figure 25)**. Indeed, the CPE-mediated translational activation during stress is mechanistically independent of the presence of uORFs, as reporter mRNAs containing CPE-elements but not uORFs get activated upon TG treatment. Interestingly, we also found that the two mechanisms are highly intertwined, as CPEB4, the direct mediator of the CPE-mediated activation, is itself a uORF-regulated mRNA. Moreover, both regulatory elements (uORFs and

CPEs) coexist in various mRNAs, such as *Txnip*, *Hyou1* and *Cpeb4*. We consider that it will be worth investigating the extent of the regulatory interaction between the CPEs and the uORFs, and how they synergize to fine-tune the production of proteins during ER stress.

2. CPEB4 drives the activation of CPE-containing transcripts

In line with previous reports (Igea and Mendez, 2010) (Ortiz-Zapater et al., 2012) (Novoa et al., 2010), we find that CPEB4 mediates the translational activation of target mRNAs, even its own **(Figures 23a and 25a) (Table 1).** However, a recent study described a repressive function of CPEB4 on mRNA translation during erythroid differentiation (Hu et al., 2014). It is important to note that in the latter, to unveil the molecular mechanism of CPEB4 regulation, the authors used exogenously overexpressed CPEB4 protein way above the physiological levels. In our experience, the overexpression of CPEB4 or any other CPEB leads to experimental artifacts such as protein aggregation and cell death. Since these conditions make the interpretation of the experiments very complicated, we consider that there could be alternative mechanistic explanations for the molecular basis of CPEB4 function during erythroid differentiation. Therefore, we consider that in mammalian cells, and contrary to CPEB1, CPEB4 most likely only activates translation of target mRNAs.

But, why is CPEB4-mediated cytoplasmic polyadenylation so crucial during stressful conditions? It is known that poly(A) tail lengthening increases the capacity of an mRNA to recruit the ribosomal machinery, thereby increasing its translation efficiency. However, in homeostatic conditions, subtle changes in the length of the poly(A) tail may only have a modest impact on the translation efficiency of the mRNA due to the great abundance of the translation initiation complexes which are available even for the low efficient transcripts. On the contrary, during

ER stress, the big drop in TC availability makes the number of transcripts per initiation complex to increase dramatically. These new scenario generates enormous competition among the mRNAs for the translation resources thereby greatly benefiting the mRNAs which are highly efficient in the recruitment of the ribosome. Under these circumstances, changes in the poly(A) tail length, and thus in the translation efficiency, may really make the difference between been translated or not.

The CPEBs, and in particular CPEB4, have been shown to be essential during the meiotic and mitotic cell cycle. Interestingly, a recent report demostrated that during the mitotic phase of the cell cycle cap-mediated translation is inhibited (Pyronnet, 2001), therefore generating a similar translational conditions as ER stress. According to this model, we predict that CPEB-mediated regulation would become an essential regulatory mechanism under any condition that increases transcript competition for the translational aparatus.

3. The strong connection between CPEB4 and the cellular secretory system

Although previous studies already hinted at the potential link between CPEB4 and ER function, the relevance and mechanistic details of this connection have remained unexplored. The ER-specific location of CPEB4 was originally observed in cultured neurons (Kan et al., 2010). Intriguingly, upon TG treatment, the authors observed a quick relocalization of CPEB4 from the ER to the nucleus. Not only do we not observe this effect in any of our experimental systems, but also we suspect that the nuclear localization of CPEB4 might be provoked by the extremely high doses of TG used in those experiments (10μM, one or two orders of magnitude higher than the standard) that probably lead to an extreme stress response followed by an abrupt cell death; alternatively, we also think that given the highly specialized nature of neurons it is plausible that their regulatory mechanisms differ from other

cell types.

In another study, researchers reported the direct interaction between CPEB4 and BiP in a high-throughput screening in astrocytic tumor cells (Chen et al., 2015). Since BiP is exclusively localized inside the lumen of the ER and mRNAs cannot cross the ER membrane, we find the interpretation of these results fairly complicated. Further analysis would be needed in order to validate this interaction and to explore its biological relevance.

Given that we have also demonstrated ER-specific CPEB4 localization in mouse hepatocytes and probably MEFs **(Figure 16a,b)**, we suspect that this subcellular localization of CPEB4 might be conserved across cell types. In the same direction, the only two validated CPEB4 targets described in previous studies are secreted proteins [VEGFα (Calderone et al., 2016) and TPA (Ortiz-Zapater et al., 2012) in endothelial and pancreatic tumoral cells, respectively], which are synthesized, maturated and transported at the ER, further supporting the strong connection between CPEB4 and the secretory system.

4. The circadian clock modulates the hepatic function of CPEB4

In this study we also found that a second regulatory mechanism impacts and conditions the UPR-mediated regulation of CPEB4 levels and activity. Thus, we showed that the translational regulation exerted by the UPR on CPEB4 protein levels is dependent on the circadian oscillating *Cpeb4* mRNA levels in liver **(Figure 28)**, thus leading to changes in the amplitude of the CPEB4 response to ER stress along the day.

Through the analysis of published genome-wide datasets (Cretenet et al., 2010) we unveiled that *Cpeb4* transcription is directly regulated by the peripheral molecular clock in liver **(Figure 26b)**. Hepatic circadian gene expression has been shown

to be controlled both by the central clock (located in the supachiasmatic nucleus of the brain) or by the hepatic peripheral clock (located in every liver cell). The regulation exerted by the central clock on liver transcripts is indirect and mediated by changes in the feeding behaviour of the animal. Given that CPEB4 oscillations are maintained both in fed and fasting conditions, but are lost in clock-deficient mice, reveals that the peripheral clock is the direct mediator of *Cpeb4* mRNA oscillations. Moreover, the presence of CLOCK-binding sites within the *Cpeb4* gene promoter **(Figure 26a)** further support this conclusion.

Although previous reports had already revealed the circadian expression and translation of *Cpeb4* mRNA (Kojima et al., 2012) (Janich et al., 2015), to our knowledge, this is the first time that the functional relevance of these oscillations is addressed. Although there are many of biological advantages in synchronizing an ER-protective mechanism to the daily oscillations in hepatic metabolism, it remains to be explored why hepatocytes rely more on the CPEB4 system at earlier times of the day than at night. We speculate that, since the hepatic protein secretion rhythms peak in the morning (Mauvoisin et al., 2014), precisely when *Cpeb4* mRNA level reaches its maximum, the circadian clock might work to protect the ER integrity by increasing the CPEB4-mediated ER stress response when protein synthesis demand is at its highest.

5. The distinctive role of CPEB4 inside the CPEB-family

Although all four members of the CPEB-family bind the same CPE-element (Afroz et al., 2014), thereby having theoretical overlapping mRNA target populations (Igea and Mendez, 2010; Novoa et al., 2010), CPEB4 is the only member whose expression is regulated by ER stress **(Figure 24),** and the only one acting as a crucial regulator in UPR. In fact, and to our knowledge, this CPEB4 function in stress response has no precedent among RNA-binding proteins. On the other hand, our results demonstrate a functional interaction between CPEB1 and CPEB4 in

the regulation of hepatic metabolism **(Figure 29)**. The simultaneous depletion of CPEB1 and CPEB4 aggravates the phenotypes present in CPEB4^{KO} mice, thereby indicating that the two CPEBs cooperate, although by different mechanisms, to maintain proper hepatic metabolism.

From an evolutionary perspective, the diversification of functions between the CPEB paralogs would allow organisms to increase their genetic regulatory potential. It is interesting to note that, while evolution has conserved the same RNA-binding specificity for the different CPEBs, especially among CPEB2-4 (Afroz et al., 2014), their N-terminal regulatory domain (NTD) has undergone strong sequence divergence. As a result, while all the CPEBs bind the same mRNA targets, they are subject to distinct regulatory inputs through diverse post-translational modifications in their NTD. In addition, not all the CPEBs are simultaneously expressed in all cell types.

In our view, this differential regulation endows the CPEB-family with the potential to build up complex regulatory networks that modulate the translation of CPE-containing mRNAs based on information integrated from various signalling pathways. Interestingly, the mRNAs encoding the CPEBs harbour CPE-elements in their 3' UTRs, thereby generating cross-regulatory interactions that could confer robustness and flexibility to the network.

6. CPEB4 protects from NAFLD development

This work also underscores that the CPEB4-regulated branch of the UPR could have substantial implications in the pathogenesis of non-alcoholic fatty liver disease (NAFLD), one of the most common causes of chronic liver disease that can progress to non-alcoholic steatohepatitis (NAS), fibrosis, cirrhosis and liver cancer (Angulo, 2002; Michelotti et al., 2013). Strikingly, in the US, NAFLD is currently the second leading cause of liver transplantation, and it is expected

to rise in the coming decades. In spite of its alarming prevalence and the fatal progression that it entails, there is currently not a single pharmacological treatment approved for NAFLD (Angulo, 2002). Therefore, improving our understanding of the molecular basis of the disease is key for the development of treatments and diagnostic techniques, which is becoming a global health priority.

In our study, we believe that we have deepen our understanding of the pathophysiological mechanisms that originate NAFLD by uncovering a new genetic regulatory circuit that is essential to prevent abnormal hepatic lipid accumulation in liver. Therefore, we found that during the increase in hepatic ER stress caused by age or HFD-feeding, CPEB4-mediated translation is required to sustain mitochondrial respiration and β-oxidation **(Figure 16c,e,f)** and hepatic lipoprotein secretion **(Figure 16j)**. In the absence of CPEB4, hepatocytes are rendered susceptible to metabolic stress thereby accumulating excessive amounts of lipids.

We think that our results could help in the identification of potential therapeutic targets for this life-threatening disease. To advance in this direction, further experiments will be needed to address whether the artificially activation of the CPEB4-pathway in steatotic livers could serve as a protective mechanism from uncontrolled ER stress and lipid accumulation in conditions of hyper-nutrition or advanced age. Unpublished results from our lab have unveiled that CPEB4 activation relies on the hyper-phosphorylation of its N-terminal domain. Interestingly, we suspect that the UPR not only triggers a rise in CPEB4 levels but also in its phosphorylation status, as revealed by a shift in the mobility of CPEB4 upon TG treatment **(Figure 23a).** Investigating the kinase(s) responsible of such phosphorylation will greatly contribute the development of CPEB4-targeted therapies.

Contrary to CPEB1 function in insulin signalling, we found that CPEB4 is

mostly involved in lipid metabolism. However, we did detect and increase in the gluconeogenic capacity of CPEB4-depleted livers upon pyruvate administration **(Figure 13h)**. This contrasts with the normal glucose production observed upon glucagon stimulation in mice **(Figure 13f)** or primary hepatocytes **(Figure 13g)** depleted of CPEB4. We think that these results could reflect a glucose metabolism defect in CPEB4^{KO} cells that is only revealed upon conditions of gluconeogenic-substrate saturation. However, since these conditions rarely occur in any physiological contexts, we do not consider the function of CPEB4 a major determinant of glucose metabolism.

The relevance of CPEB4 in human disease is further supported by the identification, through Genome Wide Association Studies (GWAS), of several single nucleotide polymorphisms (SNPs) within the *Cpeb4* gene associated to human pathology. There are two genetic variants of *Cpeb4* (Rs6861681 and Rs1106693) that strongly correlate with obesity-related traits (Heid et al., 2010) (Comuzzie et al., 2012). And there are two more (Rs17695092 and Rs17763373) associated to inflammatory and prion-derived diseases (Jostins et al., 2012) (Mead et al., 2012), two disorders characterized to be highly dependent on ER stress and the UPR pathway. Importantly, every SNP identified within the *Cpeb4* gene is located in intronic regions, indicating that these variants might affect the production or the nuclear proccessing of the *Cpeb4* mRNA, thereby altering the levels of CPEB4 protein or favouring the production of alternative isoforms. It would be interesting to test whether individuals with the different variants present changes in the CPEB4 protein, which could endow them with different susceptibilities to ER stress.

There is increasing evidence that the UPR is closely associated with cell differentiation (Reimold AM et al., 2001) (Zhang K1, 2005), stem cell functions (van Galen et al., 2014) (Mohrin M et al., 2015) (Wang et al., 2014), and cancer development and vascularization (Clarke et al., 2014), processes for which high CPEB4 levels are

also required (Hu et al., 2014) (Garcia-Pras et al., 2016) (Ortiz-Zapater et al., 2012) (Calderone et al., 2016). In fact, CPEB4 is essential during embryonic terminal erythroid differentiation (Hu et al., 2014) and its depletion during this process leads to partial early neonatal lethality. Interestingly, mice knockout of components of the PERK-signaling axis of the UPR also present perinatal lethality (Scheuner D et al., 2001). Mice knockout for PERK or non-phophorilable mutants of eIF2α die very early after birth of hypoglycemia associated with defective hepatic gluconeogenesis(Scheuner D et al., 2001). It would be very interesting to test whether ER stress-derived hypoglycemia contributes to the demise of CPEB4-depleted newborns.

In conclusion, this study has unveiled a novel role of CPEB4 in the UPR pathway *in vivo*. This novel CPEB4-driven adaptive response to ER stress adds an important player in the UPR field and might be critical for understanding the pathogenesis of NAFLD and other diseases.

Conclusions

The present study identifies CPEB4 as a novel regulatory component of the UPR pathway thereby uncovering a novel translational regulation mechanism that is key for cellular ER stress adaptation. Furthermore, we have found that this gene regulatory mechanism is biologically relevant and prevents the development of hepatic steatosis in mice.

The main conclusions reached in this study are the following:

1. CPEB4 ubiquitous knockout mice develop hepatic steatosis upon aging or high-fat diet feeding.

2. The prevention of hepatic steatosis mediated by CPEB4 is a cell autonomous mechanism.

3. CPEB4-depleted hepatocytes show impaired mitochondrial respiration, FFA β-oxidation and VLDL secretion.

4. In liver, CPEB4 preferentially binds transcripts encoding proteins involved in ER homeostasis. Although it is located at the ER, CPEB4 does not control mRNA localization.

5. The absence of CPEB4 renders cells vulnerable to HFD- or TM-induced ER stress.

6. CPEB4 is translationally and transcriptionally induced by the UPR signalling cascade, and this regulation is not shared by any other CPEB.

7. The 5' UTR of *Cpeb4* mRNA confers translational activity during conditions of ER stress and eIF2α phosphorylation.

8. ER stress triggers the translational activation of CPE-containing mRNAs by a mechanism independent of uORFs and mediated by CPEB4.

9. *Txnip* mRNA translation is activated by CPEB4 during ER stress.

10. The mRNA levels of CPEB4 are circadianly controlled by the hepatic molecular clock, which provides a temporal regulation of the UPR-mediated activation of CPEB4.

11. CPEB1 and CPEB4 cooperate through independent mechanisms to maintain hepatic metabolism homeostasis.

References

Afroz, T., Skrisovska, L., Belloc, E., Guillen-Boixet, J., Mendez, R., and Allain, F.H.T. (2014). A fly trap mechanism provides sequence-specific RNA recognition by CPEB proteins. Genes & Development *28*, 1498-1514.

Aguilera, A. (2005). Cotranscriptional mRNP assembly: from the DNA to the nuclear pore. Curr Opin Cell Biol *17*, 242-250.

Alexandrov, I.M., Ivshina, M., Jung, D.Y., Friedline, R., Ko, H.J., Xu, M., O'Sullivan-Murphy, B., Bortell, R., Huang, Y.T., Urano, F.*, et al.* (2012). Cytoplasmic polyadenylation element binding protein deficiency stimulates PTEN and Stat3 mRNA translation and induces hepatic insulin resistance. PLoS Genet *8*, e1002457.

Anderson, N., and Borlak, J. (2008). Molecular mechanisms and therapeutic targets in steatosis and steatohepatitis. Pharmacol Rev *60*, 311-357.

Angulo, P. (2002). Nonalcoholic Fatty Liver Disease. N Engl J Med *346*, 1221-1231.

Asher, G., and Schibler, U. (2011). Crosstalk between components of circadian and metabolic cycles in mammals. Cell Metab *13*, 125-137.

Atger, F., Gobet, C., Marquis, J., Martin, E., Wang, J., Weger, B., Lefebvre, G., Descombes, P., Naef, F., and Gachon, F. (2015). Circadian and feeding rhythms differentially affect rhythmic mRNA transcription and translation in mouse liver. Proc Natl Acad Sci U S A *112*, E6579-6588.

Atkins, C.M., Nozaki, N., Shigeri, Y., and Soderling, T.R. (2004). Cytoplasmic polyadenylation element binding protein-dependent protein synthesis is regulated by calcium/calmodulin-dependent protein kinase II. J Neurosci *24*, 5193-5201.

Barnard, D.C., Ryan, K., Manley, J.L., and Richter, J.D. (2004). Symplekin and xGLD-2 are required for CPEB-mediated cytoplasmic polyadenylation. Cell *119*, 641-651.

Bass, J., and Takahashi, J.S. (2010). Circadian integration of metabolism and energetics. Science *330*, 1349-1354.

Bava, F.A., Eliscovich, C., Ferreira, P.G., Minana, B., Ben-Dov, C., Guigo, R., Valcarcel, J., and Mendez, R. (2013). CPEB1 coordinates alternative 3'-UTR formation with translational regulation. Nature *495*, 121-125.

Belloc, E., and Mendez, R. (2008). A deadenylation negative feedback mechanism governs meiotic metaphase arrest. Nature *452*, 1017-1021.

Berlanga, J.J., Santoyo, J., and De Haro, C. (1999). Characterization of a mammalian homolog of the GCN2 eukaryotic initiation factor 2alpha kinase. Eur J Biochem *265*, 754-762.

Bertolotti, A., Zhang, Y., Hendershot, L., Harding, H., and Ron, D. (2000). Dynamic interaction of BiP and ER stress transducers in the unfolded-protein response. Nat Cell Biol *2*, 326-332.

Birky, T.L., and Bray, M.S. (2014). Understanding circadian gene function: animal models of tissue-specific circadian disruption. IUBMB Life *66*, 34-41.

Boustani, M.R., Mehrabi, F., Yahaghi, E., Khoshnood, R.J., Shahmohammadi, M., Darian, E.K., and Goudarzi, P.K. (2016). Somatic CPEB4 and CPEB1 genes mutations spectrum on the prognostic predictive accuracy in patients with high-grade glioma and their clinical significance. J Neurol Sci *363*, 80-83.

Bray, M.S., and Young, M.E. (2011). Regulation of fatty acid metabolism by cell autonomous circadian clocks: time to fatten up on information? J Biol Chem *286*, 11883-11889.

Brown, M.K., and Naidoo, N. (2012). The endoplasmic reticulum stress response in aging and age-related diseases. Front Physiol *3*, 263.

Browning, J.D., and Horton, J.D. (2004). Molecular mediators of hepatic steatosis and liver injury. Journal of Clinical Investigation *114*, 147-152.

Burns, D.M., and Richter, J.D. (2008). CPEB regulation of human cellular senescence, energy metabolism, and p53 mRNA translation. Genes Dev *22*, 3449-3460.

Calderone, V., Gallego, J., Fernandez-Miranda, G., Garcia-Pras, E., Maillo, C., Berzigotti, A., Mejias, M., Bava, F.-A., Angulo-Urarte, A., Graupera, M.*, et al.* (2016). Sequential Functions of CPEB1 and CPEB4 Regulate Pathologic Expression of Vascular Endothelial Growth Factor and Angiogenesis in Chronic Liver Disease. Gastroenterology *150*, 982-997.e930.

Calfon, M., Zeng, H., Urano, F., Till, J.H., Hubbard, S.R., Harding, H.P., Clark, S.G., and Ron, D. (2002). IRE1 couples endoplasmic reticulum load to secretory capacity by processing the XBP-1 mRNA. Nature *415*, 92-96.

Chang, Y.W., and Huang, Y.S. (2014). Arsenite-activated JNK signaling enhances CPEB4-Vinexin interaction to facilitate stress granule assembly and cell survival. PLoS One *9*, e107961.

Chen, P.J., and Huang, Y.S. (2012). CPEB2-eEF2 interaction impedes HIF-1alpha RNA translation. EMBO J *31*, 959-971.

Chen, W., Hu, Z., Li, X.Z., Li, J.L., Xu, X.K., Li, H.G., Liu, Y., Liu, B.H., Jia, W.H., and Li, F.C. (2015). CPEB4 interacts with Vimentin and involves in progressive features and poor prognosis of patients with astrocytic tumors. Tumour Biol.

Chitnis, N., Pytel, D., and Diehl, J.A. (2013). UPR-inducible miRNAs contribute to stressful situations. Trends in Biochemical Sciences *38*, 447-452.

Cho, H., Zhao, X., Hatori, M., Yu, R.T., Barish, G.D., Lam, M.T., Chong, L.W.,

DiTacchio, L., Atkins, A.R., Glass, C.K., *et al.* (2012). Regulation of circadian behaviour and metabolism by REV-ERB-alpha and REV-ERB-beta. Nature *485*, 123-127.

Clarke, H.J., Chambers, J.E., Liniker, E., and Marciniak, S.J. (2014). Endoplasmic reticulum stress in malignancy. Cancer Cell *25*, 563-573.

Cnop, M., Foufelle, F., and Velloso, L.A. (2012). Endoplasmic reticulum stress, obesity and diabetes. Trends in Molecular Medicine *18*, 59-68.

Comuzzie, A.G., Cole, S.A., Laston, S.L., Voruganti, V.S., Haack, K., Gibbs, R.A., and Butte, N.F. (2012). Novel genetic loci identified for the pathophysiology of childhood obesity in the Hispanic population. PLoS One *7*, e51954.

Cretenet, G., Le Clech, M., and Gachon, F. (2010). Circadian clock-coordinated 12 Hr period rhythmic activation of the IRE1alpha pathway controls lipid metabolism in mouse liver. Cell Metab *11*, 47-57.

Crick, F. (1970). Central Dogma of Molecular Biology. Nature *227*, 561-563.

Crick, F.H.C. (1958). On protein synthesis. Symp Soc Exp biol *XII*, 138.163.

Deng, J., Liu, S., Zou, L., Xu, C., Geng, B., and Xu, G. (2012). Lipolysis Response to Endoplasmic Reticulum Stress in Adipose Cells. Journal of Biological Chemistry *287*, 6240-6249.

Di Giammartino, D.C., Nishida, K., and Manley, J.L. (2011). Mechanisms and consequences of alternative polyadenylation. Mol Cell *43*, 853-866.

Douris, N., Kojima, S., Pan, X., Lerch-Gaggl, A.F., Duong, S.Q., Hussain, M.M., and Green, C.B. (2011). Nocturnin regulates circadian trafficking of dietary lipid in intestinal enterocytes. Curr Biol *21*, 1347-1355.

Drisaldi, B., Colnaghi, L., Fioriti, L., Rao, N., Myers, C., Snyder, A.M., Metzger, D.J., Tarasoff, J., Konstantinov, E., Fraser, P.E., *et al.* (2015). SUMOylation Is an Inhibitory Constraint that Regulates the Prion-like Aggregation and Activity of CPEB3. Cell reports *11*, 1694-1702.

Eckel-Mahan, K.L., Patel, V.R., Mohney, R.P., Vignola, K.S., Baldi, P., and Sassone-Corsi, P. (2012). Coordination of the transcriptome and metabolome by the circadian clock. Proc Natl Acad Sci U S A *109*, 5541-5546.

Elkon, R., Ugalde, A.P., and Agami, R. (2013). Alternative cleavage and polyadenylation: extent, regulation and function. Nat Rev Genet *14*, 496-506.

Fabbrini, E., Sullivan, S., and Klein, S. (2010). Obesity and nonalcoholic fatty liver disease: biochemical, metabolic, and clinical implications. Hepatology *51*, 679-689.

Feldstein, A. (2010). Novel insights into the pathophysiology of nonalcoholic fatty liver disease. Semin Liver Dis *30*, 393-401.

Fernandez-Miranda, G., and Mendez, R. (2012). The CPEB-family of proteins, translational control in senescence and cancer. Ageing research reviews *11*, 460-472.

Fioriti, L., Myers, C., Huang, Y.Y., Li, X., Stephan, J.S., Trifilieff, P., Colnaghi, L., Kosmidis, S., Drisaldi, B., Pavlopoulos, E., *et al.* (2015). The Persistence of Hippocampal-Based Memory Requires Protein Synthesis Mediated by the Prion-like Protein CPEB3. Neuron *86*, 1433-1448.

Fong, S.W., Lin, H.C., Wu, M.F., Chen, C.C., and Huang, Y.S. (2016). CPEB3 Deficiency Elevates TRPV1 Expression in Dorsal Root Ganglia Neurons to Potentiate Thermosensation. PLoS One *11*, e0148491.

Fu, S., Watkins, S.M., and Hotamisligil, G.S. (2012). The role of endoplasmic

reticulum in hepatic lipid homeostasis and stress signaling. Cell Metab *15*, 623-634.

Fu, Y., Dominissini, D., Rechavi, G., and He, C. (2014). Gene expression regulation mediated through reversible m(6)A RNA methylation. Nat Rev Genet *15*, 293-306.

Gachon, F., and Bonnefont, X. (2010). Circadian clock-coordinated hepatic lipid metabolism: only transcriptional regulation? Aging *2*, 101-106.

Galabru, J., Katze, M.G., Robert, N., and Hovanessian, A.G. (1989). The binding of double-stranded RNA and adenovirus VAI RNA to the interferon-induced protein kinase. Eur J Biochem *178*, 581-589.

Gao, X., Wan, J., Liu, B., Ma, M., Shen, B., and Qian, S.B. (2015). Quantitative profiling of initiating ribosomes in vivo. Nat Methods *12*, 147-153.

Garbarino-Pico, E., and Green, C.B. (2007). Posttranscriptional regulation of mammalian circadian clock output. Cold Spring Harb Symp Quant Biol *72*, 145-156.

Garcia-Pras, E., Gallego, J., Coch, L., Mejias, M., Fernandez-Miranda, G., Pardal, R., Bosch, J., Mendez, R., and Fernandez, M. (2016). Role and therapeutic potential of vascular stem/progenitor cells in pathological neovascularisation during chronic portal hypertension. Gut.

Gentile, C.L., Frye, M., and Pagliassotti, M.J. (2011). Endoplasmic reticulum stress and the unfolded protein response in nonalcoholic fatty liver disease. Antioxid Redox Signal *15*, 505-521.

Gerstberger, S., Hafner, M., and Tuschl, T. (2014). A census of human RNA-binding proteins. Nat Rev Genet *15*, 829-845.

Giangarra, V., Igea, A., Castellazzi, C.L., Bava, F.A., and Mendez, R. (2015). Global Analysis of CPEBs Reveals Sequential and Non-Redundant Functions in Mitotic

Cell Cycle. PLoS One *10*, e0138794.

Glisovic, T., Bachorik, J.L., Yong, J., and Dreyfuss, G. (2008). RNA-binding proteins and post-transcriptional gene regulation. FEBS Lett *582*, 1977-1986.

Gray, N.K., and Wickens, M. (1998). Control of translation initiation in animals. Annual review of cell and developmental biology *14*, 399-458.

Hagele, S., Kuhn, U., Boning, M., and Katschinski, D.M. (2009). Cytoplasmic polyadenylation-element-binding protein (CPEB)1 and 2 bind to the HIF-1alpha mRNA 3'-UTR and modulate HIF-1alpha protein expression. Biochem J *417*, 235-246.

Hake, L.E., Mendez, R., and Richter, J.D. (1998). Specificity of RNA binding by CPEB: requirement for RNA recognition motifs and a novel zinc finger. Mol Cell Biol *18*, 685-693.

Halbeisen, R.E., Galgano, A., Scherrer, T., and Gerber, A.P. (2008). Post-transcriptional gene regulation: from genome-wide studies to principles. Cell Mol Life Sci *65*, 798-813.

Harding, H., Zhang, Y., Bertolotti, A., Zeng, H., and Ron, D. (2000). Perk is essential for translational regulation and cell survival during the unfolded protein response. Mol Cell *5*, 897-904.

Harding, H.P., Zhang, Y., Zeng, H., Novoa, I., Lu, P.D., Calfon, M., Sadri, N., Yun, C., Popko, B., Paules, R.*, et al.* (2003). An Integrated Stress Response Regulates Amino Acid Metabolism and Resistance to Oxidative Stress. Molecular Cell *11*, 619-633.

Harding, H.P., Zhang, Y. & Ron, D. (1999). Protein translation and folding are coupled by an endoplasmic-reticulum-resident kinase. Nature *397*, 271-274.

Heid, I.M., Jackson, A.U., Randall, J.C., Winkler, T.W., Qi, L., Steinthorsdottir, V., Thorleifsson, G., Zillikens, M.C., Speliotes, E.K., Magi, R.*, et al.* (2010). Meta-analysis identifies 13 new loci associated with waist-hip ratio and reveals sexual dimorphism in the genetic basis of fat distribution. Nat Genet *42*, 949-960.

Hollien, J., Lin, J.H., Li, H., Stevens, N., Walter, P., and Weissman, J.S. (2009). Regulated Ire1-dependent decay of messenger RNAs in mammalian cells. J Cell Biol *186*, 323-331.

Hotamisligil, G.S. (2010). Endoplasmic Reticulum Stress and the Inflammatory Basis of Metabolic Disease. Cell *140*, 900-917.

Hu, W., Yang, Y., Xi, S., Sai, K., Su, D., Zhang, X., Lin, S., and Zeng, J. (2015). Expression of CPEB4 in Human Glioma and Its Correlations With Prognosis. Medicine (Baltimore) *94*, 979.

Hu, W., Yuan, B., and Lodish, H.F. (2014). Cpeb4-mediated translational regulatory circuitry controls terminal erythroid differentiation. Dev Cell *30*, 660-672.

Huang, Y.S., Carson, J.H., Barbarese, E., and Richter, J.D. (2003). Facilitation of dendritic mRNA transport by CPEB. Genes Dev *17*, 638-653.

Huang, Y.S., Kan, M.C., Lin, C.L., and Richter, J.D. (2006). CPEB3 and CPEB4 in neurons: analysis of RNA-binding specificity and translational control of AMPA receptor GluR2 mRNA. EMBO J *25*, 4865-4876.

Hummasti, S., and Hotamisligil, G.S. (2010). Endoplasmic reticulum stress and inflammation in obesity and diabetes. Circ Res *107*, 579-591.

Igea, A., and Mendez, R. (2010). Meiosis requires a translational positive loop where CPEB1 ensues its replacement by CPEB4. EMBO J *29*, 2182-2193.

Itoh, N., and Okamoto, H. (1980). Translational control of proinsulin synthesis by

glucose. Nature *283*, 100-102.

Ivshina, M., Alexandrov, I.M., Vertii, A., Doxsey, S., and Richter, J.D. (2015). CPEB regulation of TAK1 synthesis mediates cytokine production and the inflammatory immune response. Mol Cell Biol *35*, 610-618.

Ivshina, M., Lasko, P., and Richter, J.D. (2014). Cytoplasmic polyadenylation element binding proteins in development, health, and disease. Annual review of cell and developmental biology *30*, 393-415.

Jackson, R.J., Hellen, C.U., and Pestova, T.V. (2010). The mechanism of eukaryotic translation initiation and principles of its regulation. Nat Rev Mol Cell Biol *11*, 113-127.

Jacob, F., and Monod, J. (1961). Genetic regulatory mechanisms in the synthesis of proteins. J Mol Biol *3*, 318-356.

Janich, P., Arpat, A.B., Castelo-Szekely, V., Lopes, M., and Gatfield, D. (2015). Ribosome profiling reveals the rhythmic liver translatome and circadian clock regulation by upstream open reading frames. Genome Res *25*, 1848-1859.

Jostins, L., Ripke, S., Weersma, R.K., Duerr, R.H., McGovern, D.P., Hui, K.Y., Lee, J.C., Schumm, L.P., Sharma, Y., Anderson, C.A.*, et al.* (2012). Host-microbe interactions have shaped the genetic architecture of inflammatory bowel disease. Nature *491*, 119-124.

JS., O.N., and Reddy, A. (2011). Circadian Clocks in Human Red Blood Cells. Nature *469*, 498-503.

Kaczmarczyk, L., Labrie-Dion, E., Sehgal, K., Sylvester, M., Skubal, M., Josten, M., Steinhauser, C., De Koninck, P., and Theis, M. (2016). New Phosphospecific Antibody Reveals Isoform-Specific Phosphorylation of CPEB3 Protein. PLoS

One *11*.

Kan, M.C., Oruganty-Das, A., Cooper-Morgan, A., Jin, G., Swanger, S.A., Bassell, G.J., Florman, H., van Leyen, K., and Richter, J.D. (2010). CPEB4 is a cell survival protein retained in the nucleus upon ischemia or endoplasmic reticulum calcium depletion. Mol Cell Biol *30*, 5658-5671.

Kaufman, R.J. (2002). Orchestrating the unfolded protein response in health and disease. J Clin Invest *110*, 1389-1398.

Keene, J.D. (2007). RNA regulons: coordination of post-transcriptional events. Nat Rev Genet *8*, 533-543.

Khan, Z., Ford, M.J., Cusanovich, D.A., Mitrano, A., Pritchard, J.K., and Gilad, Y. (2013). Primate transcript and protein expression levels evolve under compensatory selection pressures. Science *342*, 1100-1104.

Kim, J.H., and Richter, J.D. (2006). Opposing polymerase-deadenylase activities regulate cytoplasmic polyadenylation. Mol Cell *24*, 173-183.

Kojima, S., Gendreau, K.L., Sher-Chen, E.L., Gao, P., and Green, C.B. (2015). Changes in poly(A) tail length dynamics from the loss of the circadian deadenylase Nocturnin. Sci Rep *5*, 17059.

Kojima, S., Sher-Chen, E.L., and Green, C.B. (2012). Circadian control of mRNA polyadenylation dynamics regulates rhythmic protein expression. Genes & Development *26*, 2724-2736.

Kornberg, D. (1999). Eukaryotic transcriptional control. Trends in Genetics *15*, 46-49.

Lackner, D.H., and Bähler, J. (2008). Translational Control of Gene Expression: from transcripts to transcriptomes. *271*, 199-251.

Lee, A., Scapa, E., Cohen, D., and Glimcher, L. (2008). Regulation of hepatic lipogenesis by the transcription factor XBP1. Science *320*, 1492-1496.

Lee, A.H., Iwakoshi, N.N., and Glimcher, L.H. (2003). XBP-1 Regulates a Subset of Endoplasmic Reticulum Resident Chaperone Genes in the Unfolded Protein Response. Molecular and Cellular Biology *23*, 7448-7459.

Lin, C.L., Huang, Y.T., and Richter, J.D. (2012). Transient CPEB dimerization and translational control. RNA *18*, 1050-1061.

Lu, L., Han, A.P., and Chen, J.J. (2001). Translation initiation control by heme-regulated eukaryotic initiation factor 2alpha kinase in erythroid cells under cytoplasmic stresses. Mol Cell Biol *21*, 7971-7980.

Maerkeen, K. (2010). Tauroursodeoxycholic Acid May Improve Liver and Muscle but Not Adipose Tissue Insulin Sensitivity in Obese Men and Women. Diabetes *59*, 1899-1905.

Malhi, H., and Kaufman, R.J. (2011). Endoplasmic reticulum stress in liver disease. J Hepatol *54*, 795-809.

Malhotra, J.D., and Kaufman, R.J. (2011). ER stress and its functional link to mitochondria: role in cell survival and death. Cold Spring Harb Perspect Biol *3*.

Mauvoisin, D., Wang, J., Jouffe, C., Martin, E., Atger, F., Waridel, P., Quadroni, M., Gachon, F., and Naef, F. (2014). Circadian clock-dependent and -independent rhythmic proteomes implement distinct diurnal functions in mouse liver. Proc Natl Acad Sci U S A *111*, 167-172.

Mead, S., Uphill, J., Beck, J., Poulter, M., Campbell, T., Lowe, J., Adamson, G., Hummerich, H., Klopp, N., Ruckert, I.M.*, et al.* (2012). Genome-wide association study in multiple human prion diseases suggests genetic risk factors additional to

PRNP. Hum Mol Genet *21*, 1897-1906.

Mendez, R., Hake, L.E., Andresson, T., Littlepage, L.E., Ruderman, J.V., and Richter, J.D. (2000a). Phosphorylation of CPE binding factor by Eg2 regulates translation of c-mos mRNA. Nature *404*, 302-307.

Mendez, R., Murthy, K., Ryan, K., Manley, J., and Richter, J. (2000b). Phosphorylation of CPEB by Eg2 mediates the recruitment of CPSF into an active cytoplasmic polyadenylation complex. Mol Cell *6*, 1253-1259.

Merkel, D.J., Wells, S.B., Hilburn, B.C., Elazzouzi, F., Perez-Alvarado, G.C., and Lee, B.M. (2013). The C-terminal region of cytoplasmic polyadenylation element binding protein is a ZZ domain with potential for protein-protein interactions. J Mol Biol *425*, 2015-2026.

Michelotti, G.A., Machado, M.V., and Diehl, A.M. (2013). NAFLD, NASH and liver cancer. Nat Rev Gastroenterol Hepatol *10*, 656-665.

Minshall, N., Reiter, M.H., Weil, D., and Standart, N. (2007). CPEB interacts with an ovary-specific eIF4E and 4E-T in early Xenopus oocytes. J Biol Chem *282*, 37389-37401.

Mohrin M, Shin J, Liu Y, Brown K, Luo H, Xi Y, Haynes CM, and D., C. (2015). Stem cell aging. A mitochondrial UPR-mediated metabolic checkpoint regulates hematopoietic stem cell aging. Science *347*, 1374-1377.

Moore, M.J. (2005). From birth to death: the complex lives of eukaryotic mRNAs. Science *309*, 1514-1518.

Nagaoka, K., Fujii, K., Zhang, H., Usuda, K., Watanabe, G., Ivshina, M., and Richter, J.D. (2015). CPEB1 mediates epithelial-to-mesenchyme transition and breast cancer metastasis. Oncogene.

Nagaoka, K., Udagawa, T., and Richter, J.D. (2012). CPEB-mediated ZO-1 mRNA localization is required for epithelial tight-junction assembly and cell polarity. Nat Commun *3*, 675.

Novoa, I., Gallego, J., Ferreira, P.G., and Mendez, R. (2010). Mitotic cell-cycle progression is regulated by CPEB1 and CPEB4-dependent translational control. Nature Cell Biology *12*, 447-456.

Oakes, S.A., and Papa, F.R. (2015). The role of endoplasmic reticulum stress in human pathology. Annu Rev Pathol *10*, 173-194.

Orphanides, G., and Reinberg, D. (2002). A unified theory of gene expression. Cell *108*, 439-451.

Ortiz-Zapater, E., Pineda, D., Martinez-Bosch, N., Fernandez-Miranda, G., Iglesias, M., Alameda, F., Moreno, M., Eliscovich, C., Eyras, E., Real, F.X*., et al.* (2012). Key contribution of CPEB4-mediated translational control to cancer progression. Nat Med *18*, 83-90.

Ota, T., Gayet, C., and Ginsberg, H.N. (2008). Inhibition of apolipoprotein B100 secretion by lipid-induced hepatic endoplasmic reticulum stress in rodents. J Clin Invest *118*, 316-332.

Ozcan, U., Cao, Q., Yilmaz, E., Lee, A., Iwakoshi, N., Ozdelen, E., Tuncman, G., Görgün, C., Glimcher, L., and Hotamisligil, G. (2004). Endoplasmic Reticulum Stress Links Obesity, Insulin Action, and Type 2 Diabetes. Science *306*, 457-461.

Ozcan, U., Yilmaz, E., Ozcan, L., Furuhashi, M., Vaillancourt, E., Smith, R.O., Görgün, C.Z., and Hotamisligil, G.S. (2006). Chemical Chaperones Reduce ER Stress and Restore Glucose Homeostasis in a Mouse Model of Type 2 Diabetes. Science *313*, 1137-1140.

Papasaikas, P., and Valcarcel, J. (2016). The Spliceosome: The Ultimate RNA Chaperone and Sculptor. Trends Biochem Sci *41*, 33-45.

Pavitt, G.D., and Ron, D. (2012). New insights into translational regulation in the endoplasmic reticulum unfolded protein response. Cold Spring Harb Perspect Biol *4*.

Pavlopoulos, E., Trifilieff, P., Chevaleyre, V., Fioriti, L., Zairis, S., Pagano, A., Malleret, G., and Kandel, E.R. (2011). Neuralized1 Activates CPEB3: A Function for Nonproteolytic Ubiquitin in Synaptic Plasticity and Memory Storage. Cell *147*, 1369-1383.

Peek, C.B., Affinati, A.H., Ramsey, K.M., Kuo, H.Y., Yu, W., Sena, L.A., Ilkayeva, O., Marcheva, B., Kobayashi, Y., Omura, C.*, et al.* (2013). Circadian Clock NAD+ Cycle Drives Mitochondrial Oxidative Metabolism in Mice. Science *342*.

Peng, W., Nan, Z., Liu, Y., Shen, H., Lin, C., Lin, L., and Yuan, B. (2014). Dendritic cells transduced with CPEB4 induced antitumor immune response. Exp Mol Pathol *97*, 273-278.

Pique, M., Lopez, J.M., Foissac, S., Guigo, R., and Mendez, R. (2008). A combinatorial code for CPE-mediated translational control. Cell *132*, 434-448.

Postic, C., and Girard, J. (2008). Contribution of de novo fatty acid synthesis to hepatic steatosis and insulin resistance: lessons from genetically engineered mice. J Clin Invest *118*, 829-838.

Postic, C., Shiota, M., Niswender, K.D., Jetton, T.L., Chen, Y., Moates, J.M., Shelton, K.D., Lindner, J., Cherrington, A.D., and Magnuson, M.A. (1999). Dual roles for glucokinase in glucose homeostasis as determined by liver and pancreatic beta cell-specific gene knock-outs using Cre recombinase. J Biol Chem *274*, 305-315.

Proud, C.G. (2002). Regulation of mammalian translation factors by nutrients. Eur J Biochem *269*, 5338-5349.

R., L., and AJ., S. (2013). The global NAFLD epidemic. Nat Rev Gastroenterol Hepatol *10*, 686-690.

Raabe, M., Veniant, M.M., Sullivan, M.A., Zlot, C.H., Bjorkegren, J., Nielsen, L.B., Wong, J.S., Hamilton, R.L., and Young, S.G. (1999). Analysis of the role of microsomal triglyceride transfer protein in the liver of tissue-specific knockout mice. J Clin Invest *103*, 1287-1298.

Rao, M.S., and Reddy, J.K. (2001). Peroxisomal β-Oxidation and Steatohepatitis. Semin Liver Dis *21*, 43-55.

Reid, D.W., Chen, Q., Tay, A.S., Shenolikar, S., and Nicchitta, C.V. (2014). The unfolded protein response triggers selective mRNA release from the endoplasmic reticulum. Cell *158*, 1362-1374.

Reimold AM, Iwakoshi NN, Manis J, Vallabhajosyula P, Szomolanyi-Tsuda E, Gravallese EM, Friend D, Grusby MJ, Alt F, and LH., G. (2001). Plasma cell differentiation requires the transcription factor XBP-1. Nature *412*, 300-307.

Reinke, H., and Asher, G. (2016). Circadian Clock Control of Liver Metabolic Functions. Gastroenterology *150*, 574-580.

Richter, J.D., and Coller, J. (2015). Pausing on Polyribosomes: Make Way for Elongation in Translational Control. Cell *163*, 292-300.

Richter, J.D., and Sonenberg, N. (2005). Regulation of cap-dependent translation by eIF4E inhibitory proteins. Nature *433*, 477-480.

Ron, D., and Walter, P. (2007). Signal integration in the endoplasmic reticulum unfolded protein response. Nature Reviews Molecular Cell Biology *8*, 519-529.

Rutkowski, D.T., Arnold, S.M., Miller, C.N., Wu, J., Li, J., Gunnison, K.M., Mori, K., Sadighi Akha, A.A., Raden, D., and Kaufman, R.J. (2006). Adaptation to ER stress is mediated by differential stabilities of pro-survival and pro-apoptotic mRNAs and proteins. PLoS Biol *4*, e374.

Rutkowski, D.T., Wu, J., Back, S.H., Callaghan, M.U., Ferris, S.P., Iqbal, J., Clark, R., Miao, H., Hassler, J.R., Fornek, J.*, et al.* (2008). UPR pathways combine to prevent hepatic steatosis caused by ER stress-mediated suppression of transcriptional master regulators. Dev Cell *15*, 829-840.

Sachs, A.B., Sarnow, P., and Hentze, M.W. (1997). Starting at the beginning, middle, and end: translation initiation in eukaryotes. Cell *89*, 831-838.

Sagara, Y., and Inesi, G. (1991). Inhibition of the sarcoplasmic reticulum Ca2+ transport ATPase by thapsigargin at subnanomolar concentrations. J Biol Chem *266*, 13503-13506.

Scheuner D, Song B, McEwen E, Liu C, Laybutt R, Gillespie P, Saunders T, Bonner-Weir S, and RJ., K. (2001). Translational control is required for the unfolded protein response and in vivo glucose homeostasis. Mol Cell *7*, 1165-1176.

Schwanhausser, B., Busse, D., Li, N., Dittmar, G., Schuchhardt, J., Wolf, J., Chen, W., and Selbach, M. (2011). Global quantification of mammalian gene expression control. Nature *473*, 337-342.

Shen, J., Chen, X., Hendershot, L., and Prywes, R. (2002). ER stress regulation of ATF6 localization by dissociation of BiP/GRP78 binding and unmasking of Golgi localization signals. Dev Cell *3*, 99-111.

Shi, Y., Vattem, K.M., Sood, R., An, J., Liang, J., Stramm, L., and Wek, R.C. (1998). Identification and characterization of pancreatic eukaryotic initiation factor 2 alpha-subunit kinase, PEK, involved in translational control. Mol Cell Biol *18*,

7499-7509.

Singh, G., Pratt, G., Yeo, G.W., and Moore, M.J. (2015). The Clothes Make the mRNA: Past and Present Trends in mRNP Fashion. Annu Rev Biochem *84*, 325-354.

So, J. (2012). Silencing of lipid metabolism genes through IRE1α-mediated mRNA decay lowers plasma lipids in mice. Cell Metab *16*, 487-499.

Sonenberg, N., and Hinnebusch, A.G. (2009). Regulation of translation initiation in eukaryotes: mechanisms and biological targets. Cell *136*, 731-745.

Stebbins-Boaz, B., Cao, Q., de Moor, C.H., Mendez, R., and Richter, J.D. (1999). Maskin is a CPEB-associated factor that transiently interacts with elF-4E. Mol Cell *4*, 1017-1027.

Stephan, J.S., Fioriti, L., Lamba, N., Colnaghi, L., Karl, K., Derkatch, I.L., and Kandel, E.R. (2015). The CPEB3 Protein Is a Functional Prion that Interacts with the Actin Cytoskeleton. Cell reports *11*, 1772-1785.

Sun, H.T., Wen, X., Han, T., Liu, Z.H., Li, S.B., Wang, J.G., and Liu, X.P. (2015). Expression of CPEB4 in invasive ductal breast carcinoma and its prognostic significance. Onco Targets Ther *8*, 3499-3506.

Tabas, I., and Ron, D. (2011). Integrating the mechanisms of apoptosis induced by endoplasmic reticulum stress. Nat Cell Biol *13*, 184-190.

Tarun, S.Z., Jr., and Sachs, A.B. (1995). A common function for mRNA 5' and 3' ends in translation initiation in yeast. Genes Dev *9*, 2997-3007.

Theis, M., Si, K., and Kandel, E.R. (2003). Two previously undescribed members of the mouse CPEB family of genes and their inducible expression in the principal cell layers of the hippocampus. Proc Natl Acad Sci U S A *100*.

Topisirovic, I. (2011). Cap and cap-binding proteins in the control of gene expression. Wiley Interdiscip Rev RNA *2*, 277-298.

Tsai, L.Y., Chang, Y.W., Lin, P.Y., Chou, H.J., Liu, T.J., Lee, P.T., Huang, W.H., Tsou, Y.L., and Huang, Y.S. (2013). CPEB4 knockout mice exhibit normal hippocampus-related synaptic plasticity and memory. PLoS One *8*.

Udagawa, T., Swanger, S.A., Takeuchi, K., Kim, J.H., Nalavadi, V., Shin, J., Lorenz, L.J., Zukin, R.S., Bassell, G.J., and Richter, J.D. (2012). Bidirectional control of mRNA translation and synaptic plasticity by the cytoplasmic polyadenylation complex. Mol Cell *47*, 253-266.

van Galen, P., Kreso, A., Mbong, N., Kent, D.G., Fitzmaurice, T., Chambers, J.E., Xie, S., Laurenti, E., Hermans, K., Eppert, K.*, et al.* (2014). The unfolded protein response governs integrity of the haematopoietic stem-cell pool during stress. Nature *510*, 268-272.

Vattem, K.M., and Wek, R.C. (2004). Reinitiation involving upstream ORFs regulates ATF4 mRNA translation in mammalian cells. Proceedings of the National Academy of Sciences *101*, 11269-11274.

Vollmers, C., Gill, S., DiTacchio, L., Pulivarthy, S.R., Le, H.D., and Panda, S. (2009). Time of feeding and the intrinsic circadian clock drive rhythms in hepatic gene expression. Proc Natl Acad Sci U S A *106*.

Volmer, R., and Ron, D. (2015). Lipid-dependent regulation of the unfolded protein response. Curr Opin Cell Biol *33*, 67-73.

Walter, P., and Ron, D. (2012). The Unfolded Protein Response: From Stress Pathway to Homeostatic Regulation.

Wang, L., Zeng, X., Ryoo, H.D., and Jasper, H. (2014). Integration of UPRER and

oxidative stress signaling in the control of intestinal stem cell proliferation. PLoS Genet *10*.

Wang, M., and Kaufman, R.J. (2016). Protein misfolding in the endoplasmic reticulum as a conduit to human disease. Nature *529*, 326-335.

Wang, S. (2012). IRE1α-XBP1s induces PDI expression to increase MTP activity for hepatic VLDL assembly and lipid homeostasis. Cell Metab *16*, 473-486.

Wang, S., and Kaufman, R.J. (2014). How does protein misfolding in the endoplasmic reticulum affect lipid metabolism in the liver? Curr Opin Lipidol *25*, 125-132.

Wang, X.P., and Cooper, N.G. (2010). Comparative in silico analyses of cpeb1-4 with functional predictions. Bioinform Biol Insights *4*, 61-83.

Weill, L., Belloc, E., Bava, F.A., and Mendez, R. (2012). Translational control by changes in poly(A) tail length: recycling mRNAs. Nat Struct Mol Biol *19*, 577-585.

Weingarten-Gabbay, S., Elias-Kirma, S., Nir, R., Gritsenko, A.A., Stern-Ginossar, N., Yakhini, Z., Weinberger, A., and Segal, E. (2016). Systematic discovery of cap-independent translation sequences in human and viral genomes. Science *351*.

Wek, R.C., Jiang, H.Y., and Anthony, T.G. (2006). Coping with stress- eIF2 kinases and translational control. Biochem Soc Trans *34*, 7-11.

Wijnen, H., and Young, M.W. (2006). Interplay of circadian clocks and metabolic rhythms. Annual review of genetics *40*, 409-448.

Wu, L., Candille, S.I., Choi, Y., Xie, D., Jiang, L., Li-Pook-Than, J., Tang, H., and Snyder, M. (2013). Variation and genetic control of protein abundance in humans. Nature *499*, 79-82.

Yoshida, H., Matsui, T., Yamamoto, A., Okada, T., and Mori, K. (2001). XBP1

mRNA Is Induced by ATF6 and Spliced by IRE1 in Response to ER Stress to Produce a Highly Active Transcription Factor. Cell *107*, 881-891.

Zhang K1, W.H., Song B, Miller CN, Scheuner D, Kaufman RJ. (2005). The unfolded protein response sensor IRE1alpha is required at 2 distinct steps in B cell lymphopoiesis. J Clin Invest *115*, 268-281

Zhong, X., Xiao, Y., Chen, C., Wei, X., Hu, C., Ling, X., and Liu, X. (2015). MicroRNA-203-mediated posttranscriptional deregulation of CPEB4 contributes to colorectal cancer progression. Biochem Biophys Res Commun *466*, 206-213.

Appendix

Table 1. Top enriched candidates of the RIP-seq analysis.

symbol	log2FC	symbol	log2FC	symbol	log2FC
Npm3	3,69	Tat	2,65	Ptplb	2,47
Brd3	3,53	Mex3c	2,64	Atp11b	2,47
Pck1	3,47	Cmip	2,64	Dpyd	2,46
Cadm1	3,40	Snx9	2,64	Snrnp40	2,46
Elovl2	3,37	Csgalnact2	2,63	Grb7	2,46
Cpeb4	3,29	Ubl4	2,63	Ppil3	2,44
Socs1	3,29	Slc10a3	2,63	Lif	2,44
Prpf40a	3,25	Wtap	2,62	Tank	2,43
Cog6	3,15	Nfkbia	2,62	Akirin1	2,43
Cstf1	3,08	Tsen15	2,61	Adk	2,43
l830012O16Rik	3,05	Tiparp	2,61	Ugdh	2,43
Sqrdl	3,04	Tjp1	2,60	Phip	2,42
Gm15441	3,01	Dek	2,60	Smarca5	2,42
Txnip	3,01	Slc35b3	2,59	Dr1	2,42
Tcp11l2	3,00	Cks1bGm6340	2,59	Slc2a2	2,41
Hnrnpd	2,99	Gyk	2,58	Dmxl1	2,41
Xpot	2,97	Cmpk2	2,58	Pcgf5	2,41
Cpsf1	2,95	Hdac1	2,58	l7Rn6	2,41
Trp53	2,93	Wbp5	2,58	Krt5	2,40
Clcc1	2,92	Mier3	2,58	Jak2	2,40
Gpsm2	2,92	Gbp3	2,57	Yaf2	2,40
Sde2	2,90	Efna1	2,56	Rala	2,40
Tap1	2,90	Sap130	2,56	Nedd1	2,39
Snrpb2	2,89	Atg5	2,56	Lsm3	2,39
Tshz1	2,89	NA	2,55	Sf3a3	2,39
Bhmt	2,87	Tgds	2,55	Vezf1	2,38
Bcl3	2,87	Srek1ip1	2,55	Hmgb1	2,38
Ginm1	2,87	Nfkb1	2,55	Jag1	2,38
Foxq1	2,86	Dnajc2	2,55	Clic1	2,37
Mzt1	2,85	Psma1	2,55	Gjb2	2,37
Gabpa	2,84	Pprc1	2,55	Mitd1	2,37
Josd2	2,84	Cdk4	2,54	Tbp	2,36
Psmd11	2,83	Psmb9	2,54	M6pr	2,36
Med31	2,80	Enpp4	2,53	Cyp1a2	2,36
Setd4	2,80	Efnb1	2,53	Rsad2	2,36
Ier3ip1	2,80	Spryd7	2,53	Tgfbr2	2,35
Hdhd2	2,80	00Rik	2,52	Rcn2	2,35
Gm4788	2,79	Scpep1	2,52	Slmap	2,34

Gtpbp10	2,79	Stx4a	2,52	Pex11a	2,34
Nae1	2,79	Kdm6b	2,52	Uroc1	2,34
Bcl10	2,78	Heatr5a	2,52	Serinc5	2,34
Tma7-psTma7	2,78	Slco1b2	2,52	Bud13	2,33
Fam49b	2,77	Cnep1r1	2,51	Art3	2,32
Sema3e	2,77	Sbds	2,51	Cxcl10	2,32
Cldn25	2,74	Pcmtd2	2,51	Nipsnap3b	2,32
Tpra1	2,73	Pdcl3	2,51	Hpd	2,32
Acat1	2,72	Sacm1l	2,51	Sema4b	2,32
Kdm2a	2,72	Samd1	2,50	Mkl1	2,31
Coq10b	2,72	Eny2	2,50	Kdm5a	2,31
Lmnb1	2,71	Polr2d	2,49	Tomm22	2,31
Arg1	2,71	H2afv	2,49	Rap2c	2,31
Cyp2c50	2,70	Herpud2	2,49	Apaf1	2,31
Usb1	2,70	Ppif	2,49	Slc30a1	2,31
00Rik	2,70	Git2	2,48	Ccar1	2,31
Yipf4	2,68	Snx3	2,48	Cnot3	2,31
Abhd16a	2,68	Eif4a3Gm5576	2,48	Leng1	2,31
Copb1	2,68	Ssr2	2,48	Slc25a32	2,30
F2r	2,68	Polr2hGm7511	2,48	Ifit3	2,30
Tmem64	2,67	Vprbp	2,48	Il1rap	2,30
Naf1	2,67	Manf	2,48	Ctdp1	2,30
Il1rn	2,66	Nampt	2,47	Arl6ip6	2,30
Tcf12	2,65	00Rik	2,47	Wipi1	2,30
Tmem39a	2,30	Cpox	2,22	Sp1	2,14
Fgfr2	2,29	Ocln	2,22	Zfyve16	2,14
Oat	2,29	Snx7	2,21	Zfp422	2,14
Eed	2,29	Mex3d	2,21	Rnf149	2,14
Zfp507	2,29	Kdelr2	2,20	Anp32a	2,14
Cks2	2,29	Psma7	2,20	Snx1	2,14
Lrrc40	2,29	Rap1a	2,20	Top2b	2,14
Ing3	2,29	D19Bwg1357e	2,20	Hspa13	2,14
Tma16	2,29	Mettl2	2,20	Metap2	2,13
Atp2b1	2,29	Rcc1	2,20	Tor3a	2,13
Sult1d1	2,29	Twsg1	2,20	Prkaa1	2,13
Rpia	2,28	Elf1	2,20	Katnbl1	2,13
Rbm22	2,28	Naga	2,20	Dync1i2	2,13
Ube2d1	2,28	Plagl1	2,19	Bbx	2,13
00Rik	2,28	Lgals8	2,19	Cdkn1b	2,13
Ppib	2,28	Kif21a	2,19	Smndc1	2,13

Table 2. mRNAs with reduced localization at the ER upon CPEB4 depletion

Gene symbol	log2 FoldChange	padj
Irf7	-0,427	0,096
Bst2	-0,430	0,044
Mid1ip1	-0,449	0,096
Isg15	-0,480	0,096
Paqr7	-0,501	0,065
Cyp2d40	-0,509	0,047
Gbp6	-0,547	0,044
Gck	-0,889	1,13E-7